








Review

Chitosan-Based Biomaterials: Insights into Chemistry, Properties, Devices, and Their Biomedical Applications

Simona Petroni ¹, Irene Tagliaro ², Carlo Antonini ², Massimiliano D'Arienzo ², Sara Fernanda Orsini ², João F. Mano ³, Virginia Brancato ¹, João Borges ^{3,*} and Laura Cipolla ^{1,*}

¹ Department of Biotechnology and Biosciences, University of Milano-Bicocca, 20126 Milano, Italy

² Department of Materials Science, University of Milano-Bicocca, 20125 Milano, Italy

³ CICECO–Aveiro Institute of Materials, Department of Chemistry, University of Aveiro, 3810-193 Aveiro, Portugal

* Correspondence: joaborges@ua.pt (J.B.); laura.cipolla@unimib.it (L.C.); Tel.: +351-234372585 (J.B.); +39-0264483460 (L.C.)

Abstract: Chitosan is a marine-origin polysaccharide obtained from the deacetylation of chitin, the main component of crustaceans' exoskeleton, and the second most abundant in nature. Although this biopolymer has received limited attention for several decades right after its discovery, since the new millennium chitosan has emerged owing to its physicochemical, structural and biological properties, multifunctionalities and applications in several sectors. This review aims at providing an overview of chitosan properties, chemical functionalization, and the innovative biomaterials obtained thereof. Firstly, the chemical functionalization of chitosan backbone in the amino and hydroxyl groups will be addressed. Then, the review will focus on the bottom-up strategies to process a wide array of chitosan-based biomaterials. In particular, the preparation of chitosan-based hydrogels, organic–inorganic hybrids, layer-by-layer assemblies, (bio)inks and their use in the biomedical field will be covered aiming to elucidate and inspire the community to keep on exploring the unique features and properties imparted by chitosan to develop advanced biomedical devices. Given the wide body of literature that has appeared in past years, this review is far from being exhaustive. Selected works in the last 10 years will be considered.

Keywords: chitosan; marine-origin polysaccharides; chitosan-based materials; hydrogels; layer-by-layer devices; 3D printing; organic–inorganic hybrids; drug delivery; tissue engineering; regenerative medicine



Citation: Petroni, S.; Tagliaro, I.; Antonini, C.; D'Arienzo, M.; Orsini, S.F.; Mano, J.F.; Brancato, V.; Borges, J.; Cipolla, L. Chitosan-Based Biomaterials: Insights into Chemistry, Properties, Devices, and Their Biomedical Applications. *Mar. Drugs* **2023**, *21*, 147. <https://doi.org/10.3390/md21030147>

Academic Editor: Hitoshi Sashiwa

Received: 14 January 2023

Revised: 17 February 2023

Accepted: 20 February 2023

Published: 24 February 2023



Copyright: © 2023 by the authors. Licensee MDPI, Basel, Switzerland. This article is an open access article distributed under the terms and conditions of the Creative Commons Attribution (CC BY) license (<https://creativecommons.org/licenses/by/4.0/>).

1. Introduction

Glucose and its 2-acetamido-2-deoxy derivatives are the most abundant organic compounds found on earth, in the form of their β -1,4-homopolymers cellulose and chitin, respectively (Figure 1). Notably, glucose and 2-acetamido-2-deoxy-glucose (namely *N*-acetylglucosamine, GlcNAc) are biosynthetically connected [1], being glucose 6-phosphate their common precursor; similarly, the resulting homopolysaccharides share a role in supporting the integrity, protection and structure of plants (cellulose), or arthropods and fungi (chitin) [2,3].

After cellulose, chitin is the second most abundant polysaccharide on earth. It is estimated that every year 10^{10} – 10^{12} tons of chitin are produced by living organisms (for more details, the reader may visit the GlycoPedia chitosan section at <https://www.glycopedia.eu/e-chapters/from-chitin-to-chitosan/article/abstract-introduction>, accessed on 23 December 2022). Over the years, the chitin content has been described in different species, ranging from 75% of dry mass of the exoskeleton in lobsters, to 2% of the dry mass of mycelium in fungi [4], while the degree of acetylation (DA) is commonly 100% [5].

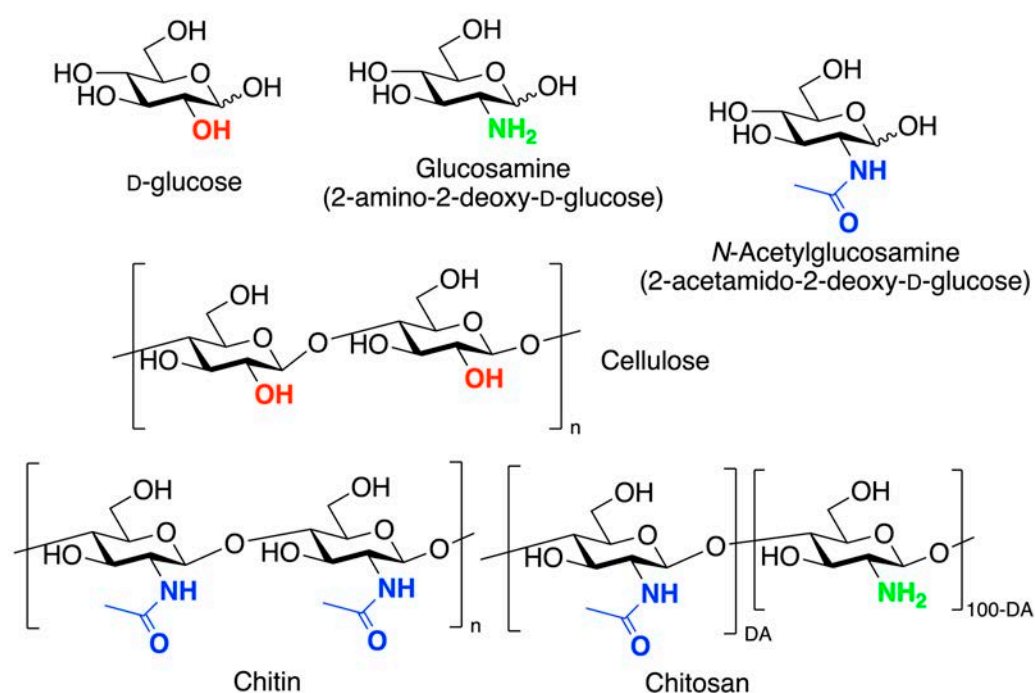


Figure 1. Structure of glucose, glucosamine, *N*-acetylglucosamine, and their homopolymers cellulose (the most abundant polysaccharide on earth), fully acetylated chitin (the second most abundant biopolymer on earth) and chitosan (partially deacetylated chitin).

Chitin was first reported as a chemical stable material in 1799 by the English scientist Charles Hachett [6]; however, only a few years later scientists gained interest in the chemistry of this polymer extracted from mushrooms (1811, Henri Braconnot, who named it fungine) [7] and insect exoskeleton (1823, Auguste Odier, who gave it its actual name, chitin). The definite chemical structure of chitin as a polymer made by β-(1 → 4) repeating units of 2-acetamido-2-deoxy-D-glucopyranose was elucidated in 1946 by Earl R. Purchase and Charles E. Braun. CHT was described for the first time in 1859 by Charles Rouget [8], who obtained an acid soluble polymer after boiling chitin in alkali. This soluble polymer was named chitosan in 1894 by Felix Hoppe-Seyler [9]. However, only since the 1970s chitin and CHT begun to be considered as promising materials to be exploited in several applications.

Due to its extensive hydrogen bond network, chitin is totally insoluble in water, as well as in most organic solvents [10,11]. This feature has hampered its characterization [12], and accounts for its chemical and biological stability on the one hand, and its poor industrial application, on the other hand [13].

CHT, which is partially deacetylated chitin in which *N*-acetylglucosamine residues are replaced with glucosamine (2-amino-2-deoxy-D-glucose, GlcN), is less widespread in nature and can be found mainly in the cell wall of a few fungi and green algae. Deacetylation converts the homopolymer chitin into a random copolymer of GlcNAc and GlcN monomers; the free amino groups can be protonated in acidic media, affecting the physicochemical properties such as solubility, hydrogen bonding and reactivity.

The molecular weight, strictly related to the degree of polymerization (DP), the degree of acetylation (DA) and the pattern of acetylation (PA) are fundamental parameters determining the CHT properties, firstly, in terms of solubility; and secondly, in terms of physicochemical properties and structure-activity relationship [14–16].

The average molecular weight of CHT affects its solution viscosity, mechanical, chemical, and optical properties, as well as chain orientation and entanglement. While chitin is reported to have an average molecular weight up to millions Da (in the range 1×10^6 – 2.5×10^6 Da, that is a DP comprised between 5 and 10 thousands of monomeric units), CHT average molecular weight is commonly comprise between 50 thousand and

1 million Da [17], while most widespread commercial CHT is within the range of a few thousand Da (3800 Da) to 500 kDa [18].

DA, defined as the average number of GlcNAc units per 100 monomers given as a percentage, can be determined with different techniques, including spectroscopic methods [18,19], or potentiometric titrations [20]. When the DA is less than 50%, CHT becomes soluble in slightly acidic aqueous media (pH < 6), and ¹H-NMR may be the technique of choice for DA determination [21]. Although there is no consensus on the DA value determining the name switch from chitin to CHT, commercial CHT is commonly featured with a DA in the range 2–45% [18]. However, more than a decade ago, the European Chitin Society (<https://euchis.org/>, accessed on 21 February 2023) proposed the use of the terms chitin/CHT based on the solubility in 0.1 M acetic acid, being chitin is the insoluble polymer and CHT the soluble one [22].

Beside DP and DA, the PA is an additional key feature in assessing CHT properties. Recent studies showcase the relationship between a specific sequence of GlcN and GlcNAc monomers and CHT biological activity: a “CHT code” is coming to light [23]. However, while DP and DA have been extensively studied over the last decades, and several techniques developed, PA has been understated mainly because of the lack of methods to obtain defined PA in CHT samples, accompanied by the limited development of specific analytical techniques with suitable sensitivity and robustness [24].

Commercial interest in CHT is due to its numerous features, including biodegradability, biocompatibility, nonimmunogenic, antimicrobial, chelating and polyelectrolyte properties encompassing the food, cosmetic, and pharma industries, and medicine, agriculture and aquaculture, wastewater treatment, textile and pulp sectors.

The industrial chitin and CHT production started in Japan in the early 1970s as a niche material. Currently, society and market demand for renewable feedstocks and new materials in place of fossil-based polymers are boosting industrial interest, and several start-ups and projects are populating the CHT scenario [25].

The CHT industrial market in 2019 was valued globally at 1.7 billion USD, and it is expected to grow at a 14.5% CAGR (compound annual growth rate) from 2020 to 2027, when it is expected to reach a 4.7 billion USD value. The market can be analyzed on the basis of CHT production geographic area, source and application [26]. From a geographical perspective, the Asia-Pacific region is the main production area due to large crustacean consumption, making shell wastes readily available; North America follows, due to the increasing production demand and expanding market of CHT-based biomedical products.

CHT's main source is seafood industry waste [27], which has been increasing over recent years, and together with the circular economy and waste reuse strategies is supporting the CHT market [28]. CHT is obtained after the deacetylation of chitin found in crustaceans' exoskeleton, mainly shrimps, crabs, krill, squids (bone plate) and lobsters. Different chemicals and conditions are used for CHT production, depending on the chitin source [29]. Besides the chemical methodologies, a few steps processing chitin into CHT (i.e., deacetylation) can be performed by following more sustainable approaches using biocatalysis [30] or fermentation processes [31,32]. However, biotechnological approaches are still far from being optimized for largescale production [33]. In the future, it is expected that CHT will be obtained from fungi, either as agriculture waste or dedicated fungi cultures, and from snails and other terrestrial mollusks. Cultured fungi CHT production is expected to grow for food and beverage applications due to dietary ethno-religious restrictions [34].

Currently, marketed CHT and its derivatives are mainly used in wastewater treatment, due to its effectiveness in the removal of toxic contaminants. The pharmaceutical and biomedical sector is the second player in CHT industrial applications [35], followed by the cosmetic, and food and beverage sectors, for instance, as a dietary supplement or preservative. Patients and pharmaceutical industries will benefit from the chitosan-based products that will enter into the market, due to their potentialities as drug delivery systems, pharmaceutical formulation components, and active ingredients for different medical treatments. Formulations and drug delivery systems containing chitosan, for example, can

help in the delivery of therapeutically relevant active proteins (i.e., growth factors), and peptides, nucleic acids and genes. Patients would benefit in the sectors of regenerative medicine, oncology, dermatology, ophthalmology, dentistry and many others both from a therapeutic and diagnostic point of view.

The use of CHT as a biopesticide and soil supplement for improving plant growth is also expected to grow. More recently, news accounts have highlighted the relevance of circular economy approaches in driving the CHT market. For example, at COP 27, held in Egypt 7–8 November 2022 (<https://cop27.eg/#/>, accessed on 21 February 2023), at the event focused on circular bio-based solutions, Chitosan Egypt (<https://chitosaneg.com/>, accessed on 21 February 2023) promoted local waste recycling towards chitosan-based bio-pesticides and bio-fertilizers, also entering the market as a CHT producer [32].

The growing interest towards CHT is witnessed by the increasing number of publications and patents since 1990, as denoted in Figure 2. Notably, the number of patents (Figure 2b) exceeds the number of publications (Figure 2a), thus revealing its attractiveness for applied research and industry innovation.

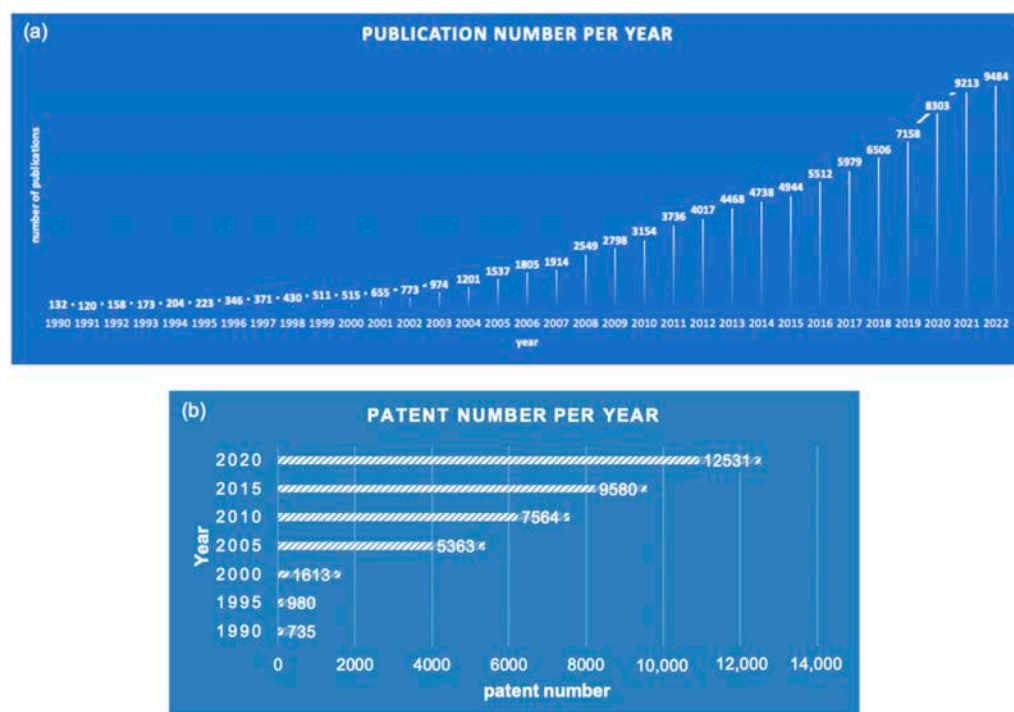


Figure 2. (a) Publication number returned by Scopus® for “Chitosan” since 1990; (b) Patent number returned by Scopus® for “Chitosan” from 1990 to 2020 (retrieved date: 12 December 2022).

This review aims at providing an overview of CHT properties and chemistry in the design of innovative materials for biomedical applications. Differently from other reviews about chitosan, this review will be organized in sections defined as a function of material typology, rather than as a function of the targeted biomedical application. Strategies towards CHT-based hydrogels, organic–inorganic hybrids, layer-by-layer systems and (bio)inks will be considered organic–inorganic hybrids; layer-by-layer and inks are commonly overlooked in reviews dealing with chitosan. Particular emphasis will be given to the chemistry beyond chitosan material design, highlighting limitations and opportunities. The examples reported here will be far from being exhaustive, given the huge number of published articles; except for seminal papers, the main cited literature spans from 2010 to date.

2. Chitosan Functionalities: Friend or Foe?

The switch from chitin to CHT renders the latter less crystalline than chitin and greatly ameliorates its solubility and, hence, reactivity. However, the functional groups

present in CHT, which are still able to act as both donor and acceptor of inter/intra molecular hydrogen bonds, are responsible for its water insolubility, unless in slightly acidic conditions (*vide infra*), thus opening the way to chemical derivatization. The chemical modification of CHT enables tuning its physicochemical and biological properties, ideally embracing any field of application. The chemical functionalization of CHT may involve the two hydroxyl groups, respectively at C-6 (primary) and C-3 (secondary), both on GlcN and GlcNAc units, and the 2-amino groups unique to glucosamine units (Figure 3).

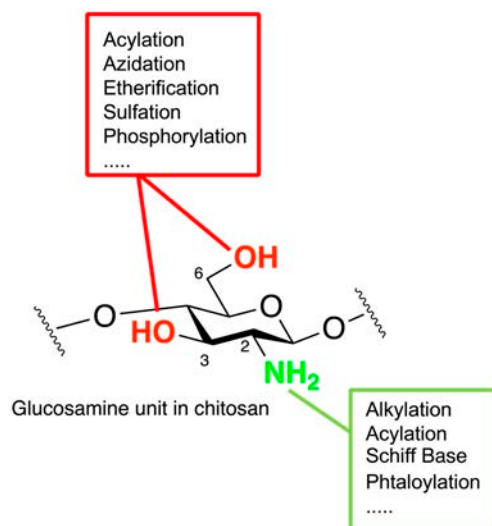


Figure 3. Sites of derivatization of GlcN units in CHT. The modification of the GlcNAc unit is limited to the 3- and 6-OH.

Hydroxyl and amino functional groups can react as nucleophiles with electrophilic reagents, being amines more reactive than hydroxyls. Chemoselective and regioselective issues may apply in CHT modification; this lack of selectivity may afford heterogeneous mixtures of derivatives, limiting reproducibility and applications; in light of these observations, robust chemistry allowing the strict control over selectivity is needed for CHT derivatization. Additionally, CHT functionalization is more effective in homogenous conditions, usually requiring aqueous acids as solvents: in these conditions, it should be taken into account that water may be a competing nucleophile in the reaction, lowering derivatization yields. At the same time, acidic pH may promote reagent decomposition. Moreover, at acidic pH, usually needed for chitosan solubilization, amine groups are partially converted into the corresponding ammonium ions, thus reducing their nucleophilicity. On the other hand, CHT derivatization in the heterogeneous phase allows the use of non-nucleophilic solvents and non-acidic pH. However, the degree of substitution is usually low and harsh conditions (*i.e.*, high temperature, excess of reagents) may be required, thus reducing the control over chemo- and regioselectivity, affording structurally heterogeneous mixtures of products, possibly containing degradation byproducts as well [10,36].

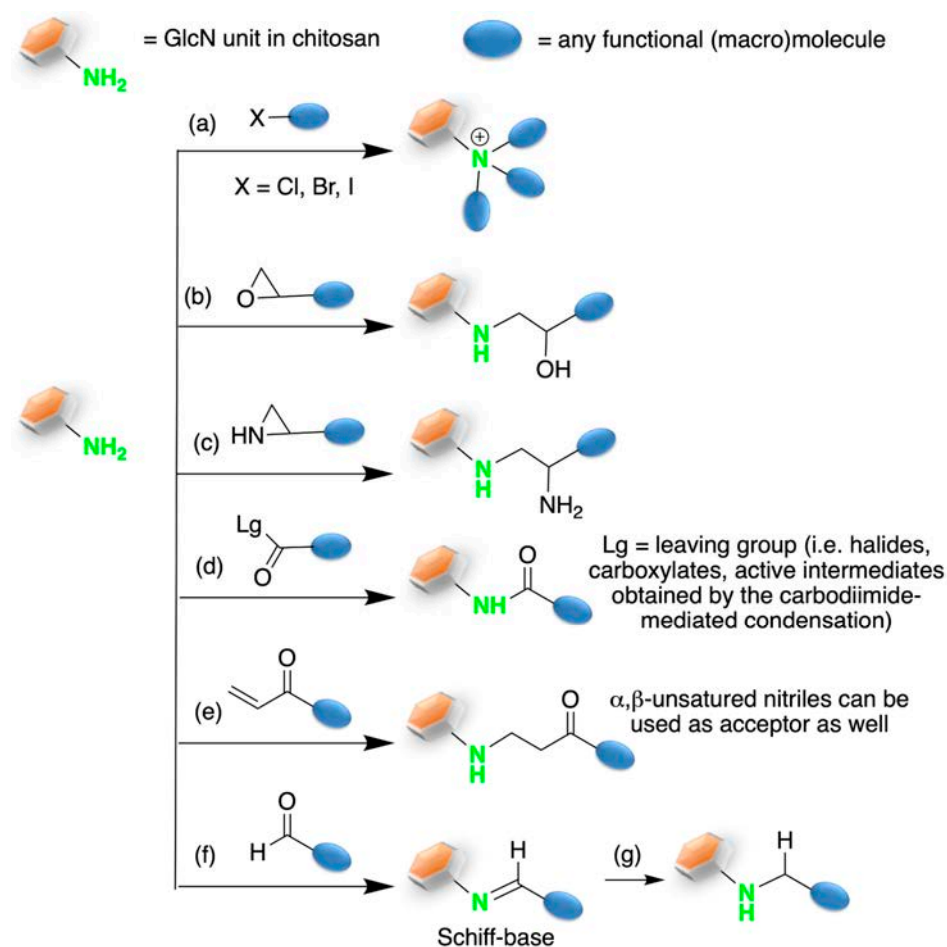
The specific chemical nature of the alkyl or acyl group of the derivatizing agents allows the introduction of several functional groups, resulting in the fine tuning of the physicochemical properties of the CHT derivatives [37]. For example, the introduction of hydrophilic groups [38], such as carboxylic [39], sulfates and sulfonates [40], or phosphate groups [41], which at suitable pH are in their anionic form, allows to obtain CHT derivatives, with properties variable as a function of the substitution's degree. As the main result, these derivatives may become soluble in water at neutral pH; and have better coordination ability towards metal cations, tunable viscosity, hydrogel forming ability, and different biological activity spanning from anticoagulant to antibacterial effects.

When hydrophobic groups are added to CHT, for example by acylation with fatty acids or alkylation with hydrocarbon chains, amphiphilic derivatives can be obtained, useful for their surface active properties and aggregation behavior, affording nanoparti-

cles, micelles and hydrogels [42–45]. These derivatives find interesting applications in the biomedical field as drug delivery systems and for lipophilic water contaminants absorption (i.e., oils). Additionally, hydrophobic derivatization increases both antibacterial and hemostatic activity [46].

If the derivatization reagents contain sulfhydryl groups (-SH), thiolated CHT derivatives can be obtained [47,48]. Thiol groups may be useful as adhesive groups and antibacterial properties, or their chemical reactivity can be exploited for further chemoselective derivatization reactions through click chemistry approaches [49] or by oxidation to the corresponding disulfide adducts [50]. Disulfide bond formation may be a limitation as well, if undesired.

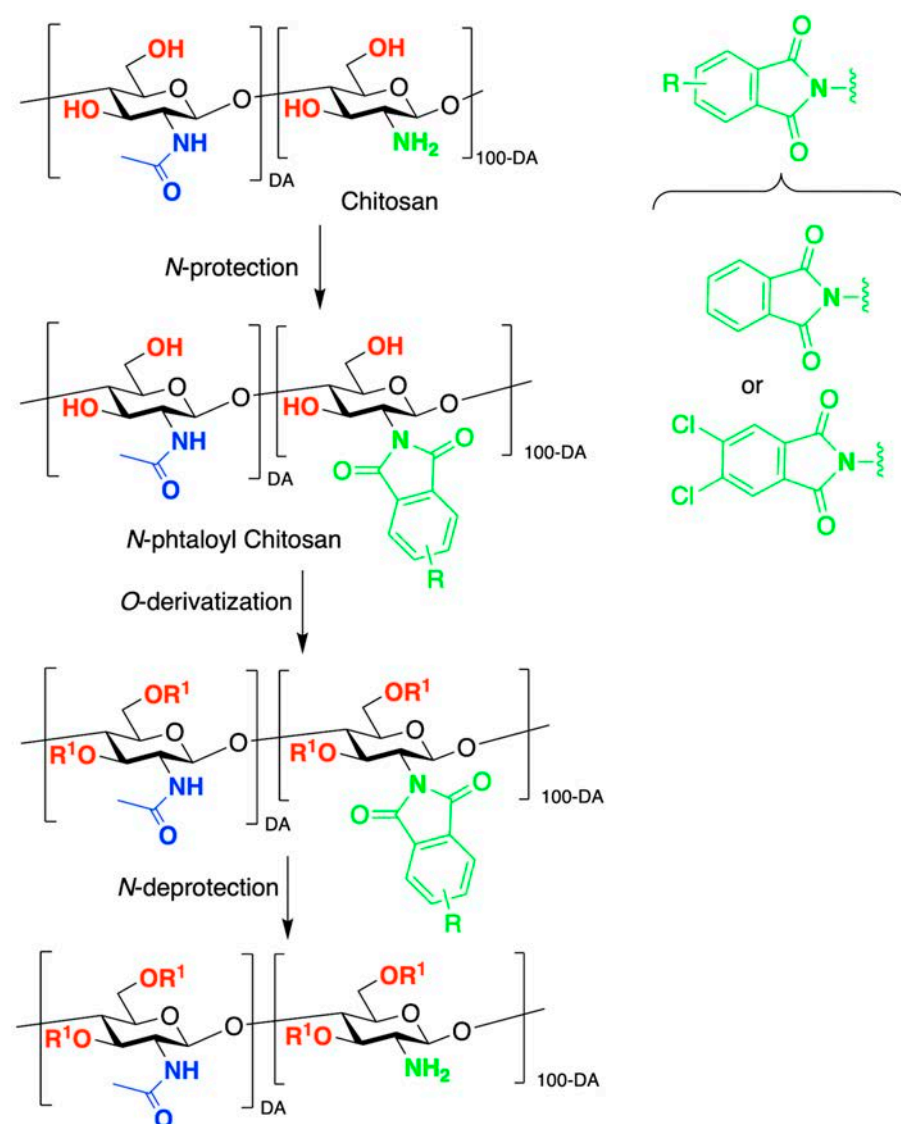
Taking advantage of the higher nucleophilicity of the amine groups (as the free base) when compared to the hydroxyl groups, several strategies can be applied for the chemoselective chitosan functionalization (Scheme 1). The amine group can act as a nucleophile in nucleophilic substitution to (per)alkylated ammonium derivatives (Scheme 1a) [51], nucleophilic opening of epoxides (Scheme 1b) [52] or aziridines (Scheme 1c) [53], nucleophilic acyl substitution to the corresponding amides (Scheme 1d) [54], donor in 1,4-Michael additions (Scheme 1e) [55], Schiff base adducts formation (Scheme 1f) [47,56], eventually followed by reductive amination to the corresponding secondary or tertiary amines (Scheme 1g). Notably, the nucleophilic attack of carbonyl derivatives towards the formation of imines (Schiff base) or amines (reductive amination), as well as Michael additions, is fully chemoselective, allowing the derivatization of the sole C-2 position of CHT, while nitrogen peralkylation affords ammonium derivatives, characterized with a pH-independent polycationic character [57].



Scheme 1. Chemistry of GlcN unit modifications at the 2-amino group; (a,b,c) alkylation; (d) acylation; (e) Michael addition; (f,g) reductive amination.

A robust strategy for fully chemoselective and effective *N*-acylation was proposed by Másson et al., through a Design of Experiment approach (DoE), affording the synthesis of CHT conjugates with cinnamic, *p*-coumaric, ferulic and caffeic acid, with substitution degrees ranging from 3 to 60% [58]. Cinnamyl moieties confer interesting properties when grafted onto different materials, such as antioxidant and antimicrobial properties [59] or exploited for light-triggered processes [60]. The synthetic strategy involves the reaction of 3,6-di-*O*-*tert*-butyldimethylsilyl CHT with *tert*-butyldimethylsilyl-protected acyl chlorides (except for cinnamoyl chloride), followed by an acidic deprotection step. The antimicrobial activity of cinnamoyl CHT resulted analogously in the unsubstituted CHT for the low substituted conjugates, while the higher the substitution, the lower the antibacterial activity. This observation is ascribed to the loss of quaternized primary amino groups. On the other hand, the antioxidant activity is not shown by the cinnamic acid derivatives, but it is strongly promoted by hydroxy cinnamic acid moieties, with the best performance being accomplished with caffeic acid conjugation, affording antioxidant activity 4000 times higher than pristine CHT.

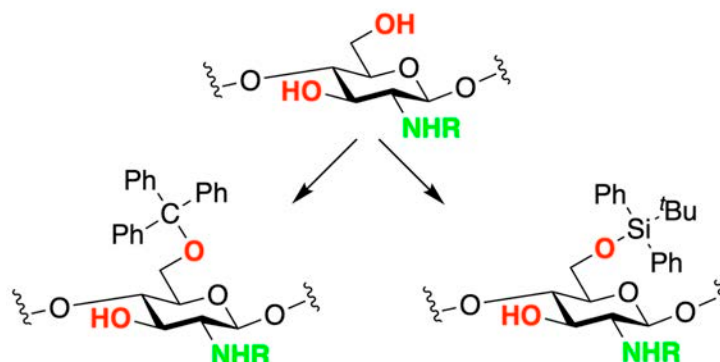
Chemoselective *O*-derivatization over *N*-substitution can usually be achieved after cumbersome protection/deprotection steps. The most commonly used group for selective *N*-protection is the phthaloyl group [61,62], and its derivatives containing electron withdrawing groups [63], which can be deprotected in mild conditions (Scheme 2).



Scheme 2. Protection/deprotection strategy towards chemoselective *O*-derivatization of CHT.

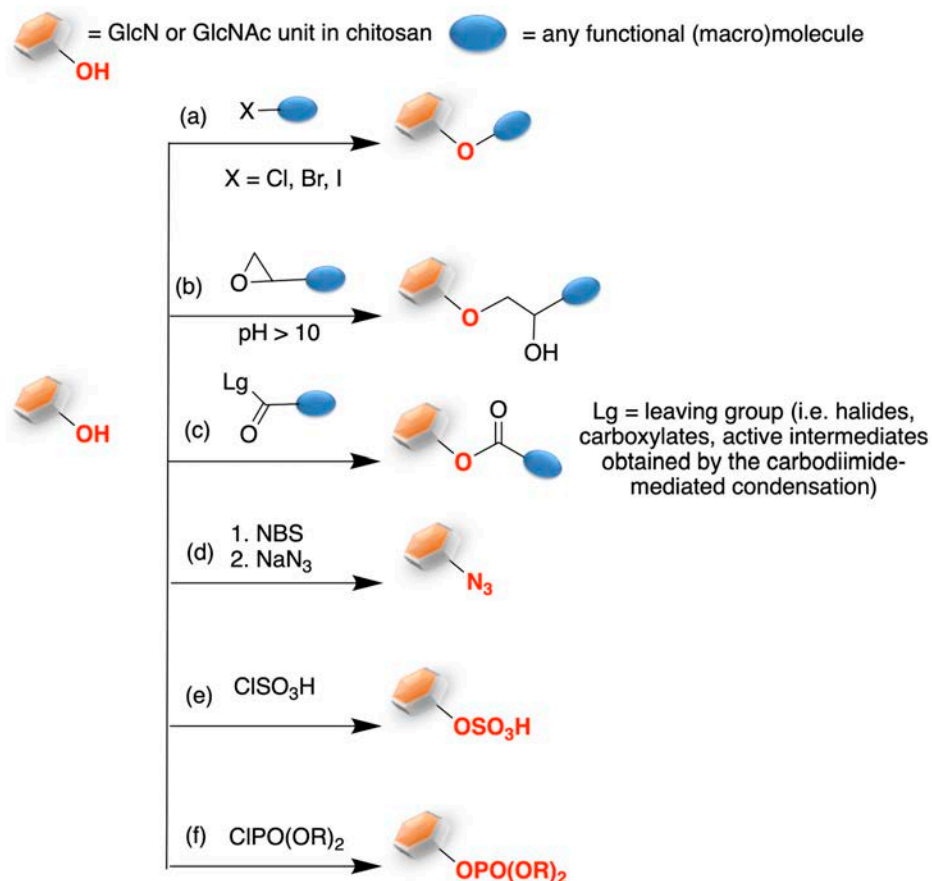
Additionally, the *O*-derivatization adds a regioselectivity issue, since both the 6-OH and/or the 3-OH groups may undergo the reaction, affording product mixtures. Depending on the reaction conditions and derivatization agents, 6-OH may be derivatized with fair regioselectivity due to its reduced steric hindrance, when compared to the secondary 3-OH. The favored access to 6-OH can be exploited for its regioselective protection (Scheme 3), thus opening the way to selective 3-OH derivatization; however, multistep protection/deprotection steps are needed.

R = H (GlcN); CH₃CO (GlcNAc); protecting group



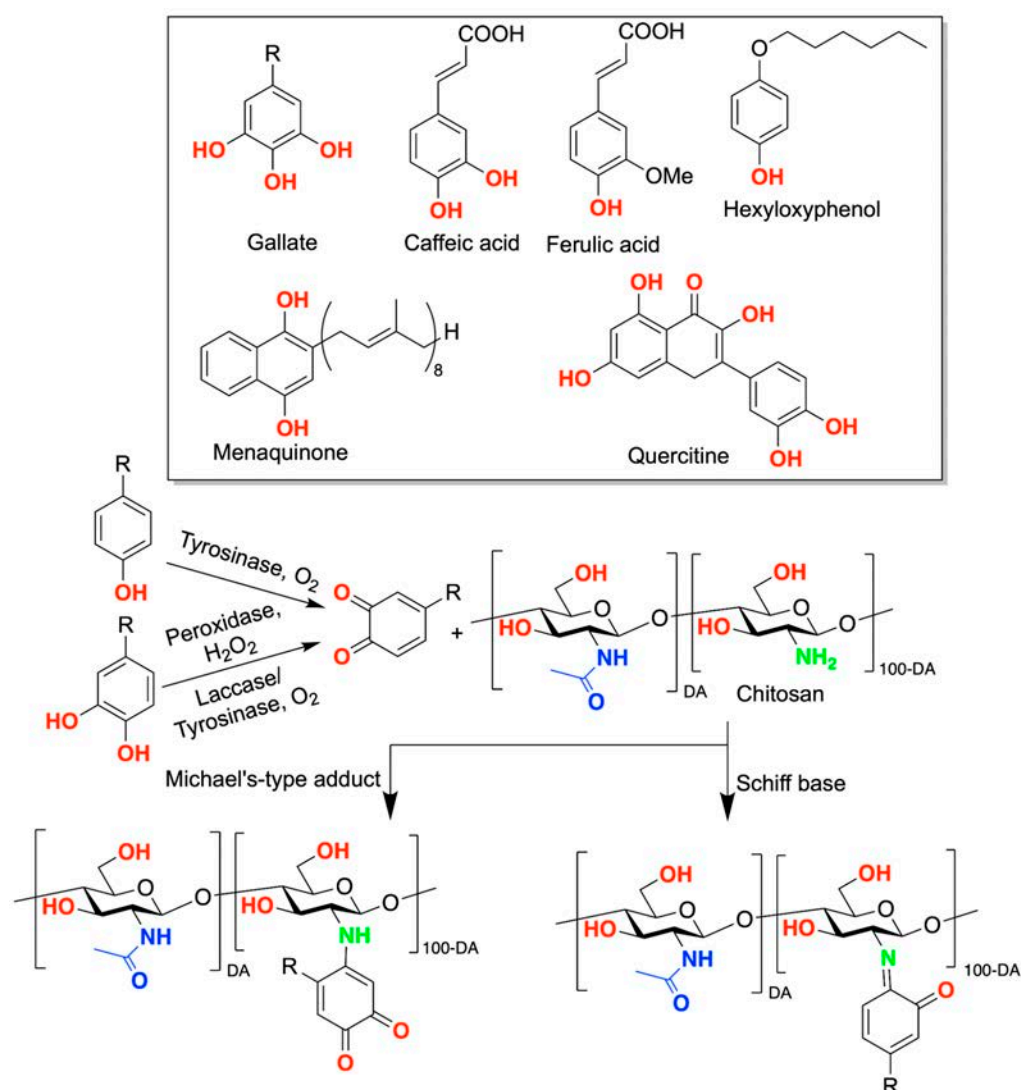
Scheme 3. 6-*O*-protected units in CHT.

Several reactions can be performed on the hydroxyl groups (Scheme 4), including etherification and acylation (Scheme 4a,b and 4c, respectively) [64], azidation (Scheme 4d) [65], sulfation and sulfonation (Scheme 4e) [66], phosphorylation (Scheme 4f) [67].



Scheme 4. Hydroxyl group modification in chitosan; (a,b) alkylation; (c) acylation; (d) azidation; (e) sulfation; (f) phosphorylation.

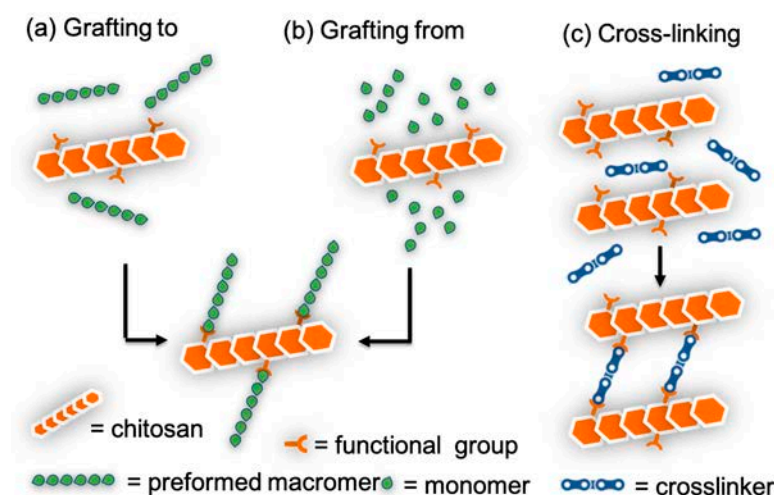
Chemo- and regioselectivity in CHT functionalization may be obtained via biocatalytic processes [68]. Interesting approaches affording non-random *N*-acylation patterns start from polyglucosamine polymers, i.e., fully deacetylated chitin, that can be chemo- and regioselectively amidated to chemically defined CHT through chitin deacetylase [69]. Oxidases [70] are interesting enzymes for the chemoselective amine derivatization with phenolic compounds (Scheme 5, inset): gallates, cinnamyl derivatives (i.e., caffeic acid, chlorogenic acid), ferulic acid, hexyloxy phenol, menaquinone, quercetin, and tyrosine containing (macro)molecules have been chemoselectively introduced as *N*-substituents. Different oxidases, such as tyrosinases [71], laccases [72], or horseradish peroxidases [73] were proposed (Scheme 5) [74]. Most of these derivatives have antioxidant and antimicrobial properties, thus improving the biological activity of CHT with features that can be exploited in both the biomedical and food packaging sectors.



Scheme 5. Enzyme-mediated chemoselective *N*-functionalization of GlcN units.

CHT can also act as a macromer in the synthesis of different copolymers, where the additional macromer component(s) may be of natural or synthetic origin [75]. The chemical nature of the co-macromer often dictates the synthetic strategy [76], and the final physicochemical, biological, and biodegradation properties [77] and applications [78]. Thus, proteins and peptides, poly- and oligosaccharides, including cyclodextrins, and several synthetic macromers (polyacrylates, polyethylene glycol, polyvinyl alcohol, polylactic acid, polycaprolactone etc.) have been grafted to CHT. CHT copolymer synthesis may be

accomplished either through “grafting to”, “grafting from” [79], or cross-linking approaches (Scheme 6) [80,81]. Regardless of the approach, a key issue in the synthetic design is the complementary reactivity of CHT functional groups (the already in place -OH and -NH₂, or those introduced *ad-hoc* by derivatization) and those on the monomer/macromer towards the desired co-polymer. As previously stated, while CHT functionalities offer grafting sites, regio- and chemoselectivity issues limit the synthesis of chemically defined co-polymers. Given the higher reactivity of the C-2 nitrogen, *N*-grafting or *N*-cross-linking usually allows the synthesis of copolymers with well-defined structure and high yields. The use of click chemistry [82–84] may further improve the outcome. On the other hand, selective *O*-grafting requires additional protection/deprotection steps of CHT macromers.



Scheme 6. Synthetic approaches towards CHT copolymers: (a) grafting to; (b) grafting from; (c) cross-linking.

In this section, a general outline of the chemistry beyond the CHT functionalization was given, with particular emphasis on regioselectivity and chemoselectivity. The reader may refer to other reviews for an in-depth understanding about specific syntheses of CHT derivatives [17,64,85–88].

3. Modulation of Chitosan Solubility, and Potential Application in the Material Science Field

The type and degree of derivatization, including the degree of acetylation, molecular weight, polydispersity, and the source and chemical treatment for production are key factors modulating the CHT physicochemical properties and applications [30,89,90].

The CHT structure inherits from chitin a semicrystalline structure held together by a strong hydrogen bonding network, which accounts for CHT insolubility in water at neutral pH [91], and in most common organic solvents [14]. In the case of chitin, the hydrogen bonds between the carbonyl oxygen as acceptors, and the amide -NH- groups as donors generate crystalline fibrils that determine the three chitin allomorphs (α , β , γ -chitin) detectable by X-ray crystallography, whose patterns have relevant variation in the chain orientation [92]. Through the process of deacetylation, which weakens hydrogen bonding, CHT partially loses its original crystalline structure and maintains only a semicrystalline form. Differences in solubility were observed between α - and β -CHT, due to the modification of the chain arrangement and its interaction with solvent molecules, affecting the swelling process and stability of the filaments [93]. Besides, differences in the molecular weight and distribution of the acetyl groups along the polymer chain play a role in the CHT crystallinity and, therefore, solubility. These aspects, together with the intrinsic variability of a biologically derived product, make it more difficult to measure the CHT solubility [94]. Residual acetyl groups are deemed to favor polymer chain aggregation and packing owing to their hydrophobicity, while free amine groups ($pK_a = 6.3$) [95] are

responsible for extended intramolecular and interchain hydrogen bonding, which increases with the polymerization degree, thus accounting for water insolubility. The reduction of these non-covalent interactions either by deacetylation, acid depolymerization, and/or free amine protonation renders CHT soluble in dilute acids and eventually in water. In acidic media, CHT becomes protonated and, thus, positively charged, which turns it into a soluble biopolymer. It has been reported that the solubility is reached when the protonated amines are more than 50% [14]. Since the solubility is closely linked to the degree of charge and, hence, protonated amine groups, the lower the DA, the higher the solubility. Aqueous organic acids are usually used to solubilize CHT, being acetic acid the most commonly used solvent with a concentration ranging between 1 to 5% (pH 4). Other carboxylic acids effective in CHT dissolution are formic and lactic acids. CHT is also soluble in aqueous inorganic acids, such as hydrochloric and nitric acids, despite being insoluble in phosphoric and sulfuric acids.

The insolubility of CHT in water at neutral (physiological) pH is still a limitation in its derivatization and application, especially in the biomedical field. However, new chemical strategies are emerging to enable the dissolution of CHT in a neutral aqueous environment [96]. For instance, to circumvent the lack of solubility at neutral pH, CHT has been modified to include either ionic or highly hydrophilic groups, such as carboxylic, sulfate or *N*-alkyls [97]. The CHT amine functional groups can be derivatized into a quaternary ammonium salt, obtaining a permanent cationic charge, which has shown to improve water solubility, antimicrobial activity and mucoadhesiveness [98]. CHT with an increased solubility can be obtained also via carboxylation by introducing acidic groups into its main chain. Derivatization may increase the CHT solubility up to neutral and alkaline pH, increasing moisturizing and film-forming properties [90].

Since the solubility of CHT is highly desired towards enabling its processing and applications, several approaches have been proposed. For instance, the rupture of intra- and interchain hydrogen bonds triggered by gelation has been proposed as a strategy for enabling the dissolution of CHT, for example, in alkali-urea aqueous solution at low temperature [99]. In this system, the gelation effect is driven by the interaction between amine and hydroxyl groups of the polymer with hydroxide ions in solution, which become very competitive in the formation of hydrogen bonds. The newly established equilibrium between intra-/intermolecular hydrogen bonds and hydroxide ions is driven in favor of hydroxide ions in a basic environment, leading to the solubilization of CHT. Urea acts as both hydrogen-bonding acceptor and hydrogen-bonding donor, contributing to the establishment of a new equilibrium where intra-/intermolecular interactions among CHT chains are unfavored. Besides aqueous alkali-urea solutions, other alkali aqueous solvents were proposed for the solubilization of CHT, namely LiOH, NaOH, KOH [100].

The dissolution of CHT in organic solvents (i.e., DMF, pyridine, DMSO, dichloromethane, chloroform, or acetone) may be achieved through its derivatization into suitable derivatives [101]; fatty acid side groups were introduced onto the CHT backbone for shifting its wettability from hydrophilic to hydrophobic and even superhydrophobic, towards the development of sustainable coatings [102,103].

Besides solubility, the rheological, surface tension [45,104], adhesiveness [105,106], and self-assembling properties [107,108] can be tuned by CHT derivatization. Hence, the modulation of CHT properties could be achieved by the introduction of new functional groups, thus enabling its use for addressing several applications, including antibacterial [109] and anticancer agents [110], catalysts [111], adsorbents of organic [112] and inorganic pollutants [113], sensors [114], the stationary phase for chromatography [115], surfactants [44,116], and a wide array of biomedical applications [64,117].

All the chemical functionalizations highlighted in Section 2 open up a broad perspective for the development of CHT-based materials and coatings. In a recent paper, Tagliaro et al. [103] fabricated superhydrophobic fluorine-free CHT coatings by the chemical modification of CHT with fatty acid side groups followed by its deposition through a solvent-free method. An optimal balance was also identified to combine hydrophobicity

and transparency (Figure 4a,b), showing good durability in abrasion resistance tests, in water and acidic environments and over adhesion tape tests, although further improvement is required to increase the material adhesiveness to the substrate. This study aims at safe- and sustainable-by-design coatings with enhanced functionalities by replacing fluorinated substances, which raise concerns for their potential hazard on human health [118].

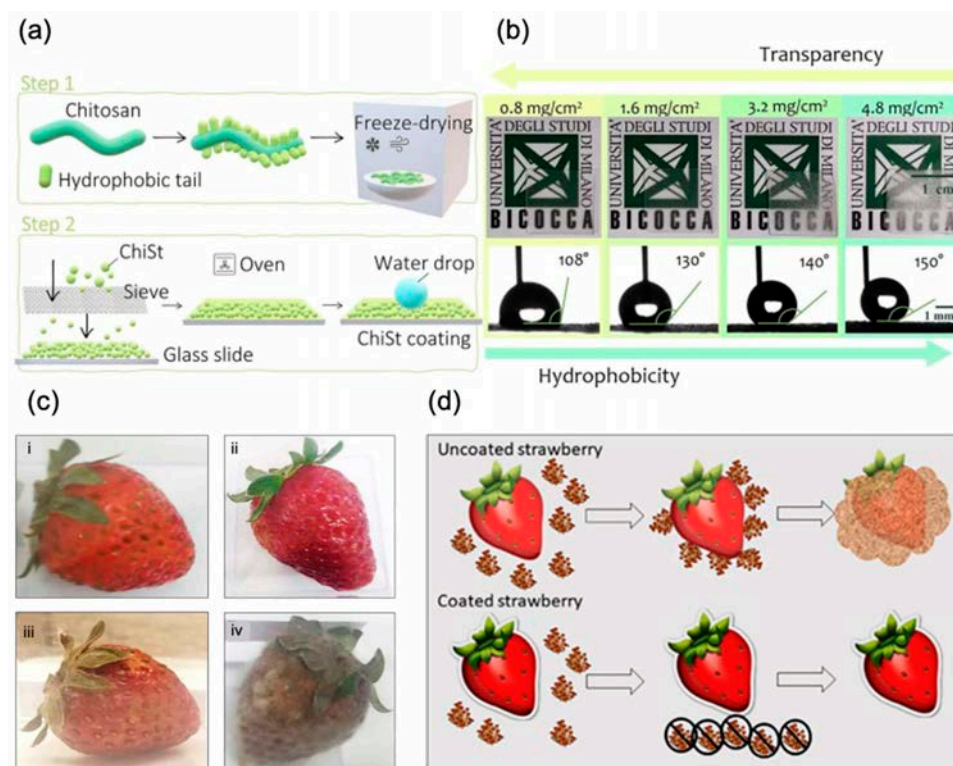


Figure 4. CHT-based coatings. (a) CHT functionalization and solvent-free hydrophobic coating deposition method; (b) contact angle and transparency of modified CHT coatings. (a,b) Reprinted from [103] Copyright (2023), with permission from Elsevier. (c) Study of a CHT-based coating applied on strawberries: (i,iii) coated strawberry before and after 7 days, (ii,iv) uncoated strawberry before and after 7 days. (d) Schematic illustration of the protection process against microorganisms in strawberries. (c,d) Reprinted and adapted with permission from [119] Copyright 2020.

CHT film coatings have also shown to increase the shelf-life of fresh products and slow down fruit decay owing to its antifungal and antimicrobial properties. Edible CHT films have been formulated both as pure CHT films or as blends with other polysaccharides, such as starch or alginate, or with proteins, such as milk and soy proteins, collagen or gelatin [120]. Vu et al. [121] have reported the efficacy of a hydrophobized palmitoyl chloride-functionalized CHT film coating in preventing discoloration and decay of fresh products, potentially doubling their shelf-life. Quintana et al. [122] showed that the addition of licorice root extracts to CHT improved the rheological properties of edible coating, as demonstrated by tests with strawberries. It was shown that the fruits not only maintained good quality parameters during storage but also showed the best microbiological preservation in comparison with controls. As such, film edibility enables the direct application of CHT as a coating for food applications (Figure 4c,d) [119], with the potential of reducing and minimizing packaging-related waste.

Besides the potential use of CHT in the food industry, CHT based-materials may also be useful to control the freezing process (nucleation, ice crystal growth and ice aging) of food for below-freezing storage. In general, polysaccharides are known to be surrounded by a hydration shell, where water molecules foster interactions with the polysaccharide functional groups (hydroxyl, -OH, and amine, -NH₂) [123]. When polysaccharides are cooled down to low temperatures, non-freezable water may be still present [124].

Non-freezable water is a non-crystalline state, which derives from the presence of both free and bound (coordinated) water molecules within the polysaccharide hydration shell (1 to 100 nm). Studies on polysaccharides with low [125] and medium molecular weight (order of 100 kDa) [126] have shown that they can inhibit ice crystal formation and growth due to micro-viscosity, gelation, and hydration. However, more fundamental studies are needed to confirm the potential of CHT to control the freezing process of water and hydrated food.

The possibility to efficiently modify CHT, greatly relying on its solubility in a reaction medium suitable for its chemical modification, renders this biopolymer suitable for multiple applications. In the next sections, insights into the processing of CHT into a wide array of CHT-based materials and devices suitable for biomedical applications are given.

4. Chitosan-Based Hydrogels for Biomedical Applications

Hydrogels based on CHT are gaining considerable interest for biomedical applications due to its biocompatibility, biodegradability, non-toxicity, and biological features, such as bio-adhesiveness, antibacterial, hemostatic, and anti-inflammatory properties. Altogether, these properties are pivotal in the design of biomedical systems for smart drug delivery [127–135], wound healing [136], and regenerative medicine [137].

Hydrogels are composed by hydrophilic macromers able to capture a large amount of water molecules without dissolving [138], suitable for mimicking the extracellular matrix (ECM) of biological tissues. The capacity to absorb water is achieved through the equilibrium between cohesive and osmotic forces, and depends on the chemical nature of the macromers, cross-linking strategies [76] and 3D structure. Since CHT is a linear polymer, cross-linking is usually needed to obtain hydrogels with suitable mechanical properties. Several synthetic strategies were applied to achieve the required functionalities [139]. Cross-linking can be obtained through physical interactions based on ionic and/or electrostatic forces [140,141] or by covalent bonds [142]. Moreover, regardless of the cross-linking approach, CHT-based hydrogels may be obtained as blends with different natural or synthetic macromers.

Following an appropriate cross-linking chemistry, hydrogels can be designed to respond to an external stimulus, such as light [143], temperature [144], pH [145], and electromagnetic field [146], and are usually referred to as smart or responsive hydrogels [147].

4.1. Chitosan-Based Hydrogels by Physical Cross-Linking

Physical cross-linking is based on non-covalent forces, such as ionic bonds, dipole-dipole, ion-dipole, Van der Waals, and hydrophobic and hydrophilic interactions. Physical hydrogels are characterized by weaker mechanical and chemical stability than chemical ones, thus being easily damaged. However, there are applications where the weakness and progressive degradation of the hydrogel is an advantage. This is the case of wound dressing applications, in which it is possible to notice a recurrence of physical hydrogels. The focus on hydrogels for wound dressings is growing since the materials traditionally used, such as gauze and bandage in cotton or wool, have several drawbacks, including low permeation to oxygen, low ability of wound drainage, limited adhesion and being painful and dangerous during removal. Innovative wound dressing materials are designed to address these issues; in this framework, hydrogels offer the advantage of their degradation ability. Additionally, hydrogel properties for damaged tissue regeneration may be improved owing to their ability to act as delivery vehicles of biomolecules for promoting tissue repair (i.e., growth factors, immunomodulators, glycans) [148–150], and limit bacterial infections (i.e., acting as anti-bacterial agents). The wound dressings based on CHT hydrogels are intrinsically biodegradable and antimicrobial [151], rendering them suited for wound healing and tissue regeneration.

Given the polycationic nature of CHT at acidic pH, a straightforward physical cross-linking can be achieved by ionic interactions with negatively charged (macro)molecules. Notably, anionic low molecular weight physical cross-linking agents such as phosphate

and carboxylate functional groups have been explored for the cross-linking of CHT biopolymer (Figure 5).

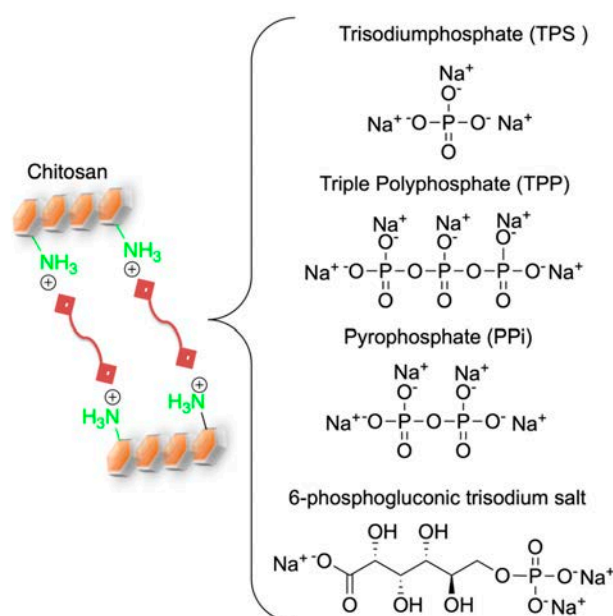


Figure 5. Physical cross-linking of CHT through phosphate and carboxylate functional groups.

CHT-based hydrogels can be obtained with trisodium phosphate (TPS) [152], pyrophosphate (PPi) [153], triple polyphosphate (TPP) [144], or 6-phosphogluconic trisodium salt [154].

In the synthesis of phosphate-based crosslinked hydrogels, the production of a homogeneous 3D matrix represents a major issue. For example, Sacco and co-workers showed that the local quick saturation of binding sites results in the formation of agglomerates, and inhomogeneous chemical and mechanical properties of the hydrogel [155]; however, a controlled diffusion of TPP anions in a CHT solution by means of a semipermeable membrane allows the production of a homogeneous hydrogel with good mechanical properties and non-cytotoxicity. Notably, TPP and PPi impart different properties on the hydrogels, the first one promoting the formation of homogeneous materials, and the second affording inhomogeneous hydrogels [156]. Moreover, the morphological analysis of the hydrogels obtained with TPP (Figure 6b) or PPi (Figure 6c) shows that TPP-crosslinked CHT possesses increased connectivity when compared with that of PPi-crosslinked, as revealed by TEM (Figure 6a). The degradability in physiological conditions, diffusion coefficient and drug release behavior reflect the different connectivity and homogeneity features of the systems [153].

6-Phosphogluconic trisodium salt was proposed for the first time as an anionic crosslinker by Martínez-Martínez et al. [154]. This low molecular weight heterobifunctional dianion can be obtained from 6-phosphogluconic acid, an intermediate in the pentose phosphate pathway involving the degradation of glucose. The obtained hydrogel is stable at neutral pH and degrades at pH below 4.5. The swelling properties, and loading and release kinetics can be tuned as a function of the amount of crosslinking agent, affording interesting features for tissue regeneration in wound healing applications.

Thermoresponsive CHT-based hydrogels can be obtained owing to polyols monophosphates [157], such as β -glycerol phosphate [158,159], glucose 1-phosphate [160] or 6-phosphate [157]. The gelation mechanism is not based on cross-linking interactions among amino and phosphate groups as observed for dianions, but instead by the modulation of hydrogen bonding networks among the polysaccharide, polyol moieties and water molecules [157].

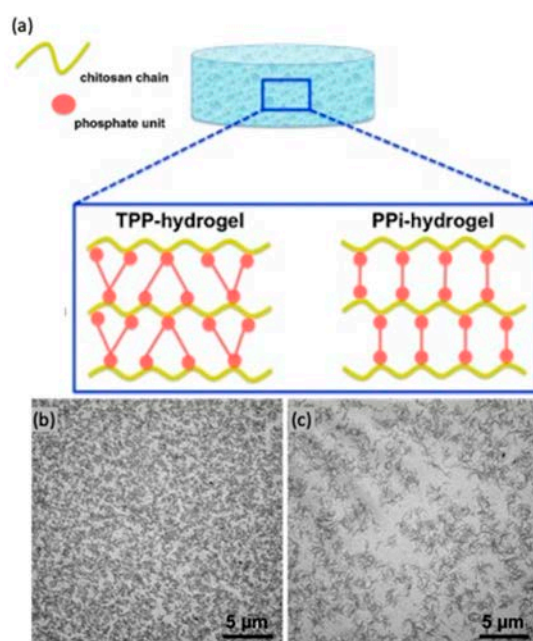


Figure 6. (a) Schematic representation of hydrogel junctions between CHT and either TPP or PPI produced by electrostatic interactions. TEM analysis with contrast of (b) TPP and (c) PPI shows differences in the homogeneity of the network. Reprinted from [156]. Copyright (2016), with permission from Elsevier.

An injectable pH-sensitive hydrogel based on carboxymethyl CHT and oligomeric procyanidin was also proposed [161]. Oligomeric procyanidins are natural flavonoids obtained from grape seeds, showing antitumor and antibacterial activity, able to act as a dynamic cross-linker through hydrogen bonding (Figure 7).

R = H, CH₂COOH: Carboxymethyl Chitosan

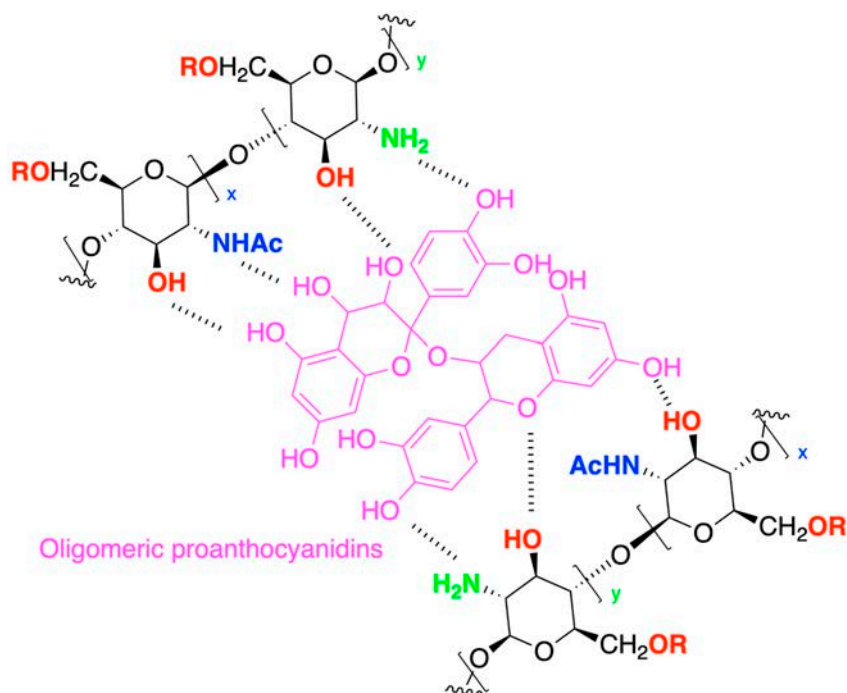


Figure 7. Cross-linking between carboxymethyl chitosan and oligomeric proanthocyanidins (hydrogen bonding interactions are highlighted).

The resulting hydrogel showed antibacterial, adhesive, self-healing, and injectable properties, being useful in regenerative medicine applications (Figure 8).

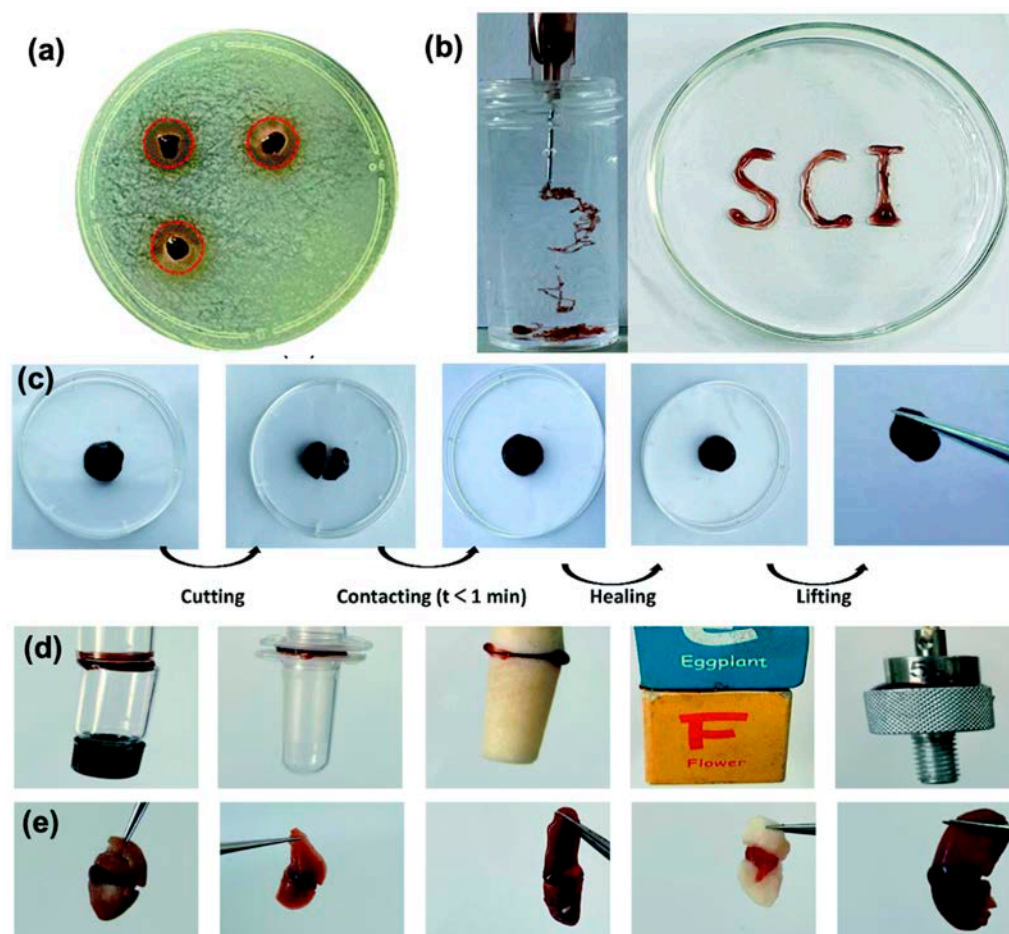


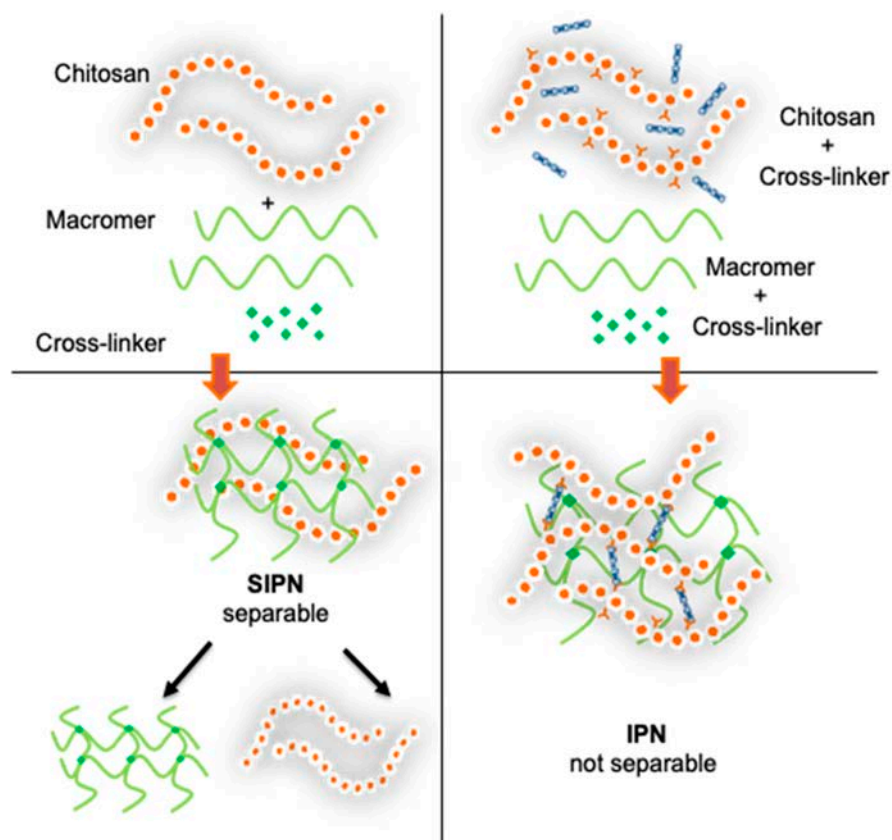
Figure 8. Carboxymethyl CHT cross-linked with oligomeric proanthocyanidins shows (a) anti-bacterial activity visualized as an inhibition zone against *E. coli*; (b) injectable properties; (c) self-healing ability; (d) adhesive properties to diverse materials, from left to right: glass, wood, plastic, rubber, iron; (e) adhesive properties to biological tissues, from left to right: heart, liver, spleen, lung, kidney. Reproduced and adapted with permission from [161] © The Royal Society of Chemistry 2022 under a Creative Commons Attribution-Non Commercial 3.0 Unported Licence.

Besides the use of small molecules for physical cross-linking, macromers such as anionic polysaccharides or proteins can also be used. Those include alginate [162], pectin [163], xanthan [164], or hyaluronan [165]. However, the inhomogeneity of the resulting hydrogels is still an issue; advancements towards improving the homogeneous distribution of electrostatic forces have been achieved through acidification of the mixture in the vapor phase, for example by resorting to CHT and pectin [166]. CHT-pectin hydrogels were optimized for 3D-printed scaffold production for regenerative medicine [167].

Proteins such as collagen and its hydrolyzed product gelatin [168] and elastin [169] have been blended with CHT for hydrogel production since they are particularly suited for tissue regeneration, fulfilling two fundamental requisites: favorable interactions with cells (i.e., adhesion) and cytocompatibility [170]. However, proteins do not have a polyanionic character as featured by some polysaccharides, and different non-covalent interactions are brought into play in the hydrogel formation, resulting in limited mechanical properties and stability. Chemical cross-linking is then the most suitable strategy to obtain stable CHT-protein hydrogels.

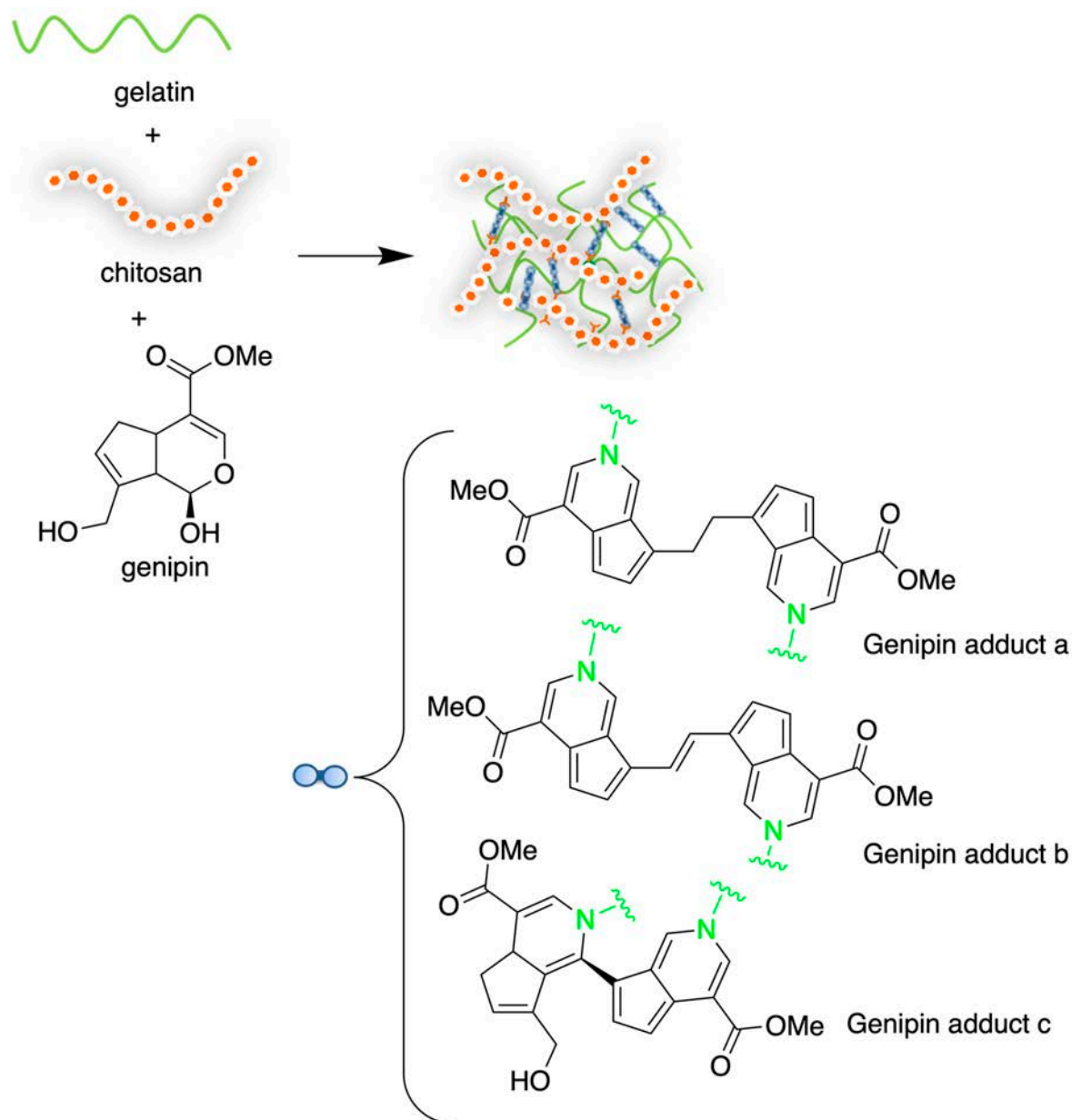
Physical cross-linked hydrogels may comprise a blend of CHT and other natural macromers. However, synthetic macromers have also been used [140]. Synthetic macromers offer several advantages, including better control over chemical structure and composition, improvement and tailoring of the mechanical properties, and stability against chemical or metabolic degradation. The chemical nature/functionality of the macromers influences the interactions with biological systems. Cell adhesion is hampered by highly hydrophobic materials with low surface energy, that are unable to establish interactions with cell membrane proteins [171]. Likewise, extremely hydrophilic materials are highly hydrated inhibiting cell adhesion [172].

Synthetic macromers are particularly attractive to address the limitations of low stability and mechanical properties through CHT-based interpenetrating (IPN) and semi-interpenetrating (SIPN) polymer networks. In IPN and SIPN, the hydrogels are still based on non-covalent interactions. However, increased network stability is achieved through macromer interpenetration. Usually, at least a synthetic polymer is needed to achieve the molecular entanglement. IPNs are defined by IUPAC as “polymers comprising two or more networks that are at least partially interlaced on a molecular scale but not covalently bonded to each other and cannot be separated unless chemical bonds are broken (Note: a mixture of two or more preformed polymer networks is not an IPN), while semi-interpenetrating polymer networks (SIPNs) are “polymers comprising one or more polymer networks and one or more linear or branched polymers characterized by the penetration on a molecular scale of at least one of the networks by at least some of the linear or branched macromolecules” (Note: an SIPN is distinguished from an IPN because the constituent linear or branched macromolecules can, in principle, be separated from the constituent polymer network(s) without breaking chemical bonds; it is a polymer blend) [173]. Several synthetic strategies can be used, mainly based on sequential or simultaneous approaches (Scheme 7).



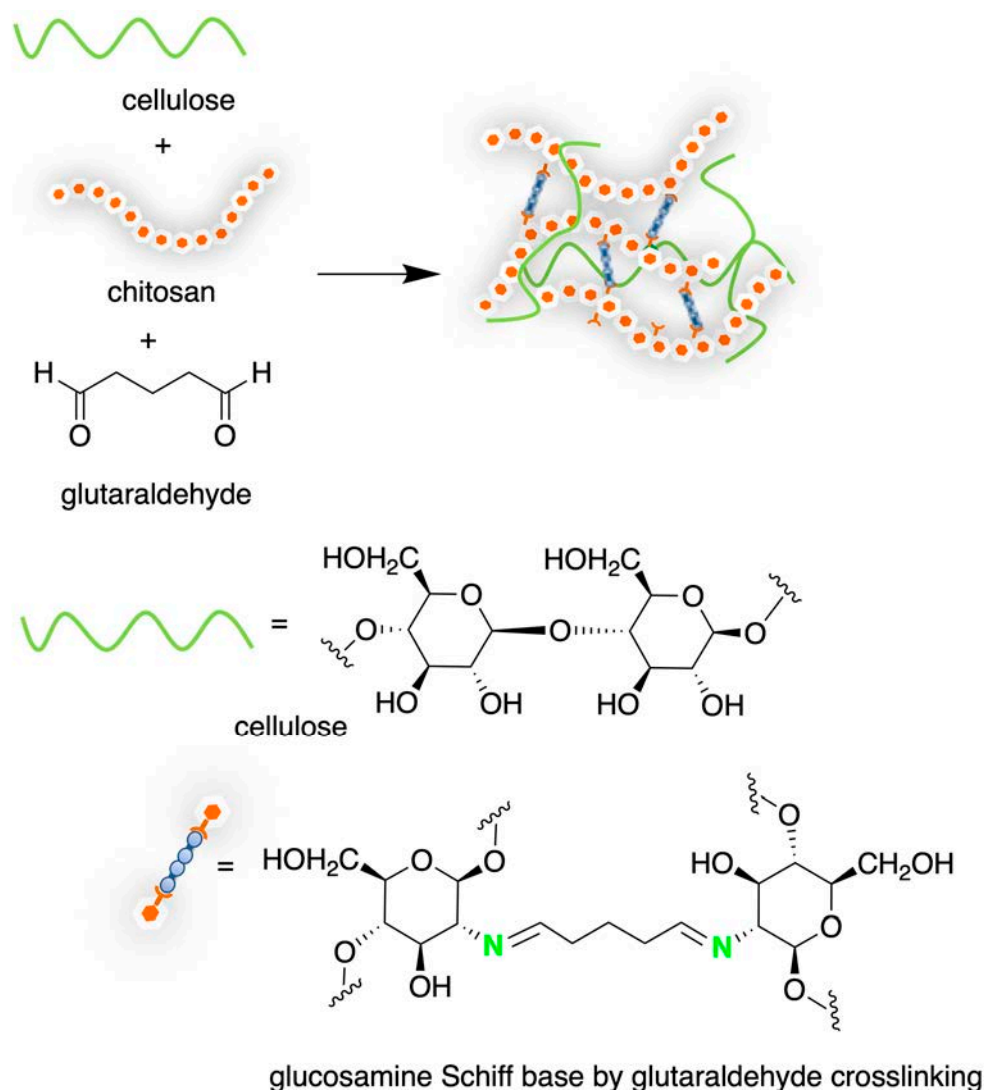
Scheme 7. Interpenetrating and semi-interpenetrating CHT-based networks obtained by a simultaneous approach.

For example, CHT-based IPN based on the simultaneous cross-linking of CHT and gelatin by the natural cross-linker genipin were proposed (Scheme 8) [174]. Genipin, a compound extracted from the *Gardenia jasminoides*, reacts in a complex multistep sequence with the primary amines of CHT and amino acid sidechains in gelatin, affording different adducts (Scheme 8). The resulting hydrogel possesses pH-responsiveness, useful for controlled drug release in biomedical applications.



Scheme 8. Interpenetrating networks obtained by genipin cross-linking of gelatin and CHT.

CHT-based SIPNs have also been proposed, showing improved mechanical and biological properties. For example, CHT was cross-linked with glutaraldehyde in the presence of bacterial cellulose (Scheme 9) [175]. The resulting hydrogel showed promising thermal stability, mechanical resistance and flexibility. The modulation of the amount of cellulose with respect to the CHT allowed finetuning of the elastic modulus: the higher the cellulose percentage, the lower the elastic modulus. Additionally, the CHT content modulates the antibacterial properties of the final hydrogel: the higher the chitosan percentage with respect to cellulose, the better the antibacterial activity.



Scheme 9. Semi-interpenetrating polymer networks based on CHT and bacterial cellulose, by chitosan cross-linking mediated by glutaraldehyde.

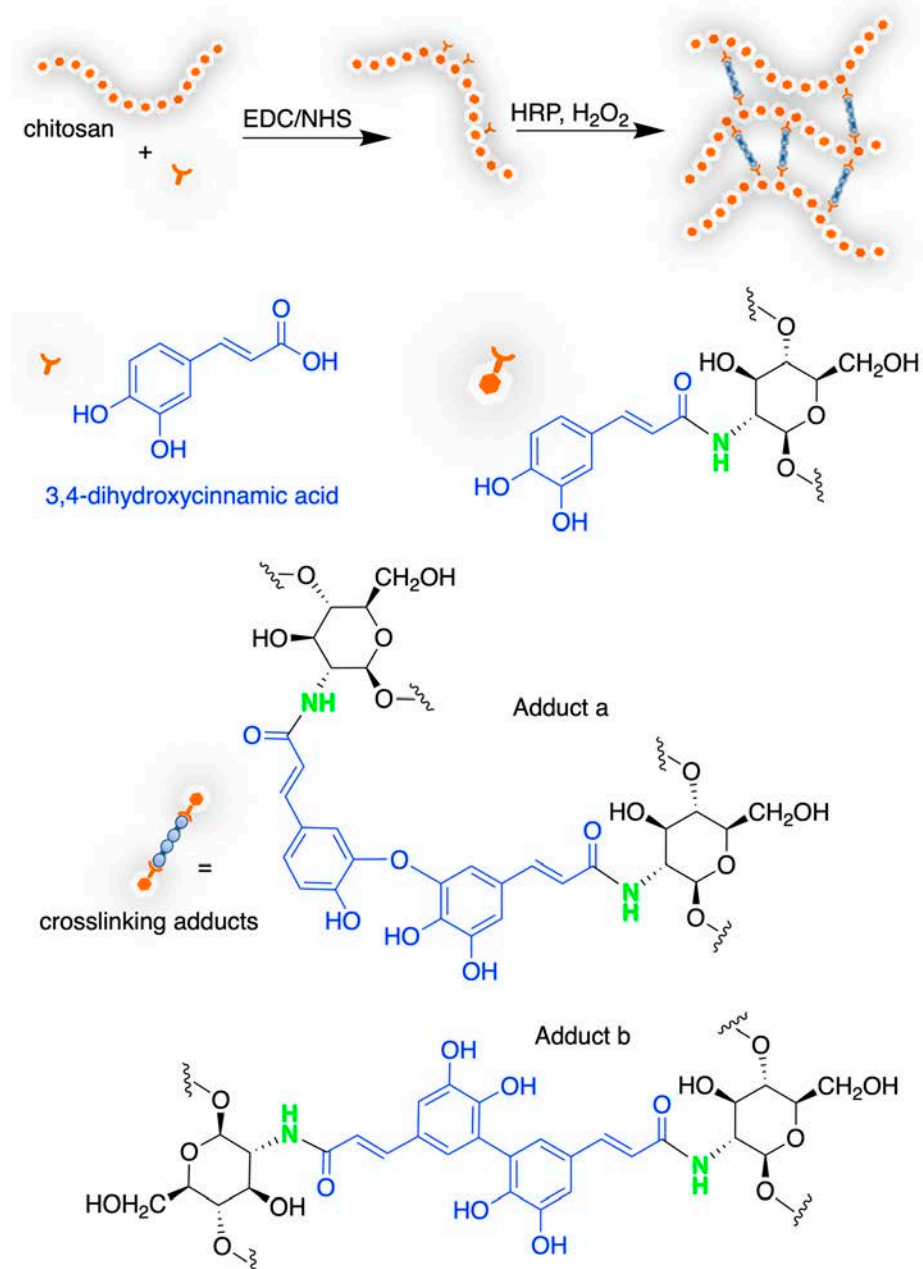
SIPN also have wide application in ex situ cell culture, as in the case of polymethacryloyl glycyglycine (poly-MAGG) cross-linked by radical polymerization with ethylene glycol dimethacrylate (EGDMA) in the presence of CHT [176], being promising for tissue engineering and controlled drug delivery applications.

4.2. Chitosan-Based Hydrogels by Chemical Crosslinking

Chemical cross-linking creates stable covalent bonds within macromers, imparting them with higher chemical, biochemical and mechanical stability. However, these features may cause reduced biodegradation and toxicity issues. In fact, the toxicity of the reagents and byproducts is frequently underscored, especially due to the intrinsic inability to wash them out of a gelled matrix [177]. Moreover, as detailed in previous sections, the CHT physicochemical features contribute to amplify the obstacles of chemical cross-linking. Glutaraldehyde [178], genipin [179], and long-chain cross-linkers with suitable reactivity, such as the polyethylene glycol (PEG) diacid [180] have been widely used as agents for enabling the cross-linking of CHT amino groups. In this case, the CHT-PEG cross-linking mechanism is attempted by reacting the glycol diacid with CHT via carbodiimide coupling chemistry. The resulting hydrogel denoted self-healing ability and enabled drug delivery for treating harmful chronic ulcers. The reticulation with a long chain cross-linker is

enforced by the dynamic intermolecular interactions due to hydrogen donors and acceptor atoms (nitrogen and oxygen) present in the system.

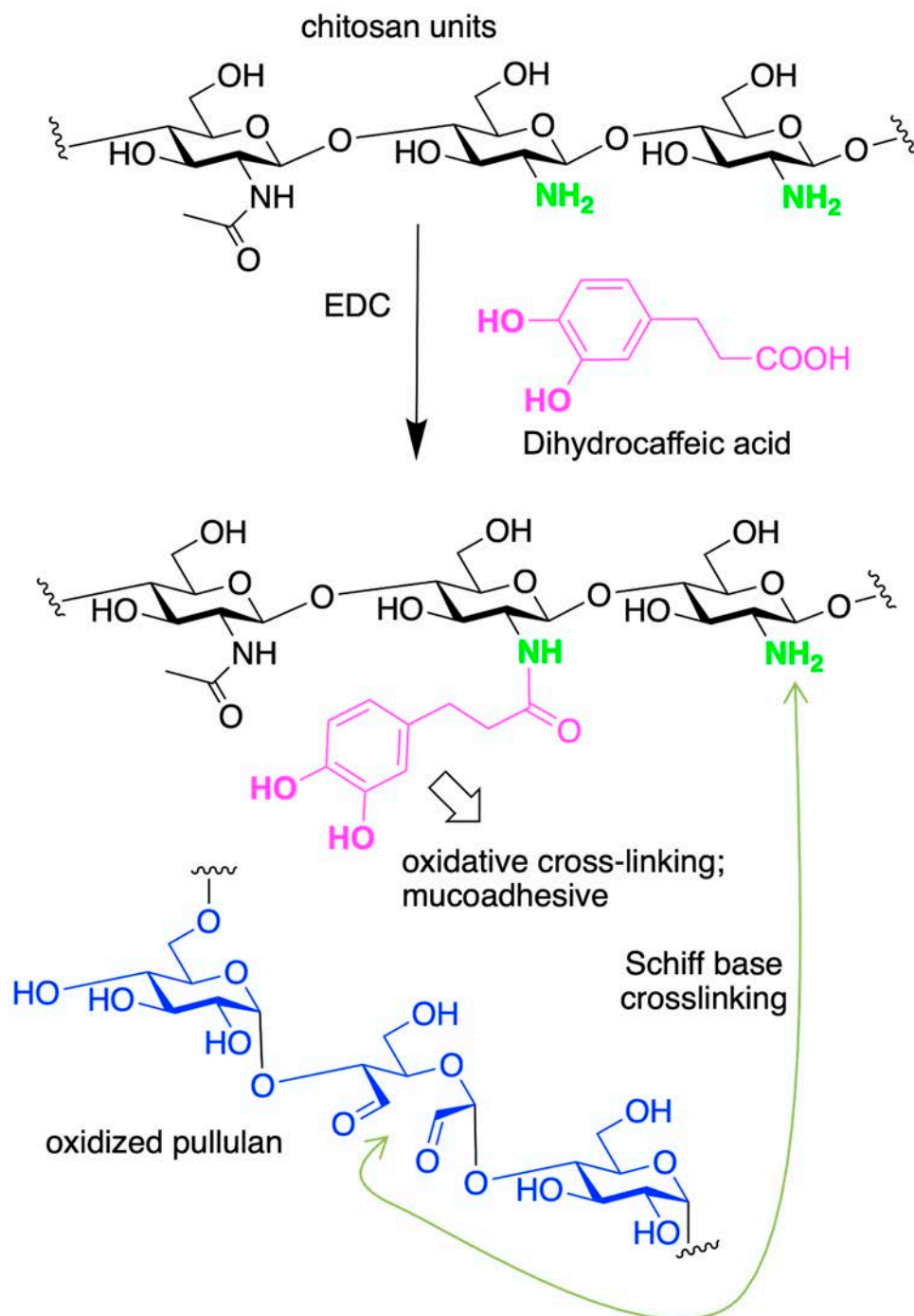
Considering the risk of byproduct toxicity, emerging cross-linking strategies involve enzymatic reactions [181]. Siqi Zhou et al. [182] reported on the functionalization of CHT with 3,4-dihydroxyhydrocinnamic acid, followed by oxidative cross-linking through horseradish peroxidase/hydrogen peroxide (HRP/H₂O₂) (Scheme 10).



Scheme 10. CHT cross-linking mechanism through enzymatic oxidation of cinnamic acid moieties.

The obtained hydrogel was studied for its ability to regenerate cartilage tissue. Bone-derived mesenchymal stem cells (BMSC) laden-hydrogel was able to induce chondrogenic differentiation and hyaline cartilage production *in vivo*, being a promising scaffold for cartilage tissue repair. The repair of articular cartilage tissue is not trivial owing to the lack of a natural regenerative mechanism. The most commonly used approach is usually based on the isolation of autologous chondrocytes or stem cells seeded in 3D scaffolds. Moreover, several studies identified CHT as a suitable biopolymer for cartilage tissue regeneration [183].

CHT has been used for the design of pH-responsive injectable hydrogels loaded with doxorubicin for chemotherapy against colon cancer, and with the antibiotic amoxicillin against *E. coli* and *S. aureus* [184]. In order to obtain a pH-responsive hydrogel, dihydrocaffeic acid moieties have been grafted to CHT through the carbodiimide chemistry to obtain a suitable hydrogel for drug delivery. The CHT-caffeic acid macromers were cross-linked with oxidized pullulan (a polysaccharide constituted by α -1,6-maltotriose repeating units) by Schiff base reaction (Scheme 11).

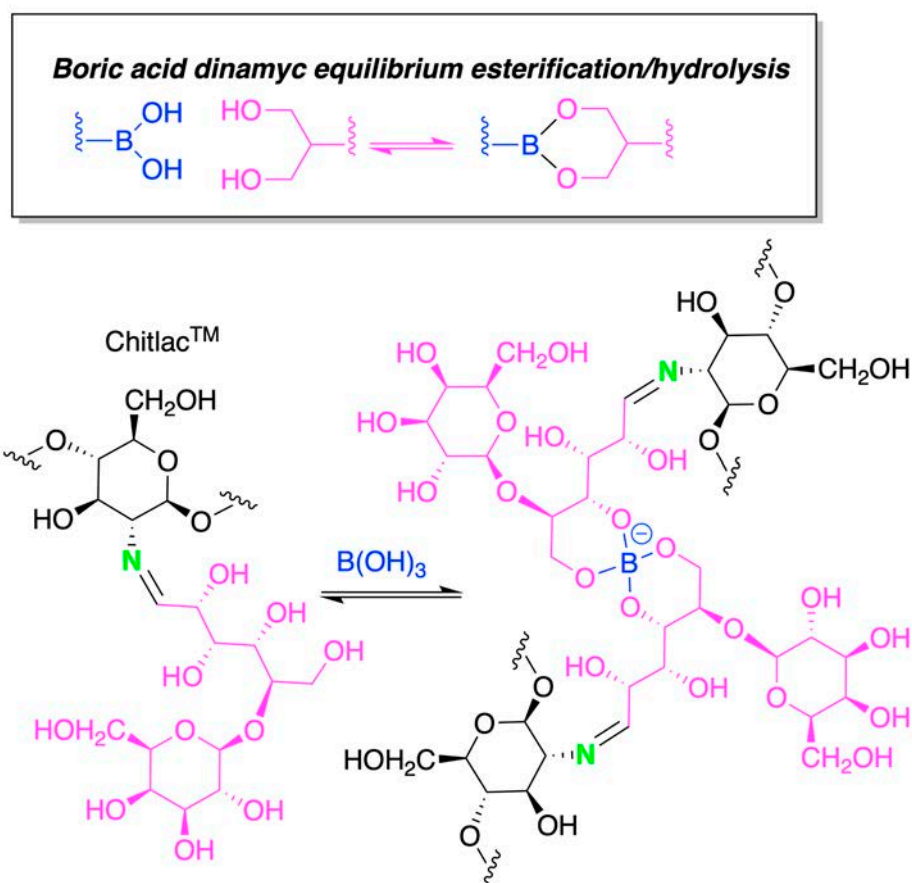


Scheme 11. pH-responsive hydrogels based on CHT and pullulan.

The grafting with dihydrocaffeic acid has multiple purposes: improved adhesion to mucus membranes, higher solubility of CHT and pH responsiveness due to the oxidative cross-linking of the catechol moieties promoted by a pH switch from acidic to physiological

media [185]. Pullulan showed to significantly improve the mucoadhesive properties when compared with the pullulan-free CHT-dihydrocaffeic acid system.

A key issue in regenerative medicine is the design of scaffolds promoting and sustaining cell adhesion, growth and differentiation, mimicking as much as possible the native ECM composition, structure, and biochemical and biomechanical stimuli. Donati et al. proposed a mechano-responsive hydrogel based on commercially available Chitlac[®] [186], obtained from CHT by reductive *N*-alkylation with the reducing end of lactose. Chitlac[®] was cross-linked with boric acid in different concentrations (Scheme 12).



Scheme 12. pH-responsive hydrogels based on Chitlac[®] and boric acid/ester dynamic chemistry (the lactose moieties are highlighted in pink).

The resulting hydrogels (Figure 9) showed increased viscosity upon thermal or mechanical energy application, due to a rearrangement of the molecular network induced by the boric acid [187]. The dynamic boric ester crosslinks generate a nonequilibrium status where anchoring points are continuously created and destroyed, as a consequence of the adaptation to stress variation [188].

Dynamic chemical bonds, such as imine formation/hydrolysis, accompanied by structural elements favoring hydrophobic intermolecular interactions (i.e., aryl moieties) are the basis for the preparation of thermoresponsive CHT-based hydrogels through a combination of physical and chemical cross-linking. In this regard, natural aldehydes [189] such as vanillin [190], salicylic aldehyde [191] and cinnamaldehyde [192] were proposed (Figure 10).

The choice of a proper aldehyde determines the self-assembling behavior of the system [193].

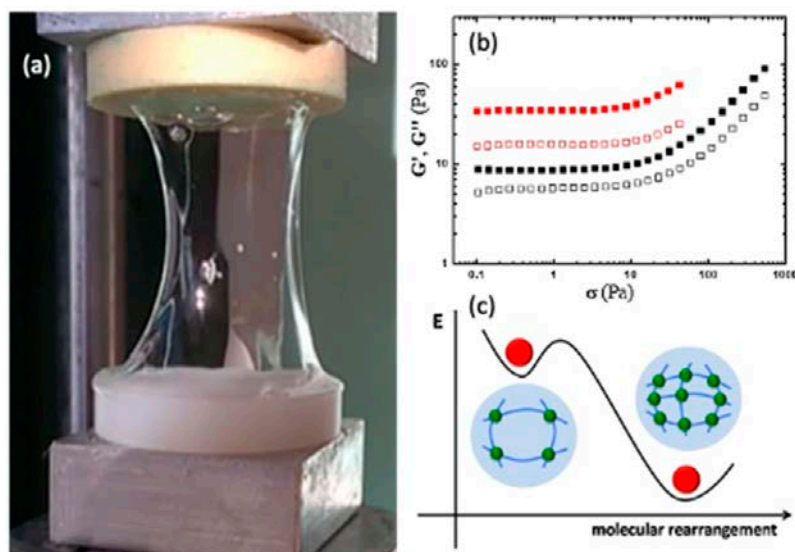


Figure 9. (a) Chitlac/boric acid active network shows strain-hardening features. (b) Dependence of G' (filled symbols) and G'' (open symbols) on stress for Chitlac/boric acid prior to (black) and after (red) continuous oscillatory shear. (c) Scheme of network rearrangement upon application of energy. Reprinted from [187]. Copyright (2019), with permission from Elsevier.

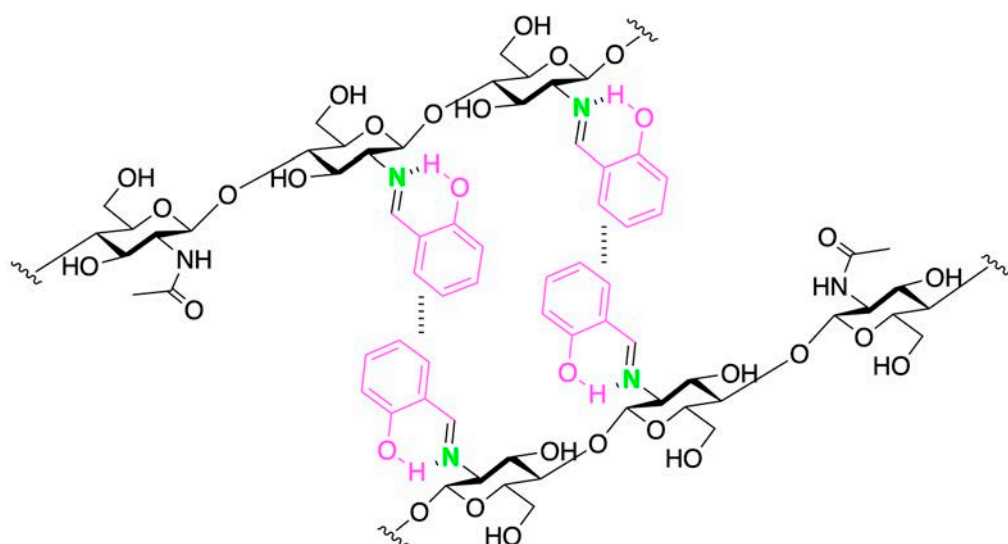
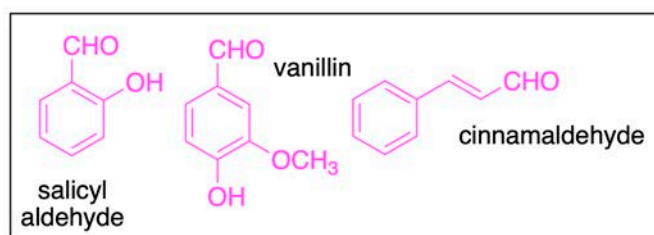


Figure 10. Physical and chemical cross-linking exemplified for the salicylic aldehyde/CHT system.

5. Chitosan-Based Organic–Inorganic Hybrids for Biomedical Applications

Based on the IUPAC definition, a hybrid material is a “material composed of an intimate mixture of inorganic components, organic components or both types of components, where the components usually interpenetrate on scales of less than $1 \mu\text{m}$ ” [173]. This definition embraces organic-inorganic hybrids containing at least one inorganic component and one organic component with an interpenetrating structure on the sub-micrometric scale. Due to

their dual composition, organic–inorganic hybrids display unique properties, offering interesting opportunities in several applications [194], including in regenerative medicine [195]. The interpenetrating network formed by the organic and inorganic matrices allows finely tuning the mechanical and biological properties, combining the high mechanical properties typical of the inorganic components, with the elasticity [196], and possibly biocompatibility and bioactivity of the organic components [197–200]. Additionally, a suitable hybrid formulation allows obtaining organic–inorganic hydrogels, monoliths, bulk materials and 3D printable inks [196].

The organic–inorganic hybrids can be further divided into two classes referred to as class I and II. In class I, the interconnected network is based on weak intermolecular forces, such as Van der Waals, hydrogen bonds, ionic and electrostatic interactions. The class II hybrids are featured with stable covalent bonds between the organic and inorganic phases. Obviously, in class II hybrids coexistence of covalent and non-covalent interactions is possible. The exploitation of CHT as the organic component is particularly attractive [201] due to its biocompatibility, biodegradability, low toxicity and biological properties, as previously highlighted. At the same time, silica and hydroxyapatites are very appealing inorganic phases to be used in hybrid synthesis for regenerative medicine, especially for bone tissue repair. Both hydroxyapatite, the native bone mineral phase, and silica are pivotal to improve the mechanical properties of the final material, besides being osteoinductive and biocompatible.

5.1. Class I Chitosan-Based Hybrids

As in the case of hydrogel design, the polycationic nature of CHT at acidic pH, or after stable *N*-peralkylation, offers an easy way to form interpenetrating organic–inorganic hybrids with anionic counterparts. A robust network produced by ionic interactions between the protonated amino groups of CHT and hydroxysilicate anions was obtained by a sol-gel process, performed in acidic conditions, by mixing CHT and hydrolyzed tetraethoxysilane (TEOS) solutions [202]. The role of pH and the acidic nature was investigated. It was found that hybrid materials with better mechanical properties could be obtained in mild acidic conditions (pH 4) in the presence of acetic acid. The modulation of the silica/CHT ratio also allowed tuning the mechanical properties: the higher the CHT content, the lower the rigidity of the resulting scaffold. The bioactivity was investigated in terms of bone-like hydroxyapatite deposition on the scaffold surface. Notably, scaffolds with CHT content higher than 50% did not trigger the formation of hydroxyapatite, thus limiting the osteoinduction properties of the silica phase.

Hydroxyapatite scaffolds can be prepared with suitable porosity and morphology. However, their mechanical properties lack the characteristic elasticity of human bone tissue. Additionally, to improve the osteogenic potential of the scaffolds, bioactive factors such as bone morphogenetic proteins are often included [203,204]. However, the biological macromolecules are often expensive, thus limiting clinical applications. To circumvent these limitations, hybrids with an organic component have been proposed: class I hybrids were prepared using CHT and hydroxyapatite doped with therapeutic metal ions, including copper (II) and strontium [205], as a low-cost and effective alternative to osteogenic macromolecules [206]. Strontium was considered due to its ability to promote osteogenesis and bone remodeling, while copper promotes angiogenesis and denotes antibacterial activity. Preliminary *in vitro* biological evaluation of MG-63 human osteoblast-like cell viability highlighted promising features of these hybrids for bone tissue regeneration (Figure 11). However, further studies are needed to prove their potential.

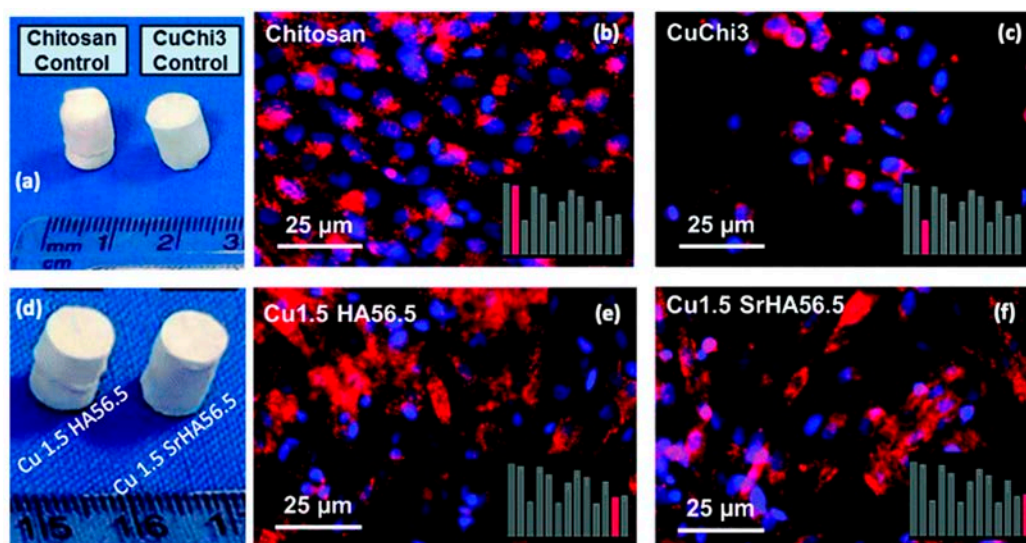


Figure 11. (a) Plain CHT and 3% Cu(II)-containing CHT scaffolds used as controls; Fluorescence images of MG-63 osteoblasts in indirect culture stained with DiI and DAPI (the bottom right panels highlight the respective cell viability measurement of each sample) with (b) plain chitosan and (c) 3% Cu-containing CHT; (d) 1.5% Cu-containing CHT scaffolds with 56.5% HA (Cu 1.5 HA56.5) and 1.5% Cu-containing CHT scaffolds with 56.5% HA and 3% Sr (Cu 1.5 SrHA56.5); fluorescence images of MG-63 osteoblasts in indirect culture stained with DiI and DAPI (the bottom right panels highlight the respective cell viability measurement of each sample) with (e) Cu 1.5 HA56.5 and (f) Cu 1.5 SrHA56.5. Cell viability on Cu-containing chitosan is lower than in scaffolds containing CHT-HA and CHT-HA-Sr. Reprinted and adapted from [205]. © The Royal Society of Chemistry 2019 under a Creative Commons Attribution 3.0 Unported Licence.

5.2. Class II Chitosan-Based Hybrids

Covalent bonds between the organic and inorganic phases in class II hybrids bring similar advantages when compared to physical interactions, as previously reported for hydrogels. In class II hybrid synthesis, the covalent bonds are commonly obtained by means of suitable cross-linking agents, possessing both a reactive moiety towards the inorganic component, and one with complementary reactivity to the organic (macro)molecule [207]. Within this framework, functional organosilanes, such as 3-glycidoxy propyl trimethoxysilane (GPTMS) [208,209] and aminopropyl triethoxysilane (APTES) have been widely used as cross-linking agents. For example, GPTMS has been used for the synthesis of hybrid scaffold with oriented structures through the sol-gel methodology, followed by a unidirectional freeze-casting step, affording a highly ordered lamellar pore structure (Figure 12a–c). The covalent bond between the inorganic silica network and organic CHT phase was obtained by the nucleophilic attack of the CHT amino group on the epoxide of the GPTMS moiety (Scheme 13), followed by silica network formation.

However, the conjugation of CHT to GPTMS has been reported to occur in very low yields due to the competing water nucleophilic attack, leading to the opening of the epoxide to the corresponding diol. However, the CHT-silane conjugate enabled obtaining covalent hybrids, and their biomechanical properties could be tuned by varying the ratio of organic/inorganic components. In particular, when the organic component was the major component (60%), the resulting scaffolds showed flexible and elastomeric behavior perpendicular to the freezing direction, while having elastic-brittle features parallel to the freezing direction (Figure 12) [210]. This anisotropic mechanical response, which is intrinsically dependent on the direction of stress, is similar to what occurs in cartilage, where the orientation of collagen fibrils depends on the articulation zone.

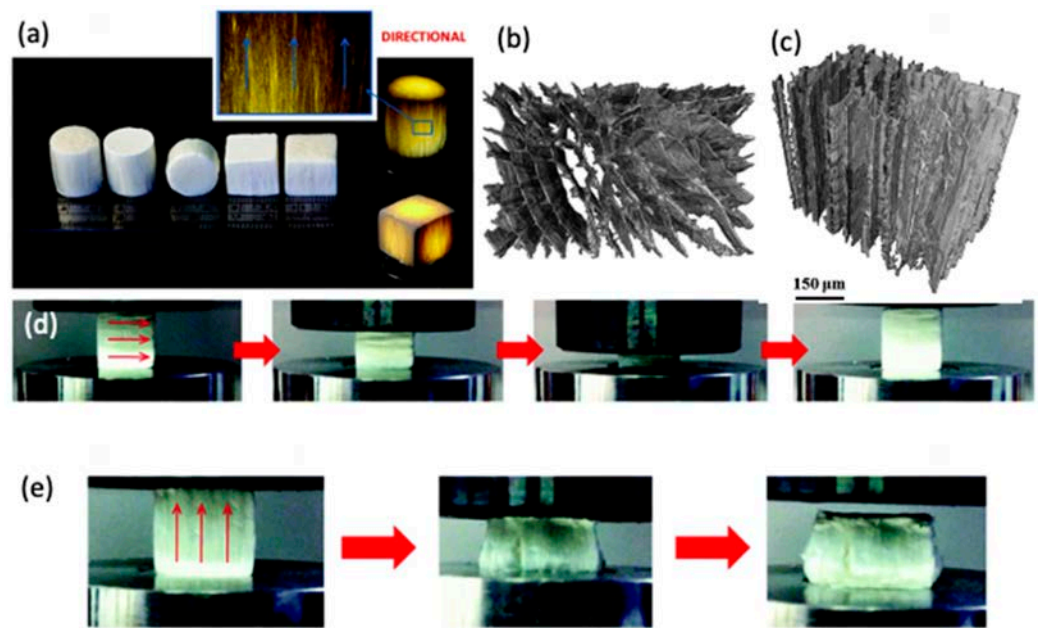
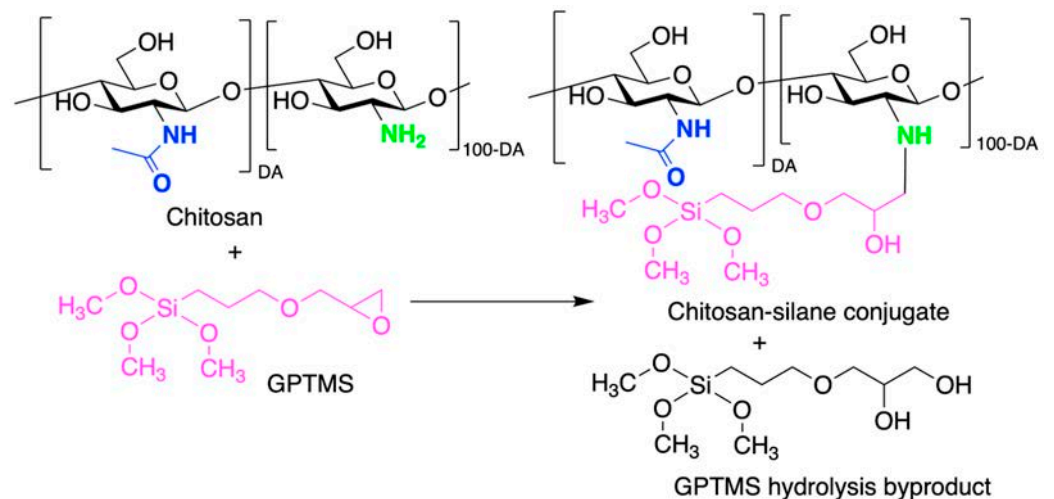


Figure 12. (a) Freeze cast silica/CHT hybrid scaffolds. (b) X-ray micro-computed tomography (μ CT) images of the freeze cast 60 wt% organic hybrid scaffold showing the typical microstructures perpendicular and (c) parallel to the freezing direction. (d) Compression behavior of the freeze cast 60 wt% organic hybrid scaffolds perpendicular to the freezing direction, showing the highly elastic behavior, and (e) parallel to the freezing direction, showing the rupture formation and failure to recover after the compression. The arrows on the sample indicate the freezing direction. Reprinted from [210]. © The Royal Society of Chemistry 2015 under a Creative Commons Attribution 3.0 Unported Licence.



Scheme 13. GPTMS-CHT conjugate for the synthesis of class II hybrids.

Sol-gel chemistry is usually based on tetraethoxysilane (TEOS) as the precursor for the inorganic phase, which upon condensation releases ethanol as the reaction by-product, that is a cytotoxic compound that inhibits cell growth and proliferation. The less toxic glycerol-modified silane precursor was proposed for the synthesis of novel CHT-containing class II hybrids, denoting a hydrogel behavior [211]. As in the previous example, the cross-linker was GPTMS; however, a mixture of CHT and a thiolated-CHT was used in the conjugation reaction. In preliminary biological assays, the hybrids showed to be cytocompatible, and revealed antibacterial activity and suitable drug delivery properties.

6. Chitosan-Based Layer-by-Layer Assemblies for Biomedical Applications

The layer-by-layer (LbL) assembly technology is an easier, cost-effective and highly versatile bottom-up methodology to readily and conformally coat surfaces and develop a wide array of multilayered devices with finely tuned properties and functions at the nanoscale. The technology simply relies on the sequential adsorption of at least two distinct building blocks exhibiting complementary intermolecular interactions on virtually any type of surface, leading to a diverse set of multilayered structures [212].

Dating back to the early works by Iler on the dip-assisted LbL assembly of oppositely charged colloidal particles on flat glass substrates in 1966 [213], and Decher and Hong on either oppositely charged bipolar amphiphiles [214] or polyelectrolyte multilayers [215], and combinations thereof [216] on charged planar surfaces in the early 1990s, the electrostatic interaction between oppositely charged materials is still the most employed build-up mechanism of multilayered assemblies. Moreover, although the dipping methodology has been by far the most used methodology owing to its feasibility in coating substrates of any size, shape or surface chemistry, the need for a large amount of materials and its time-consuming process turned attention to other processing methodologies, including the commonly employed spin-coating and spraying [217–219]. However, over the last two decades other fabrication methodologies have emerged such as fluidic- and electromagnetic-driven assembly [218], high-gravity field- and inkjet printing-assisted assembly [220–224], and LbL assembly on particles [225,226], thus opening new avenues for which the technology can be applicable [218].

The fact that the LbL assembly process can be performed under mild conditions in entirely aqueous solutions enables assembling biological molecules (e.g., proteins, enzymes, polysaccharides) and cells, preserving their biological activity, thus being highly advantageous in addressing biomedical and biotechnological applications [227–235]. However, the versatility imparted by the LbL assembly technology expands well-beyond the use of biological molecules to enable the adsorption of a wide array of constituents (e.g., nanoparticles, synthetic polymers, clays, carbon nanotubes, dyes, metal oxides) on virtually any type of substrate, regardless of size, shape, surface chemistry, and even animate or inanimate nature towards shaping multifunctional multilayered devices across multiple scale lengths [236].

Herein, we emphasize the combination of chitosan biopolymer with either other natural or synthetic ingredients to shape a wide array of LbL structures, including nanostructured multilayered thin films and thicker free-standing membranes, multilayered particles, hollow capsules and (multi)compartmentalized systems, hollow tubes, scaffolds/constructs, and animate living cell surfaces for addressing biomedical applications.

6.1. Multilayered Thin Films and Free-Standing Multilayered Membranes

Since its early-stage development, the LbL assembly technology has been widely applied to coat a wide variety of 2D flat hydrophilic and hydrophobic non-patterned substrates, ranging from glass, quartz, polystyrene, silicon wafer, and gold to produce 2D nanostructured multilayered thin coatings for biomedical and biotechnological applications. Although tightly bound to the underlying substrate, chitosan-derived nanostructured multilayered thin films have revealed to be very appealing nanocoatings for the loading, protection, transport, and on-demand controlled release of cargo, ranging from small molecules to large macromolecules, as well as to control cell functions. For instance, positively charged chitosan was combined with oppositely charged alginate (ALG) into spray-assisted ALG/CHT wholly marine polysaccharide-derived multilayered coatings on polyethyleneimine(PEI)-functionalized glass substrate for the loading and controlled release of tamoxifen (TMX), a well-known breast cancer drug [237]. It was shown that the release profile of the drug physically adsorbed onto the PEI/(ALG/CHT)₅ base layer could be modulated by playing with the number of (CHT/ALG)_n bilayers from 5 to 20, being faster for the nanocoating with the lowest number of bilayers. Moreover, irrespective of the number of bilayers, the TMX-loaded multilayers proved to be efficient therapeutic nanocoatings in reducing the MCF-7 human breast cancer cells viability in vitro, holding potential to

be used as patches for sustained TMX release. Similar biocompatible (ALG/CHT)₅ multilayered thin films were assembled on PEI-coated polystyrene cell culture plates and further cross-linked with genipin (G) towards modulating human umbilical vein endothelial cells' (HUVECs) functions [238]. It was found that the cross-linked nanocoatings enhanced cell adhesion, spreading and proliferation in both normal and serum-free medium when compared with the uncross-linked counterparts owing to their higher stiffness and lower hydration level (Figure 13). Adding to this, the addition of an extra CHT/ALG bilayer over the cross-linked nanofilm reverted the cell adhesion, spreading and proliferation to similar levels as those obtained in the uncross-linked (ALG/CHT)₅ nanofilm, mainly in the case of those cultured in serum-free conditions, thus revealing the key role of the nanocoating stiffness and surface properties in tuning both cell-nanocoating interactions and cell behavior. Quartz has been also widely employed as a template for assembling multilayered nanofilms for sustained drug release and to control cell behavior. For instance, in a recent study four CHT/hyaluronic acid (CHT/HA) bilayers were assembled as base layers into a quartz substrate followed by the adsorption of (CHT/HA-siRNA)_n bilayers ($n = 0-15$ bilayers), as monitored by UV-visible spectroscopy. This study revealed that the multilayers were only effective in enabling the controlled release of siRNA from the nanofilms when assembling up to nine siRNA-loaded bilayers. Furthermore, the siRNA-loaded multilayered thin films promoted good cell adhesion and siRNA silencing effect in enhanced green fluorescent protein (eGFP)-HEK 293T cells, as demonstrated by the decrease in the eGFP expression. These surface-mediated non-viral multilayered nanofilms hold great promise as nanoplatforms for site-specific sustained release of siRNA in mucosal tissues [239]. Besides, silicon wafer, titanium and gold have also been among the most widely used flat substrates for assembling either wholly marine polysaccharide-based or hybrid multilayered nanofilms with tunable physicochemical and biological properties and multifunctionalities for a variety of bioapplications [240–248]. Notably, the limitation imposed by the need for assembling CHT-based multilayered thin films under slightly acidic pH ($\text{pH} < \text{pK}_a \approx 6.2$) has been recently surpassed by the synthesis and further assembly of quaternized CHT (Q-CHT)/heparin multilayers under physiological conditions, holding great promise as nanoreservoirs of proteins to control cell functions under non-denaturing conditions [249]. Such an approach could be virtually translated into the assembly of Q-CHT with any oppositely charged material into multilayer films.

More recently, considerable attention has been devoted to the assembly of chitosan-derived multilayered thin nanofilms onto flat patterned substrates for biomedical purposes owing to the possibility to impart the functional multilayered coatings with topographical features reminiscent of the substrate properties. In this regard, polystyrene superhydrophobic surfaces decorated with patterned wettable regions of tunable size and geometry developed through bench-top approaches were used to build-up arrays of patterned and adhesive LbL films encompassing chitosan and oppositely charged dopamine-functionalized hyaluronic acid (HA-DN), denoting a different number of catechol groups via high-throughput screening (Figure 14a) [250]. The *in vitro* cellular assays and mechanical tests revealed that the multilayered nanofilms having the larger amount of dopamine conjugated to hyaluronic acid (HA-4DN) showcased an enhanced cell adhesion and highest adhesive strength, which increased upon increasing the number of CHT/HA4-DN bilayers (Figure 14b,c).

Although multilayered thin nanofilms cannot be easily detached from the underlying substrate and are not robust enough to be used in practical biomedical applications, they provide important information about the feasibility and growth mode, as well as of the structure and properties of the multilayered films. Such knowledge has been translated into the assembly of robust and thicker free-standing multilayered membranes encompassing a huge number of layers, which are much more prone to be translated into innovative devices to fulfill biomedical purposes. Thicker multilayered films have been widely assembled on either hydrophobic/hydrophilic non-patterned or patterned substrates by resorting to an automatic dipping robot and detached into free-standing multilayered mem-

branes. The chosen type of substrates, namely its topography, dictates the final end-use of the as-produced free-standing membranes whose topography is reminiscent of the substrate's features. Hydrophobic, inert and low surface energy non-patterned polypropylene (PP) substrates have been among the most used templates to produce readily detachable free-standing membranes, since there is no need for either harmful solvents, extreme temperatures or sacrificial layers to detach the assembled multilayered films from the underlying hydrophobic template. In fact, upon reaching a certain number of bilayers, which is dependent on the chosen material's combinations, the as-produced multilayered assemblies can be easily detached into free-standing membranes using solely tweezers. In this regard, chitosan has been combined with a diverse set of oppositely charged natural biopolymers, including ALG, chondroitin sulfate (CS) or hyaluronic acid to produce free-standing membranes with tunable properties and functions that could be applied in numerous biomedical applications [251–253]. For instance, CHT/ALG free-standing membranes were crosslinked with genipin to produce membranes with higher stiffness and better cell adhesion for tissue engineering strategies [253]. Similar CHT/ALG free-standing membranes but with gradients of increasing stiffness were produced by continuously increasing the level of genipin-induced cross-linking of the free-standing membranes along the time upon exposure to a solution with increasing levels of genipin [254]. It was found that the membranes with high cross-linking degree showcased enhanced mechanical properties and better cell adhesion and proliferation when compared with the membranes with low cross-linking degree or even the native ones (Figure 15). Such cross-linked membranes also showed to be suitable reservoirs of biomolecules, including growth factors holding great potential for being used as wound dressing devices [255].

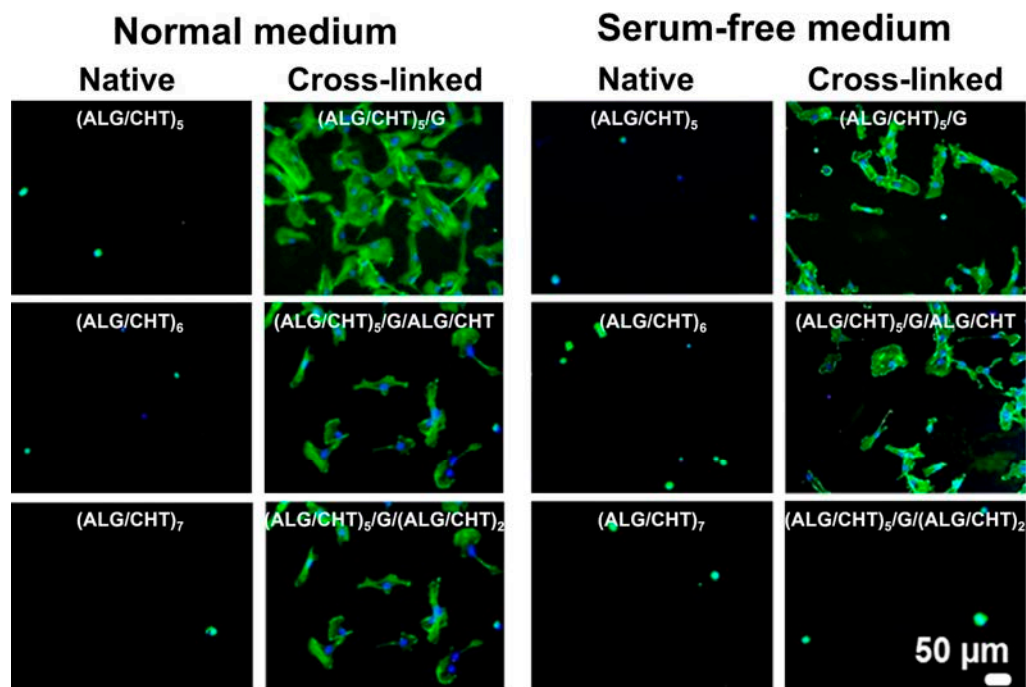


Figure 13. Representative fluorescence microscopy images of the adhesion of HUVECS on native and G cross-linked $(\text{ALG/CHT})_5$ nanofilms assembled on PEI-functionalized polystyrene cell culture plates with or without additional bilayers on the top when resuspended in normal medium or serum-free. Cells' nuclei were stained in blue by DAPI and F-actin filaments in green by phalloidin. Scale bar: 50 μm . Adapted with permission from [238]. Copyright © 2017 Elsevier.

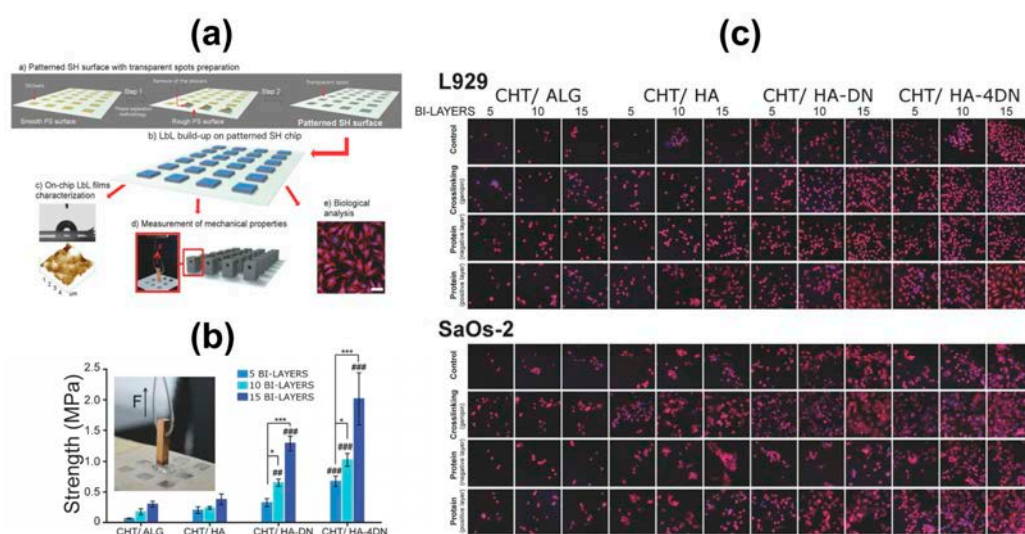


Figure 14. (a) Schematic illustration of the preparation of polystyrene superhydrophobic surfaces patterned with wettable regions of tunable size and geometry. (b) Adhesive strength between the CHT/ALG, CHT/HA, CHT/HA-DN and CHT/HA-4DN multilayer nanofilms produced over the wettable regions of the superhydrophobic microarray and the iron pillars while increasing the number of bilayers. Data shown as means SD ($n = 5$; * $p < 0.1$, and *** $p < 0.001$). The statistical differences relating to CHT/HA films with the same number of bilayers are represented by double symbols (##, $p < 0.01$) and triple symbols (###, $p < 0.001$). Representative image of an adhesion measurement in a single wettable spot where an iron pillar is pulled out with a constant strain rate. (c) Representative fluorescence microscopy images of L929 murine fibroblast and SaOs-2 human osteoblast-like cells after being cultured for 24 h on the nanofilm-coated wettable spots (control), and fibronectin-coated multilayered nanofilms and genipin cross-linked nanofilms. Cells' nuclei were stained in blue by DAPI and F-actin filaments in red by phalloidin. Scale bar: 50 μm . Adapted with permission from [250]. Copyright © 2016 Wiley-VCH Verlag GmbH & Co. KGaA, Weinheim.

Native and genipin-induced cross-linking free-standing membranes made of CHT/ALG multilayers also exhibited shape memory properties, undergoing reversible shape switching triggered by either hydration or ionic cross-linking [256,257]. Moreover, the incorporation of magnetic nanoparticles in such self-standing CHT/ALG membranes imparted them with shape memory and magneto-responsive properties, which improved cell adhesion [258]. Those membranes hold invaluable potential as smart implantable devices to be inserted in the human body in a temporary shape via minimally invasive procedures, and once reaching to the injured site and achieving a certain hydration level would adopt its permanent shape. Biomimetic mussel-inspired multilayered membranes denoting tunable and improved adhesive and mechanical properties, as well as cell adhesion and proliferation, were also produced on smooth polypropylene substrates by electrostatically assembling either 200 CHT/HA-DN bilayers [259], or integrating HA-DN in the assembly of 100 CHT/ALG/CHT/HA-DN tetralayers [260]. The in vitro biological performance of the as-produced membranes was assessed with different cell types, including human primary dermal fibroblasts and MC3T3-E1, demonstrating their intrinsic potential in skin wound healing and bone tissue engineering, respectively. Moreover, the incorporation of both HA-DN and bioactive glass nanoparticles (BG NPs) into hybrid nacre-inspired bioresorbable free-standing membranes containing CHT/HA-DN/CHT/BG NPs tetralayers rendered them not only bioadhesive but also bioactive, as showcased by the formation of a calcium-phosphate layer on their surface [261]. As such, the membranes denote immense potential to act as wound dressings, as well as bioinstructive matrices to promote guided bone tissue regeneration in addressing periodontal diseases.

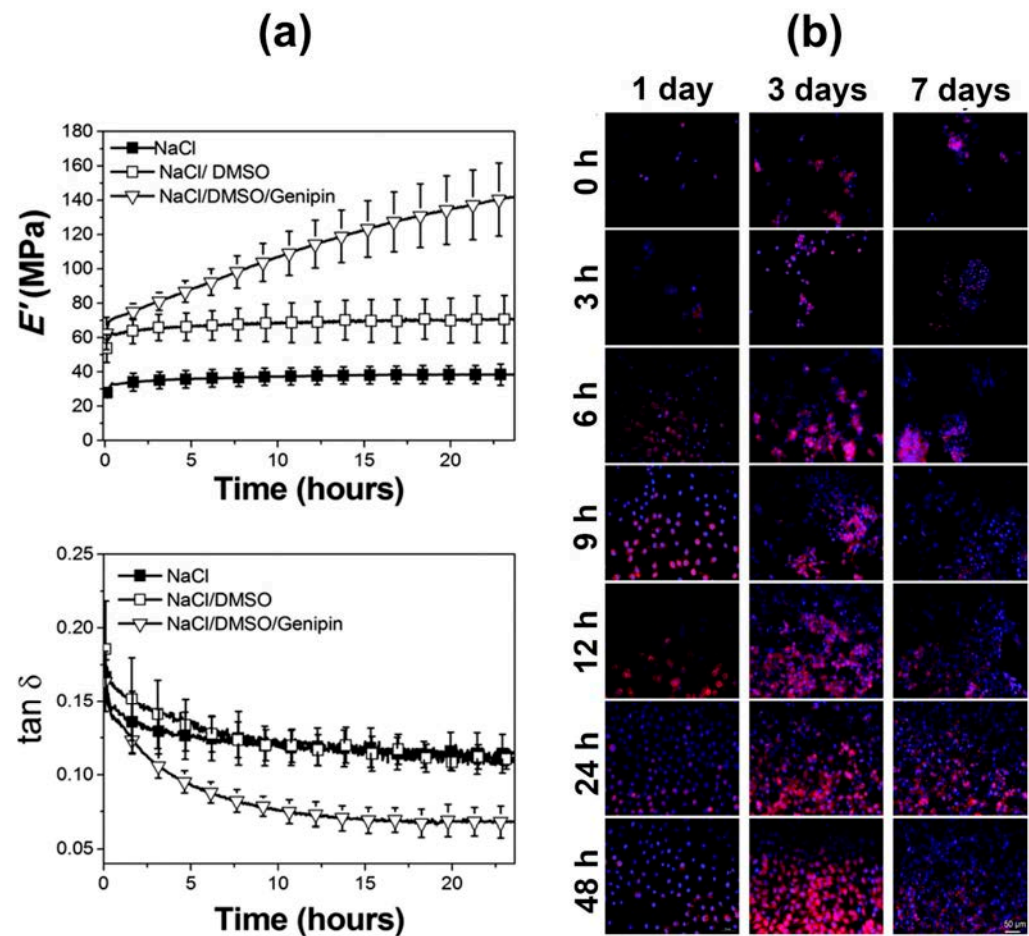


Figure 15. (a) Storage modulus (E') and loss factor ($\tan \delta$) of (CHT/ALG)₁₀₀ free-standing membranes while immersed in 0.15 M acetate buffer at pH 5.5, 0.15 M acetate buffer at pH 5.5/DMSO and 0.15 M acetate buffer at pH 5.5/DMSO/genipin solutions at 37 °C. (b) Representative fluorescence microscopy images of L929 mouse fibroblast cells after being cultured for 1, 3 and 7 days on uncross-linked (0 h) and cross-linked (CHT/ALG)₁₀₀ free-standing membranes upon increasing the cross-linking reaction time (3–48 h). Cells' nuclei were stained in blue by DAPI and F-actin filaments in red by phalloidin. Scale bar: 50 μm . Adapted with permission from [254]. Copyright © 2015 Royal Society of Chemistry.

Self-standing membranes have also been assembled on patterned hydrophobic templates aiming to better control cell functions in addressing specific tissue engineering strategies. For instance, highly aligned tissues such as muscle, blood vessels or nerves would undoubtedly benefit from the assembly of free-standing membranes whose nanoscale topographical features would be reminiscent of those of such tissues. In fact, patterned polycarbonate templates exhibiting nano-grooved features were used to produce robust self-standing nanopatterned cross-linked chitosan-chondroitin sulfate (CHT/CS) membranes that directed C2C12 myoblast cell alignment along the nanopattern direction and triggered their differentiation into myotubes when using non-differentiated growth medium, thus being promising bioinstructive matrices for muscle regeneration (Figure 16) [262]. Such a platform could be adapted to other cell types existing in highly aligned tissues, such as neuronal or endothelial cells to enable the regeneration of nerve tissue or blood vessels, respectively. Furthermore, patterned polydimethylsiloxane templates denoting an array of micro-wells with tunable geometry were designed to precisely assemble micro-pore mimetic free-standing CHT/ALG membranes in which human osteoblast-like cells tended to colonize preferentially [263]. Those membranes featuring micro-pores could be used as

micro-reservoirs for the loading, protection, and on-demand sustained release of bioactive molecules or as cell carriers in regenerative medicine strategies.

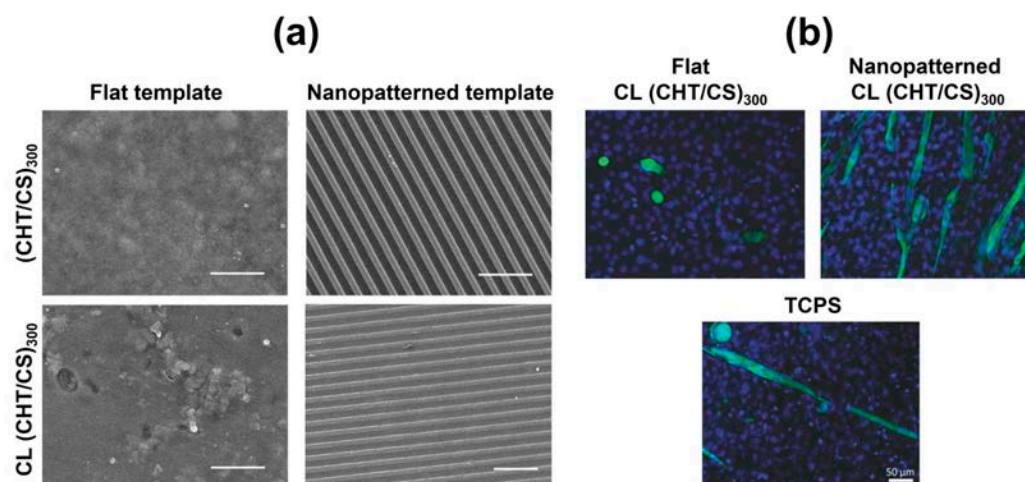


Figure 16. (a) Representative scanning electron microscopy (SEM) micrographs of native and genipin cross-linked (CL) flat and nanopatterned (CHT/CS)₃₀₀ free-standing membranes produced over flat polypropylene and patterned optical media templates, respectively. Scale bar: 5 μm. (b) Representative immunofluorescence micrographs of C2C12 myoblast cells after being cultured for 10 days on CL flat and nanopatterned (CHT/CS)₃₀₀ free-standing membranes, and tissue culture polystyrene surfaces (TCPS) using normal growth medium. Cells' nuclei were stained in blue by DAPI and myotubes in green by troponin T. Scale bar: 50 μm. Adapted with permission from [262]. Copyright © 2017 Wiley-VCH Verlag GmbH & Co. KGaA, Weinheim.

6.2. Multilayered Particles, Hollow Multilayered Capsules and Hierarchical (multi)Compartmentalized Capsules

The versatility imparted by the LbL assembly technology has been well-demonstrated by its potential to coat more convoluted 3D surfaces, including colloidal particles, tube-like, hierarchical multi-compartmentalized or porous structures, thus extending its applications in the biomedical arena. Organic and inorganic biocompatible templates have been widely used to prepare core-shell multilayered particles. Such particles are engineered by repeating the alternate and sequential adsorption of aqueous solutions of complementary materials onto the particles' surface. The use of sacrificial core templates further enables the preparation of hollow multilayered microcapsules following core template dissolution.

Microsized calcium carbonate (CaCO₃) inorganic particles have been widely employed as templates for the fabrication of core-shell LbL micro-particles and hollow microcapsules for bioapplications owing to their unique features, including easy, fast and inexpensive synthesis, highly porous structure, large surface area-to-volume ratio, biocompatibility, non-toxicity, and high mechanical stability. Chitosan has been combined with other oppositely charged natural [264], (Figure 17) or synthetic polymers [265,266] to engineer fully natural or biomimetic chitosan-derived multilayered shells, respectively, templated on spherical CaCO₃ microcores. The exposure of the sacrificial template to calcium-chelating agents such as ethylenediamine-tetraacetic acid (EDTA) enabled its decomposition and development of hollow multilayered microcapsules (Figure 17b), which are particularly attractive as multifunctional carrier vehicles of high payloads for intracellular delivery, cellular internalization (Figure 17c) or intracellular trafficking.

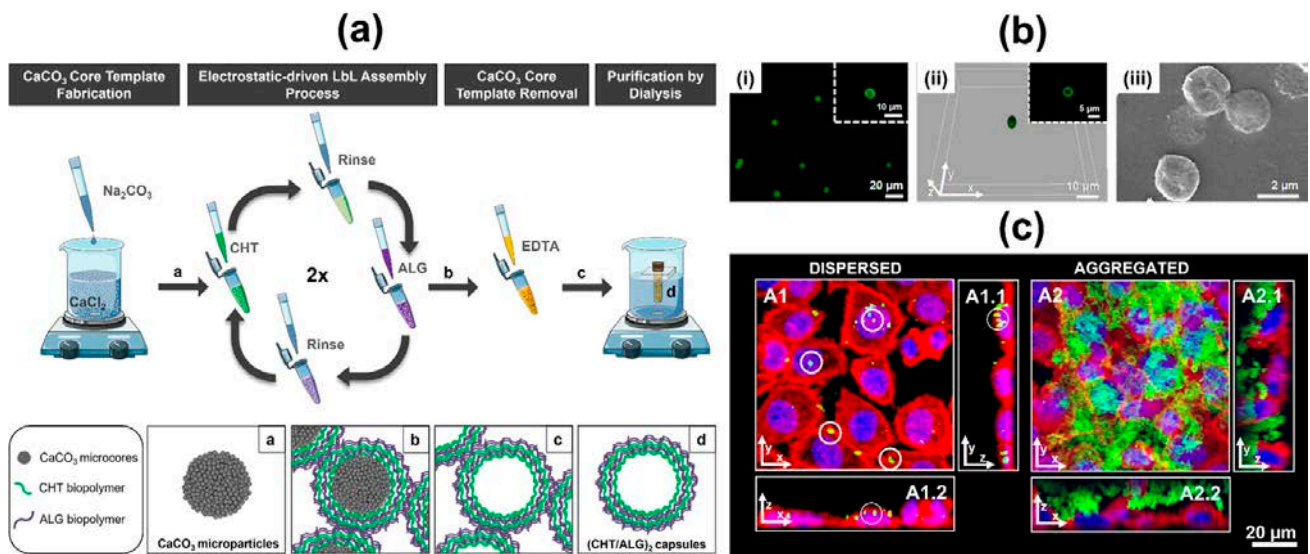


Figure 17. (a) Schematic illustration of the preparation of “a” CaCO_3 core microparticles, “b” core-shell CaCO_3 microparticles functionalized with two CHT/ALG bilayers, “c” CaCO_3 -templated (CHT/ALG)₂ hollow multilayered microcapsules after EDTA-induced core template dissolution, and “d” well-dispersed CaCO_3 -templated (CHT/ALG)₂ hollow multilayered microcapsules after EDTA-induced decomposition of the CaCO_3 core template and purification by dialysis. (b) Representative (i) fluorescence and (ii) confocal laser scanning microscopy (CLSM), and (iii) SEM images of the well-dispersed (FITC-CHT/ALG)₂-based hollow multilayered microcapsules after dialysis. (c) 3D reconstructed z-stack CLSM micrographs of L929 mouse fibroblast cells upon contacting the well-dispersed (A1) or aggregated (A2) (FITC-CHT/ALG)₂-based hollow multilayered microcapsules as seen from the top (A1, A2; view of the xy plane). A1.1–A2.1 and A1.2–A2.2 correspond to orthogonal projection images (view of the yz and xz planes, respectively). Blue channel: DAPI nuclear probe; Red channel: rhodamine-labeled phalloidin; Green channel: (FITC-CHT/ALG)₂-based hollow multilayered microcapsules. White circles intend to highlight some microcapsules internalized by L929 cells. Adapted with permission from [264]. Copyright © MDPI 2018 under a Creative Commons Attribution 4.0 International License.

Organic biocompatible and biodegradable polymers have also been employed as templates to assemble chitosan-based core-shell multilayered micro- and macroparticles and further liquefied multilayered capsules to be used for cell encapsulation in *in vitro* and *in vivo* tissue engineering and regenerative medicine strategies [267]. In particular, hybrid multilayered nanoshells encompassing oppositely charged poly(L-lysine) (PLL), ALG and CHT were templated on spherical calcium chloride cross-linked alginate micro- and macroparticles loaded with either a mono- or co-culture of cells and surface functionalized poly(L-lactic) (PLA) or poly(ϵ -caprolactone) (PCL) microparticles, providing anchorage sites for enabling cell adhesion and proliferation [225,226,267–270]. The exposure of the core-shell particles to EDTA induced the chelation of the calcium ions, producing liquefied alginate multilayered micro- and macroparticles featuring a chitosan-derived LbL shell. Such shell revealed to be permselective, enabling the inwards diffusion of nutrients and oxygen essential to sustain cell survival and the excretion of cell metabolites and waste products, while excluding the entrance of large molecules of the host immune system and other cells. On the other hand, the liquefied core maximizes the diffusion of those essential molecules along the entire system, thus surpassing the limitations of larger-size tissue constructs (above ca. 200 μm). The multilayered capsules could be cultured under dynamic tissue-like conditions and encapsulate virtually any biomolecules of interest and anchorage-dependent cell types, thus enabling the *in vitro* development of microtissues in a more close-to-native and inexpensive manner. In particular, the liquefied and multilayered microcapsules have shown to encapsulate a co-culture of human adipose-derived

stem cells (hASCs) and either human adipose-derived microvascular endothelial cells or osteoblasts anchored to collagen I-functionalized PLA or PCL microparticles and to form bone-like microtissues *in vitro* and *in vivo*, holding great promise to be applied in bone tissue engineering [267,268,270]. Besides, similar liquefied microcapsules encapsulating supportive PCL microparticles and a mono- or co-culture of HUVECs and human fibroblasts have been produced with a bioactive multilayered nanoshell encompassing PLL/ALG/CHT and an outer alginate layer functionalized with arginine-glycine-aspartic acid (RGD) tripeptide cell adhesive motif to enhance their biological performance [271]. 3D microaggregates of cells and microparticles were produced and confined within the liquefied core by cells recruiting microparticles and 3D microcapsule macroaggregates were formed in the outside by cells and deposited extracellular matrix, whose linkage is promoted by the outermost RGD bioactive peptide-functionalized microcapsules. The bioactive outer layer promoted the recruitment of new microvessels and formation of vasculature, thus enabling the diffusion of essential molecules for cell survival and possibly stimulating a proper integration of the microcapsules within the surrounding tissue *in vivo* to better foster tissue regeneration. Magnetic-responsive liquefied alginate macrocapsules denoting an LbL nanoshell encompassing oppositely charged PLL, ALG, CHT and magnetic nanoparticles (MNPs) have shown to encapsulate hASCs cells anchored to crosslinked collagen II/TGF- β 3-surface functionalized PLA microparticles and induce their chondrogenic differentiation aiming at cartilage tissue regeneration. Those self-regulated liquefied multilayered microcapsules have great potential to be applied as innovative bioencapsulation systems and platforms for multiple tissue engineering and regenerative medicine strategies.

Liquefied spherical alginate macrocapsules functionalized with a tunable CHT/ALG LbL nanoshell have also been used as reservoirs of model fluorophores and CaCO₃-templated temperature-responsive chitosan/elastin-like recombinamers (ELRs) multilayered microcapsules, thus enabling multifunctional, (multi)compartmentalized capsules with a hierarchical organization from the nano- to the macro-scale mimicking living systems [272]. The latter internal microcompartment further encapsulated either magnetic nanoparticles (MNPs) or fluorescent model molecules, whose release could be tailored and spatiotemporally controlled on-demand by playing with the temperature-sensitive nature of ELRs and magnetic field-responsive MNPs, respectively. Such multicompartmentalized capsules could encapsulate virtually any type of compartments, including multistimuli-responsive ones, thus enabling smart multifunctional systems that would be very appealing for a wide variety of biomedical and biotechnological applications.

6.3. Hollow Multilayered Tubes

Cylindrical substrates have also been coated in an LbL fashion to engineer innovative self-sustained hollow multilayered tubes, with tunable properties and functions at the nanoscale, which hold great promise in sustained drug/therapeutics delivery, tissue engineering and regenerative medicine. For instance, self-standing hollow multilayered macrotubes (*ca.* 1 mm) were engineered by dip-coating sacrificial paraffin wax-coated glass tubes in (ALG/CHT)₁₀₀ multilayered nanoshells followed by dichloromethane-induced core template leaching, without altering the nanoshell properties [273]. Owing to their softness and high hydration level, the native hollow tubes were further crosslinked with the natural cross-linking agent genipin, leading to tunable multilayered tubes with decreased water uptake, increased stiffness and improved L929 fibroblast cells adhesion and proliferation when compared with the native ones. Such a proof-of-concept study launched the seeds for a follow-up work aiming to develop tube-like artificial blood vessel substitutes for cardiovascular tissue engineering. In this regard, similar genipin cross-linked ALG/CHT hollow multilayered tubes were bioengineered and subsequently functionalized with fibronectin via EDC/NHS chemistry to further enhance cell adhesion (Figure 18a,b) [274]. The as-produced hollow tubes were successfully co-cultured with human umbilical vein endothelial cells in the inner side and human aortic smooth muscle cells in the outer side,

two cell types existing in the blood vessels' composition, thus recreating the native blood vessels (Figure 18c). Besides, (ALG/CHT)₈ hollow multilayered nanotubes templated on the inner pores of PEI-functionalized polycarbonate templates (Figure 18d,e) have shown to be internalized by cancer cells (Figure 18f), holding great potential as carrier vehicles of therapeutic agents [275].

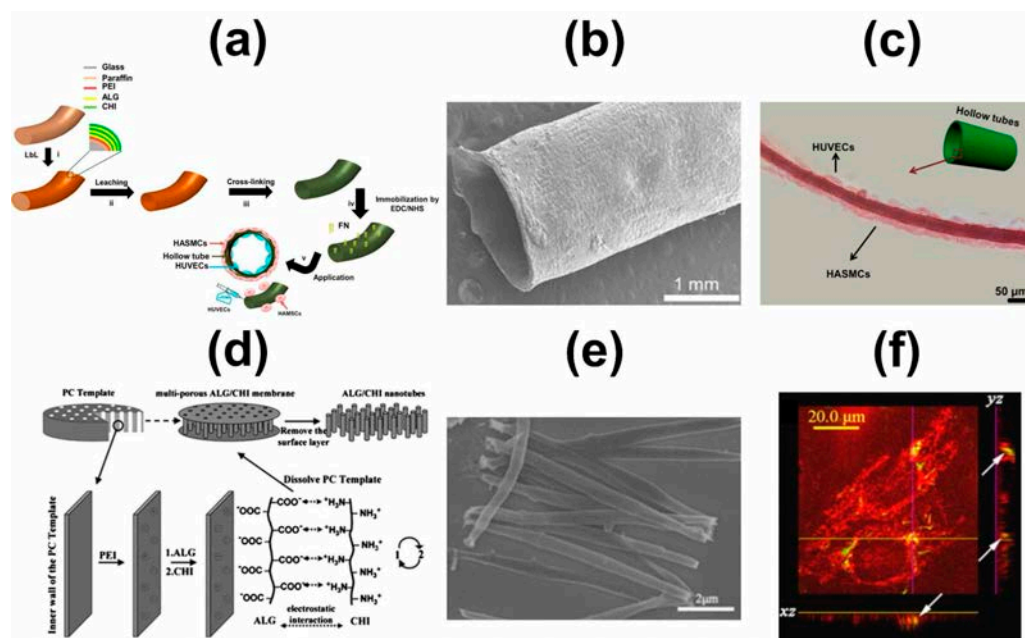


Figure 18. (a) Schematic illustration of the preparation of ALG/CHT hollow multilayered macrotubes. (b) SEM micrograph of the (ALG/CHT)₁₀₀ hollow multilayered macrotubes. Adapted with permission from [273]. Copyright © 2014 Wiley-VCH Verlag GmbH & Co. KGaA, Weinheim. (c) Histological cross-section of (ALG/CHT)₁₀₀ hollow multilayered macrotubes seeded with HUVECs (inner side) and HASMCs (outer side) stained by Haematoxylin & Eosin after 7 days of culture. (a,c) Reproduced with permission from [274]. Copyright © 2016 American Chemical Society. (d) Schematic representation of the preparation of ALG/CHT nanotubes. (e) SEM micrograph of (ALG/CHT)₈ hollow multilayered nanotubes. (f) CLSM image of MCF-7 cells upon contacting the (fluorescein dichlorotriazine labeled-ALG/CHT)₈ nanotubes, in the presence of the FM 4–64 marker, for 24 h, revealing the endocytosis of the nanotubes. Adapted with permission from [275]. Copyright © 2007 Elsevier.

The versatility imparted by the hollow multilayered tubes would enable their use as reservoirs of bioactive agents to enable long-term cell survival and trigger the formation of pre-vascularized tissues. Moreover, owing to their geometry and tunable properties and multifunctionalities at the nanoscale, the hollow multilayered tubes hold great promise as reservoirs of neuronal growth factors and neuronal cells for repairing neuronal networks in neural tissue regeneration, as well as platforms to enable the development of (multi)compartmentalized systems.

6.4. 3D Constructs

In the last decade, LbL technology has been moving a step forward to assemble even more complex 3D structures for use in the biomedical and biotechnological fields. Spherical paraffin wax particles were surface functionalized with PEI prior to their conformal ALG/CHT multilayered coating via the perfusion LbL assembly methodology, using a perforated cylindrical container, thus leading to 3D interconnected cylindrical structures encompassing multilayered microspheres denoting a regular stacking arrangement (Figure 19a(i)) [276]. The paraffin core was leached out by exposure to dichloromethane, enabling moldable 3D interconnected and porous self-supporting multilayered constructs (Figure 19a(ii)). The beneficial effect of both the LbL coating and particles' interconnectivity

on cell adhesion and viability was studied using human osteoblast-like cell lines, revealing that more than 99% of cells seeded on the construct remained viable and metabolically active after 3 days of culture through the entire structure (Figure 19a(iii)). The perfusion LbL assembly methodology and spherical template leaching have also been combined to coat 3D packet paraffin spheres with chitosan/chondroitin sulfate (CHT/CS) multilayered nanoshells, which were further leached out to assemble highly porous and interconnected nanostructured 3D CHT/CS multilayered constructs [277]. Such constructs proved to support the adhesion, proliferation, and viability of either bovine chondrocytes or multipotent bone marrow-derived stromal cells and the chondrogenic differentiation of the latter, thus holding potential to be applied in cartilage repair. This approach can be adapted to virtually any template, irrespective of the size and geometry, and a multitude of complementary LbL biopolymers can be assembled into multilayered films, which could act as a reservoir of bioactive molecules. Furthermore, virtually any type of cells can be cultured, thus opening new horizons in a wide array of tissue engineering and regenerative medicine strategies. More recently, packed calcium cross-linked cell-laden ALG beads or reeled fibers with tunable size and geometry were conformally coated with CHT/ALG multilayers via perfusion-based LbL methodology and further chelated with EDTA to produce 3D self-standing liquefied constructs (Figure 19b(i,ii)) [278,279]. Such modular constructs were revealed to be well interconnected and could be easily handled without disrupting their original 3D structure by the action of the assembled multilayers. Moreover, the assembled liquefied 3D constructs enabled the survival and proliferation of L929 fibroblast cells (Figure 19b(iii)). Additionally, the cell proliferated freely throughout the entire liquefied system, including inside the liquefied bound beads or fibers, thus revealing their cyto-compatibility and permeability of the multilayered coating, which is key to regulating the diffusion of oxygen, nutrients, and metabolic waste products to ensure cell survival.

Porous 3D hierarchical micro- and macro-scaffolds also were prepared in a straightforward way by combining the LbL assembly technology with the rapid prototyping technique. In this regard, prototyped 3D PCL macro-scaffolds were coated in an LbL fashion with bioinstructive nanocoatings encompassing oppositely charged marine-origin polysaccharides, namely CHT and carrageenan, and human platelet lysate towards assembling hierarchical cell-instructive 3D multiscale scaffolds [280]. The LbL-coated scaffolds were further freeze-dried to shape the bioinstructive nanoassemblies in the inner side of the scaffolds into fibrillar structures, which provided enhanced cell-anchorage points to induce the osteogenic differentiation of hASCs into osteoblasts. The proposed methodology could be translated into the assembly of any bioactive LbL coatings, which can act as reservoirs of bioactive molecules, and different cell types can be seeded to direct multiple tissue engineering purposes.

Other 3D scaffolds were prepared by resorting to alternative methodologies and further LbL-coated to impart the scaffolds with enhanced properties and multifunctionalities for being used in biomedical applications [281,282]. A recent original research article combined 3D printing with the LbL assembly technology to bioengineer customized large 3D constructs (Figure 20a) aimed at surpassing the bulk hydrogels-limited diffusion of oxygen and nutrients essential to sustain long-term cell survival and enable the formation of prevascular networks for vascular tissue engineering [283]. Customizable calcium cross-linked sacrificial ALG structures exhibiting tunable sizes and shapes (Figure 20b), including microfibers were 3D printed, coated with six bioinstructive chitosan/RGD-grafted alginate multilayers in an LbL fashion and further embedded in a shear-thinning and bioinert photocrosslinkable xanthan gum hydrogel (XG-GMA). The immersion of the full 3D construct in EDTA induced the liquefaction of the alginate core template, leading to perfusable bioinstructive hollow multilayered microstructures, which were fixed and sustained without collapsing by the supporting hydrogel matrix (Figure 20c). HUVECs were seeded in the inner walls of the bioinstructive LbL-coated perfusable microchannels with FBS-free culture medium, revealing a much higher number of adherent and viable cells when compared with the uncoated microchannel (90% vs. 5%, Figure 20d). The

bioinstructive LbL-coated microchannels embedded in hydrogels hold great promise to bioengineer endothelial cell-lined tubular networks as blood vessel substitutes. Moreover, the versatility imparted by the combination of 3D printing, LbL assembly technology and photocrosslinkable hydrogels open new perspectives in bioengineering large-scale 3D vascularized tissue constructs for modular tissue engineering and regenerative medicine.

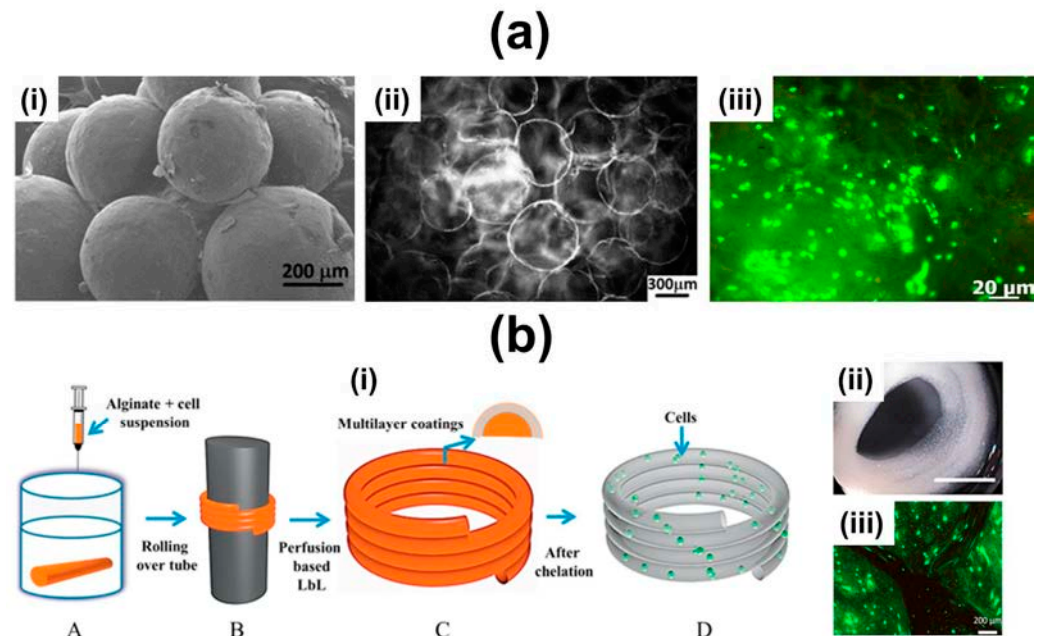


Figure 19. (a) Preparation of LbL-coated 3D porous nanostructured constructs: (i) SEM micrograph of (ALG/CHT)₁₀-coated PEI-functionalized spherical paraffin wax particles; (ii) Fluorescence microscopy micrograph of liquefied paraffin wax particles-templated (ALG/CHT)₁₀ constructs after leaching the core template; (iii) Live/Dead assay of LbL-coated 3D constructs after 3 days of culture. Live cells were stained in green by calcein-AM and dead cells were stained in red by propidium iodide (PI). Adapted with permission from [276]. Copyright © 2010 Wiley-VCH Verlag GmbH & Co. KGaA, Weinheim. (b) Preparation of self-sustained LbL-coated 3D spiral-shaped constructs. (i) Schematic illustration of the process to fabricate liquefied 3D helical structures using cell-encapsulated ALG hydrogel fibers by combining ionotropic gelation with the perfusion-based LbL assembly technology: (A) Cells were encapsulated in ALG hydrogel fibers by ionotropic gelation; (B) The fibers were reeled over the glass rod to form the spiral structure; (C) Removal of the glass rod and coating with five CHT/ALG bilayers to obtain non-liquefied 3D spiral-shaped constructs; (D) Liquefied 3D construct obtained after the EDTA-induced chelation of the ALG core template. (ii) Top view optical image of the liquefied L929 fibroblast cells-encapsulated 3D constructs after 7 days of culture. Scale bar: 5 mm. (iii) Live/Dead assay of liquefied 3D constructs at 7 days of culture using L929 cells. Living cells were stained in green by calcein-AM and dead cells were stained in red by PI. Adapted with permission from [273]. Copyright © 2015 IOP Publishing Ltd.

6.5. Living Cell Surfaces

The use of entire aqueous solutions and the mild processing conditions behind the fabrication of the LbL nanoassemblies have turned this technology into a suitable, cytocompatible methodology to functionalize animate and dynamic living cell surfaces, including single cells and cell aggregates [284–288]. In fact, probiotic microorganisms have been encapsulated in CHT/ALG multilayers to protect them from the gastro-intestinal microbiome and enhance their delivery, adhesion and growth *in vivo* (Figure 21a) [289]. Furthermore, the chitosan-based LbL nanocoating improved not only the probiotic viability, but also facilitated its mucoadhesion and growth on the porcine intestine surface when compared with the uncoated probiotic (Figure 21b).

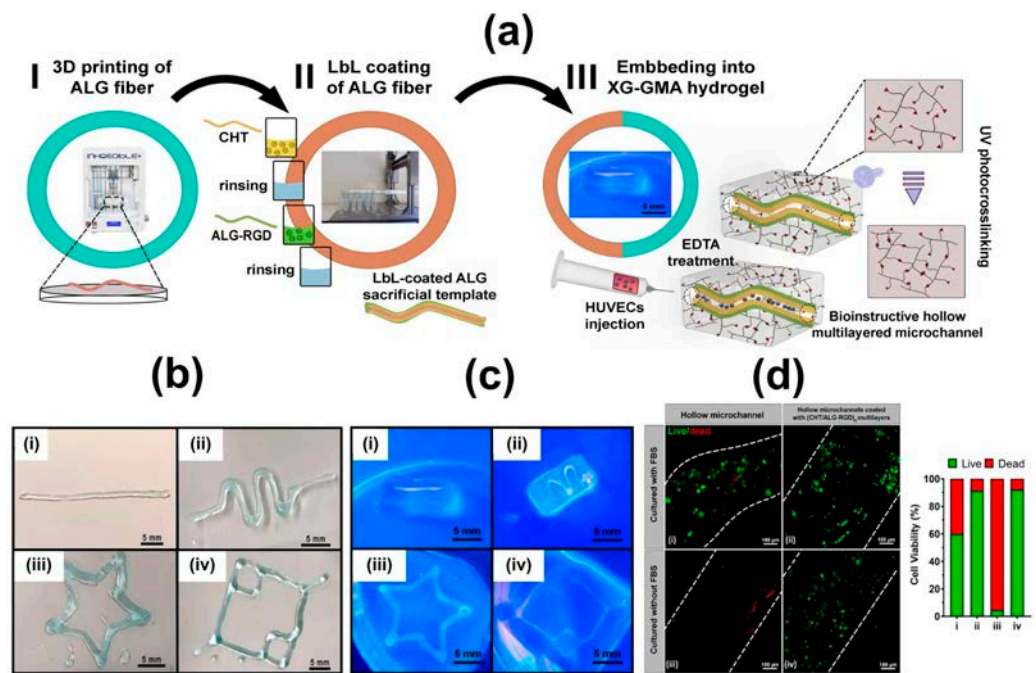


Figure 20. (a) Schematic illustration of the fabrication of perfusable 3D constructs encompassing bioinstructive (CHT/ALG-RGD)₆ multilayers templated on liquefied ALG microchannels embedded in photocrosslinkable XG-GMA supporting hydrogels. Optical images of the customizable (b) 3D printed ALG sacrificial structures, denoting different sizes and shapes, after crosslinking with CaCl₂, and (c) 3D constructs enclosing perfusable structures embedded in photocrosslinkable XG-GMA hydrogels after the injection of a fluorescent aqueous solution into the microchannel inner walls, viewed under UV light. (d) Live/Dead confocal laser scanning microscopy micrographs of HUVECs seeded for 3 days, with (i,ii) or without (iii,iv) FBS, in the (i,iii) uncoated and (ii,iv) (CHT/ALG-RGD)₆ LbL-coated hollow microchannels embedded in photocrosslinkable XG-GMA hydrogels. The white dashed lines indicate the borders of the microchannels. Quantification of cell viability in the uncoated and LbL-coated microchannels for HUVECs seeded for 3 days with or without FBS. Adapted with permission from [264]. Copyright © MDPI 2021 under a Creative Commons Attribution 4.0 International License.

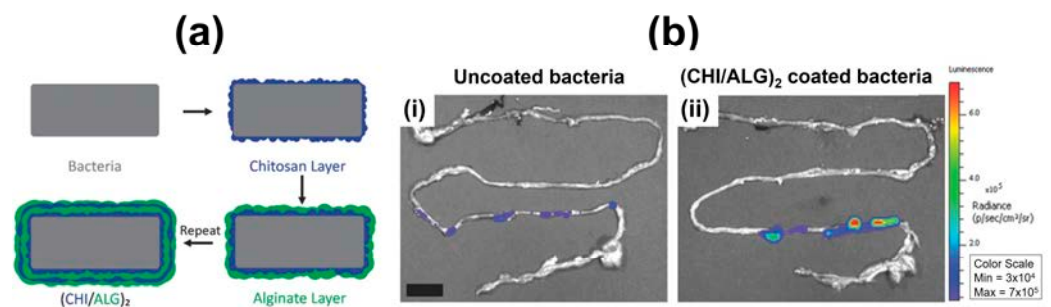


Figure 21. (a) Schematic representation of CHT/ALG LbL coating on probiotic strain *Bacillus coagulans* (BC). (b) Representative in vivo images of (i) uncoated-BC and (ii) (CHI/ALG)₂ LbL-coated BC 1 h after oral gavage. Scale bar = 1.5 cm. Adapted with permission from [273]. Copyright © 2016 Wiley-VCH Verlag GmbH & Co. KGaA, Weinheim.

In other studies, the encapsulation of the bacteria *Escherichia coli* or *Staphylococcus epidermidis* in biopolymeric nanoshells of chitosan and either alginate or dextran sulfate preserved the viability and delayed the growth of the encapsulated bacteria when compared with uncoated bacteria [290,291]. Such a strategy represents a promising approach to prevent the proliferation of both bacteria and, thus, maintain the gut or skin microbiota aiming to regulate human health. The LbL technology was also used as an efficient way to

enhance and modulate live *Bacille Calmette-Guérin* (BCG) mycobacteria's immunogenicity by functionalizing its surface with a polymeric nanocoating containing oppositely charged chitosan and strong immunostimulatory agent polyinosinic–polycytidylic acid (poly(I:C)), a synthetic analog of the double-stranded RNA [292]. It was found that the multilayered nanocoating induced a stronger and long-term protective immune response against adult pulmonary tuberculosis. The multilayered nanocoating did not affect the bacterial viability and further induced an enhanced macrophage pro-inflammatory response and expression of co-stimulatory molecules when compared with the uncoated BCG.

7. Chitosan-Based Inks for 3D Printing Applications

In the last decades, regenerative medicine and tissue regeneration may include biofabrication strategies, defined as “the automated generation of biologically functional products with structural organization from living cells, bioactive molecules, biomaterials, cell aggregates such as micro-tissues, or hybrid cell-material constructs, through bioprinting or bioassembly and subsequent tissue maturation processes” [293]. Within this framework, 3D printing, an additive manufacturing technology consisting of the LbL fabrication of 3D scaffolds with tunable sizes and geometries, programmed by means of computer-aided drafting (CAD), plays a relevant role as a promising tool for the replacement of damaged tissues. Differently from the off-of-shelf scaffold production or the common hydrogels scaffolds, 3D printing may allow the fabrication of novel 3D bioengineered tissue with promising properties [294,295].

When aiming for biomedical applications, the accurate choice of the ink, namely the development of a printing formulation with proper rheological properties that may contain bioactive (macro)molecules and biomaterials, allowing spatial organization and cell growth, is vital. In this regard, of particular interest are bioinks (Figure 22), “formulations of cells suitable for processing by an automated biofabrication technology that may also contain biologically active components and biomaterials” [296].

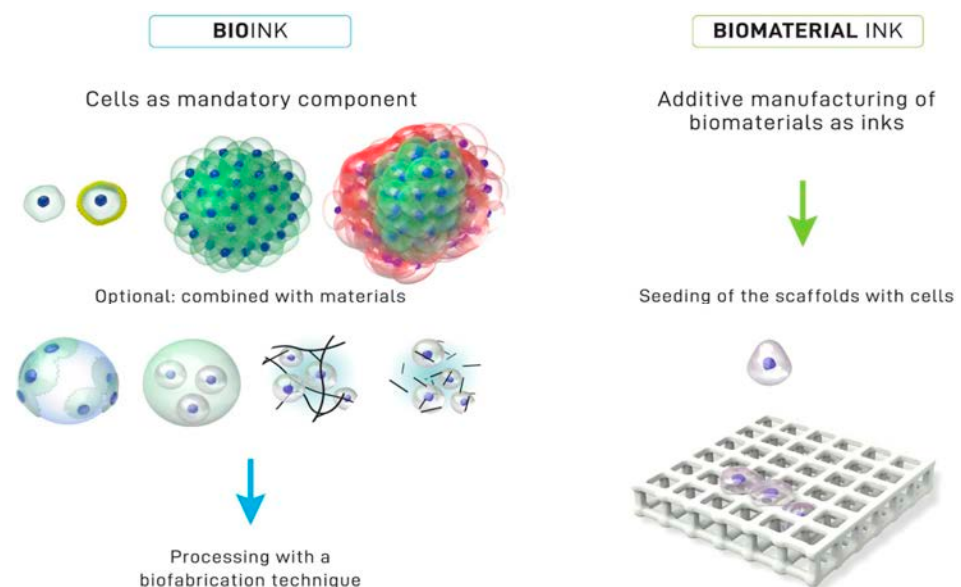


Figure 22. Difference between bioink (left) and biomaterial ink (right); in bioinks cells are intrinsic components; whereas in biomaterial inks, a biomaterial composes the ink for additive manufacturing techniques. Adapted with permission from [296]. © 2018 IOP Publishing Ltd. under the terms of the Creative Commons Attribution 3.0 license.

Designing bioinks with suitable printing properties is still a difficult task. Notably, CHT can be exploited as a (bio)ink component due to its low cost, biocompatibility and non-immunogenicity. However, its use as a component in 3D bioprinting applications is reported roughly in 4% of publications. In this section, the recent developments in the

field of 3D (bio)printing are highlighted, with a focus on the use of CHT as a (bio)ink component aiming at maximizing key parameters: the printability of the (bio)ink, cell viability after the printing step for regenerative applications and loading/release ability as drug delivery platforms [297,298].

The possibility to locally deliver drugs/therapeutics with printed scaffolds encompassing inks of varied composition has been reported for breast cancer treatment, including using a polycaprolactone/CHT ink. CHT, itself, is not suited for 3D printing due to its poor ductility and mechanical strength. However, it is well suited as a drug delivery platform, as described in the previous sections. On the other hand, PCL, due to its glass transition temperature and *in vivo* biodegradability, possess suitable features for 3D printing and biocompatible scaffold design. However, it lacks favorable interactions with cells and tissues, due to its hydrophobicity. Hence, the combination of CHT and PCL, combining their respective features, may encompass limitations of each single polymer. A two-layer 3D printed scaffold was designed: in one layer, PCL is coupled with CHT for the release of the drug (5-Fluorouracil); the second layer encompass PCL, where gold nanoparticles (AuNPs) were subsequently loaded. AuNPs may act as radiation enhancers or local heat generators upon infrared irradiation, thus contributing to cancer cells' death by local temperature enhancement. The PCL/AuNPs-PCL/CHT printed scaffold maintained a flexible structure suitable for the implant in the human body (Figure 23), showed a good drug release profile and antibacterial activity due to the CHT properties, and long scaffold degradation time owing to the PCL component, useful for the drug release profile [299].

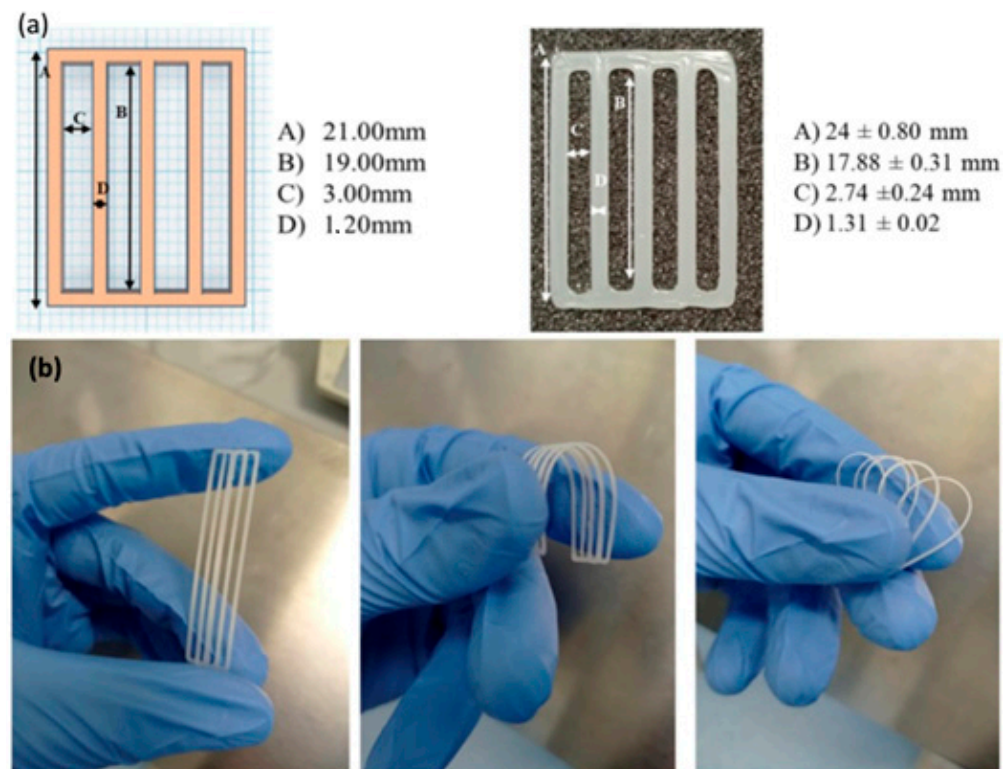


Figure 23. (a) Representation of the 3D printed first layer scaffold design loaded into the BioX software (left) and the resulting printed scaffolds (right), with their respective measurements; (b) elastic behavior of the printed scaffolds. Adapted from [299]. © 2022 Elsevier B.V. under a Creative Commons Attribution 4.0 International License.

Skin tissue engineering is an emerging field where 3D bioprinted constructs have huge potential in applications due to their ability to be used as reservoirs of drugs and *in situ* wound healing platforms. The long-term efficacy of scaffolds denoting long-term antibacterial activity and high biocompatibility mimicking the native epithelial ECM environment are highly desirable for this application. Towards this aim, an ink composed

by a soluble quaternized CHT derivative (Figure 24a), gelatin, and decellularized ECM (dECM) derived from fresh porcine skin was designed. However, since the resulting scaffolds lacked thermostability at a physiological temperature, a cross-linking step via EDC/NHS coupling chemistry was performed. Finally, to impart antibacterial properties, a polycationic polymer (Figure 24b) was incorporated within the scaffold composition.

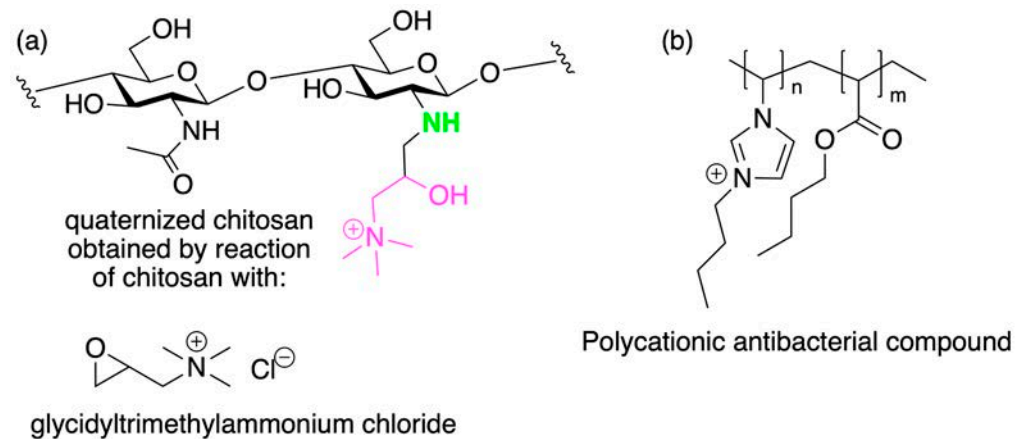


Figure 24. (a) Quaternized CHT and (b) polycationic antibacterial compound used as component in the 3D printed scaffold for skin tissue regeneration.

The resulting 3D printed scaffold (Figure 25) was studied as a wound healing platform for skin tissue regeneration in terms of hemostatic and antimicrobial activities, cell biocompatibility, adhesion and proliferation induction. The scaffold showed 100% of antibacterial activity against *E. coli* (Gram-negative) and *S. aureus* (Gram-negative) bacteria, and good hemostatic and hemocompatibility properties when compared with a quaternized CHT-free control scaffold. Additionally, it allowed the growth of fibroblasts, showing a higher ECM deposition, in particular, in terms of collagen type I, fibronectin and decorin [300].

An interesting approach towards bone tissue regeneration is provided by a bioink obtained by inducing a fast gelation (about 7 s at 37 °C) of different components, namely CHT, glycerophosphate, hydroxyethyl cellulose and cellulose nanocrystals. This bioink is printed in the presence of the pre-osteoblast lineage MC3T3-E1 cells. The presence of both cellulose nanocrystals and cells were key factors in determining the rheological properties of the bioink, and improving the mechanical features of the final CHT-based scaffold. Notably, a wide range of printing pressures could be used (12–20 kPa), without having a detrimental effect on cell viability. Increased alkaline phosphatase activity, a marker of osteogenesis, together with cell differentiation into osteoblasts, calcium phosphate nucleation and ECM deposition were observed, highlighting that CHT and cellulose nanocrystals-based bioinks could be considered as a valid approach for bone repair [301].

CHT can be functionalized with acrylic moieties, which upon photopolymerization reaction afford hydrogels suitable for bioprinting. A recent study proposed a bioink obtained by the combination of keratin and glycol CHT methacrylate, which are polymerized by UV-mediated photo-crosslinking. The produced bioink is an example of a tunable ECM mimicking material, promoting cell growth and adhesion. The optimization of the bioink composition allowed bioprinting monodispersed cells, as well as spheroids. The human adipose stem cell spheroids have been embedded in the keratin/CHT methacrylated bioink, showing a rapid migration of the cells through the matrix within five days from the cell encapsulation. In contrast to the spheroid's derived cell behavior, cell suspension remained in their round morphology, supporting the hypothesis that cells in 3D architecture strengthen the cell-cell signaling [302].

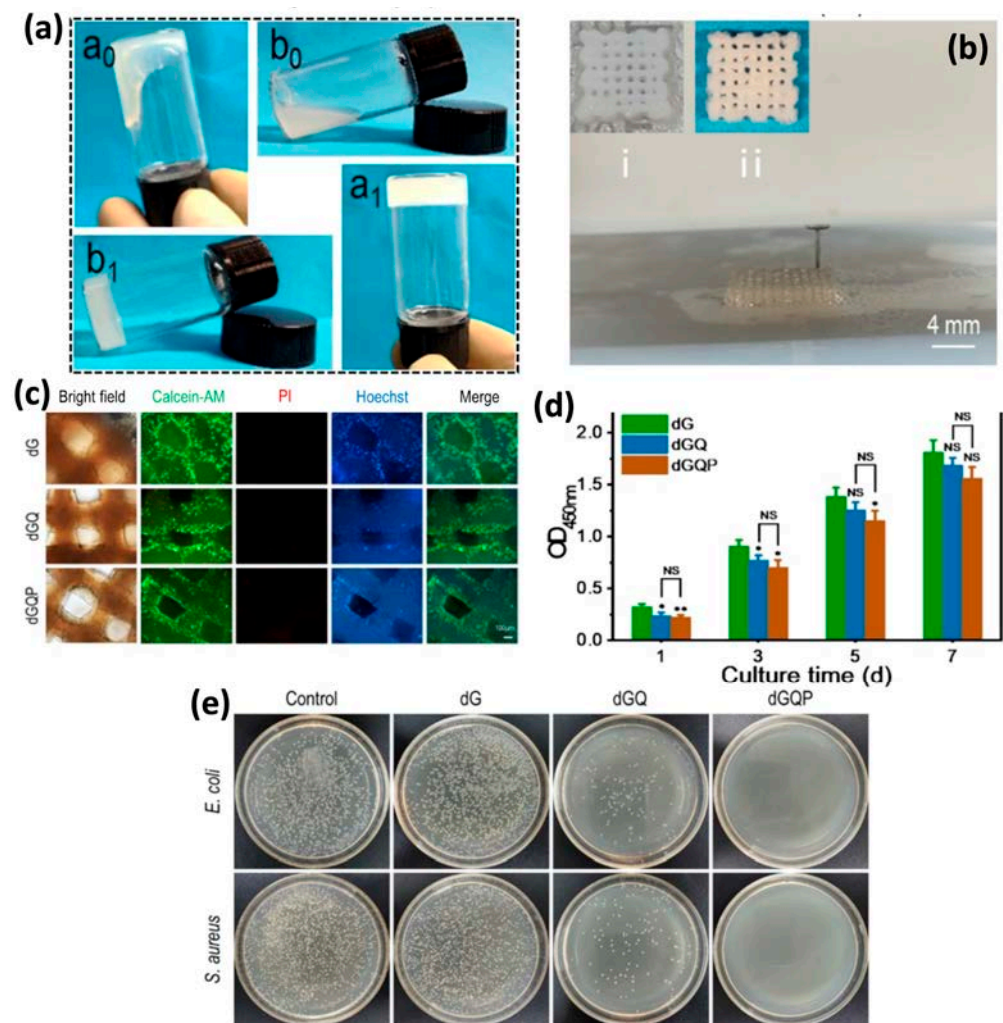


Figure 25. (a) Gelation of the bioinks at two temperatures (20 °C and 10 °C) for the dECM/gelatin scaffold (dG, a₀ and a₁), and dECM/gelatin/quaternized CHT (dGQ, b₀ and b₁); (b) 3D printed scaffolds in hydrogel and aerogel form; (c) cell biocompatibility evaluated as live-dead staining of L929 fibroblasts cultured on the scaffolds at the 7th daytime point. Live cells stained green by Calcein-AM, dead cells stained red by PI, cell nucleus stained blue by Hoechst 33258, bright field: observations in white light, scale bar: 100 μm. (d) proliferation of fibroblasts on the scaffolds quantified by the CCK8 test (Data expressed as mean ± SD (n = 3). NS: $p > 0.05$, * $p < 0.05$, ** $p < 0.01$); (e) images of the antibacterial properties of the scaffolds against *E. coli* and *S. aureus*. Reprinted and adapted with permission from [300] © 2022 Elsevier B.V.

Recent studies aimed to improve the printability conditions of CHT by formulating CHT-based bioinks that can be crosslinked by means of ionic cross-linkers in physiological conditions. One example is the use of nanohydroxyapatite, an inorganic phase widely exploited for bone tissue engineering applications, as emphasized in the previous sections. In particular, a CHT-based bioink cross-linked by glycerol phosphate and sodium hydrogen carbonate, in the presence of different ratios of nanohydroxyapatite has been proposed. The obtained 3D printed scaffolds have been analyzed in terms of morphology, rheological properties and shape fidelity to understand if the printing conditions were suitable for a robust biofabricated construct. The optimized hydroxyapatite/CHT bioink is suitable for printing with pre-osteoblastic MC3T3-E1 cells, supporting cell viability [303].

The chemistry of cross-linking may be detrimental to cell viability and growth; self-crosslinkable strategies have been studied to overcome this limitation. A recent example is an innovative self-crosslinkable ink, obtained by the conjugation of CHT to gallic acid, through the carbodiimide coupling chemistry. The CHT-gallamide derivative spontaneously undergoes oxidation at physiological pH, affording the corresponding *o*-quinones, which in turn react affording imine and 1,4-Michael addition adducts, providing the cross-links of chitosan chains (similarly to the reactions described in Scheme 5). Its biocompatibility was demonstrated with NIH3T3 cell lines, which proved to be viable after 7 days of culture post-printing. The CHT-gallamide ink has an increased mechanical strength (about 337 kPa) that can be modulated by controlling the self-cross-linking process. Due to the mechanical properties, the ink can be printed in various complex geometrical shapes with a high fidelity to the CAD prototypes (Figure 26), being promising for tissue engineering applications [304].

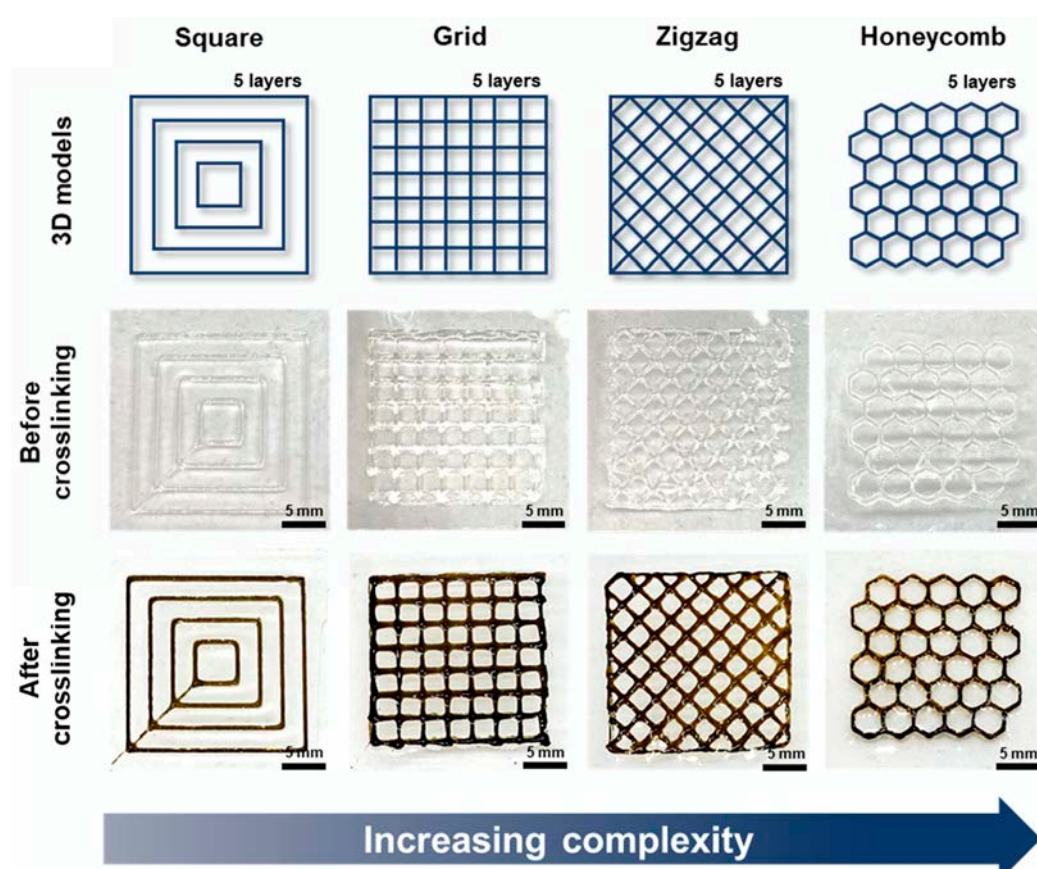


Figure 26. Printability of different 3D models (square, grid, zigzag, and honeycomb patterns). Construct dimension = $20 \times 20 \times 1.25$ mm (scale bar, 5 mm). Reprinted and adapted with permission from [304]. © 2022 Elsevier B.V.

Notably, bioprinting is not only associated with tissue engineering and regenerative medicine fields, but it can also be exploited to fabricate bioactive materials with complex geometries for immobilizing microorganisms; this approach is useful, for example, in downstream steps in microorganism-mediated biotechnological productions. Genipin is a widely explored agent to cross-link CHT (the chemistry of cross-linking is depicted in Scheme 8). However, the kinetics of the conjugation reaction is too slow (in the order of hours) to guarantee the stability of the 3D printed construct. To circumvent this limitation, alumina and alginate have been considered as components of the bioink formulation. In this regard, CHT is first dissolved in 1% acetic acid, followed by the addition of powdered alumina, and lastly, alginate and bacteria. Genipin is added as the last component, right before the printing step. The genipin-mediated slow cross-linking reaction turned out

to be an advantage, since no obstruction of the nozzle was observed. The rheological properties of the ink were modulated with different concentrations of alginate to modulate the scaffold's rheological properties to the bacterial growth (*Escherichia coli*). The observed antibacterial activity of CHT and/or genipin in control experiments of bioinks formulation without alginate was strongly reduced by the presence of the alginate. The geometry of the scaffold allows better circulation and availability of nutrients for the bacteria, sustaining their viability. This approach can be exploited to better grow bacteria in bioreactors [305].

In summary, finding the perfect match among optimized mechanical properties, printability and cell biocompatibility is the main challenge for the formulation of innovative and improved CHT-based (bio)inks. Owing to its properties, CHT is considered as an interesting biopolymeric material suitable for (bio)ink formulation in combination with other (bio)materials. Bioprinting is a successful technology that could take tissue engineering to the next level, and CHT can play a prominent role in defining a valuable class of bioinks for different applications.

8. Conclusions

From the previous sections, it clearly emerges that CHT can be exploited as a bio-based polymeric material for a huge number of applications, being included in different formulations, and manufactured towards varying structures with different compositions, morphologies, and geometries. An increasing number of research papers and patents have been published, and will continue to grow, fostered by valuable applications in regenerative medicine and following circular economy strategies. Sustainability issues will be key players in promoting CHT spreading in several industrial sectors and applications.

The increasing interest towards this polysaccharide will also drive researchers to address still existing limitations to its widespread application, such as the environmental impact caused by the extraction of chitin and its deacetylation to obtain CHT, the too high production costs to be competitive on the market with respect to other polymers, the solubility issues at physiological pH, and structural heterogeneity.

The environmental and production costs will be key issues for chitosan to enter the market as a competitive substitute of fossil-based feedstocks to produce innovative materials for several applications. In recent years, studies are emerging aimed at the detailed life cycle assessment (LCA) of chitosan production, specifically focusing on environmental and economic viability [306].

We are sure that in the next few years, CHT will strongly contribute to unprecedented advancements in the material sciences and biomedical fields, thanks to the progress in alleviating the key issues that are still a limitation to chitosan exploitation.

Author Contributions: L.C. and J.B. coordinated manuscript preparation, supported by S.P. All authors contributed to draft the manuscript, prepare the figures. All authors have read and agreed to the published version of the manuscript.

Funding: J.F.M. and J.B. acknowledge financial support by the Programa Operacional Regional do Centro–Centro 2020, in the component FEDER, and by national funds (OE) through Fundação para a Ciência e a Tecnologia/Ministério da Ciência, Tecnologia e Ensino Superior (FCT/MCTES), in the scope of the project “SUPRASORT” (PTDC/QUI-OUT/30658/2017, CENTRO-01-0145-FEDER-030658). This work was developed within the scope of the project CICECO-Aveiro Institute of Materials, UIDB/50011/2020, UIDP/50011/2020 and LA/P/0006/2020, financed by national funds through the FCT/MEC (PIDDAC). J.B. gratefully acknowledges FCT for the individual Assistant Researcher contract (2020.00758.CEECIND) under the Scientific Employment Stimulus-Individual Call. S.P., S.F.O., M.D. and L.C. gratefully thank the Cariplo Foundation with respect to the BIOSTAR-PACK project (2020-0993) for financial support.

Conflicts of Interest: The authors declare no conflict of interest.

Abbreviation

ALG	alginate
APTES	aminopropyl triethoxysilane
BCG	bacille Calmette-Guérin
BGNPs	bioactive glass nanoparticles
CAD	computer-aided drafting
CHT	chitosan
CS	chondroitin sulfate
DA	degree of acetylation
dECM	decellularized ECM
DMSO	dimethyl sulfoxide
DN	dopamine
DP	degree of polymerization
ECM	extracellular matrix
EDC	1-ethyl-3-(3-dimethylaminopropyl) carbodiimide hydrochloride
EDTA	ethylenediamine-tetraacetic acid
ELRs	elastin-like recombinamers
GlcN	2-amino-2-deoxy-D-glucose, glucosamine
GlcNAc	2-acetamido-2-deoxy-glucose N-acetylglucosamine
GPTMS	3-glycidoxy propyl trimethoxysilane
IPN	interpenetrating polymer network
LbL	layer-by-layer
MNPs	magnetic nanoparticles
NHS	N-hydroxysuccinimide
PA	pattern of acetylation
PCL	poly(ϵ -caprolactone)
PEI	polyethyleneimine
PLA	poly(L-lactic acid)
PP	polypropylene
PPi	pyrophosphate
Q-CHT	quaternized chitosan
RGD	arginine-glycine-aspartic acid peptide
SIPN	semi-interpenetrating polymer network
TEM	transmission electron microscopy
TEOS	tetraethoxysilane
TEOS	tetraethoxysilane
TMX	tamoxifen
TPP	triple polyphosphate
TPS	trisodium phosphate
XG	xanthan gum
μ CT	X-ray micro-computed tomography

References

- Skarbek, K.; Milewska, M.J. Biosynthetic and Synthetic Access to Amino Sugars. *Carbohydr. Res.* **2016**, *434*, 44–71. [[CrossRef](#)]
- Kostag, M.; El Seoud, O.A. Sustainable Biomaterials Based on Cellulose, Chitin and Chitosan Composites—A Review. *Carbohydr. Polym. Technol. Appl.* **2021**, *2*, 100079. [[CrossRef](#)]
- Brown, H.E.; Esher, S.K.; Alspaugh, J.A. Chitin: A “Hidden Figure” in the Fungal Cell Wall. *Curr. Top. Microbiol. Immunol.* **2020**, *425*, 83–111. [[CrossRef](#)] [[PubMed](#)]
- Hamed, I.; Özogul, F.; Regenstein, J.M. Industrial Applications of Crustacean By-Products (Chitin, Chitosan, and Chitooligosaccharides): A Review. *Trends Food Sci. Technol.* **2016**, *48*, 40–50. [[CrossRef](#)]
- Tolaimate, A.; Rhazi, M.; Alagui, A.; Desbrieres, J.; Rinaudo, M. Valorization of Waste Products from Fishing Industry by Production of the Chitin and Chitosane. *Phys. Chem. News* **2008**, *42*, 120–127.
- Crini, G. Historical Landmarks in the Discovery of Chitin. In *Sustainable Agriculture Reviews 35: Chitin and Chitosan: History, Fundamentals and Innovations*; Crini, G., Lichtfouse, E., Eds.; Sustainable Agriculture Reviews; Springer International Publishing: Cham, Switzerland, 2019; pp. 1–47. ISBN 978-3-030-16538-3.
- Braconnot, H. Sur la nature des champignons. *Ann. Chim. Phys.* **1811**, *79*, 265–304.
- Rouget, C. Des Substances Amylaceesdans Les Tissus Des Animaux, Specialement Des Articules (Chitine). *Comp. Rend.* **1859**, *48*, 792–795.
- Hoppe-Seyler, F. Ueber Chitin Und Cellulose. *Berichte Dtsch. Chem. Ges.* **1894**, *27*, 3329–3331. [[CrossRef](#)]

10. Kurita, K. Controlled Functionalization of the Polysaccharide Chitin. *Prog. Polym. Sci.* **2001**, *26*, 1921–1971. [[CrossRef](#)]
11. Austin, P.R. Chitin Solutions and Purification of Chitin. In *Methods in Enzymology; Biomass Part B: Lignin, Pectin, and Chitin*; Academic Press: New York, NY, USA, 1988; Volume 161, pp. 403–407.
12. Funahashi, R.; Ono, Y.; Qi, Z.-D.; Saito, T.; Isogai, A. Molar Masses and Molar Mass Distributions of Chitin and Acid-Hydrolyzed Chitin. *Biomacromolecules* **2017**, *18*, 4357–4363. [[CrossRef](#)]
13. Berezina, N. Production and Application of Chitin. *Phys. Sci. Rev.* **2016**, *1*. [[CrossRef](#)]
14. Aranaz, I.; Alcántara, A.R.; Civera, M.C.; Arias, C.; Elorza, B.; Heras Caballero, A.; Acosta, N. Chitosan: An Overview of Its Properties and Applications. *Polymers* **2021**, *13*, 3256. [[CrossRef](#)] [[PubMed](#)]
15. Dimzon, I.K.D.; Ebert, J.; Knepper, T.P. The Interaction of Chitosan and Olive Oil: Effects of Degree of Deacetylation and Degree of Polymerization. *Carbohydr. Polym.* **2013**, *92*, 564–570. [[CrossRef](#)] [[PubMed](#)]
16. Kaczmarek, M.B.; Struszczyk-Swita, K.; Li, X.; Szczesna-Antczak, M.; Daroch, M. Enzymatic Modifications of Chitin, Chitosan, and Chitooligosaccharides. *Front. Bioeng. Biotechnol.* **2019**, *7*, 243. [[CrossRef](#)] [[PubMed](#)]
17. Mourya, V.K.; Inamdar, N.N. Chitosan-Modifications and Applications: Opportunities Galore. *React. Funct. Polym.* **2008**, *68*, 1013–1051. [[CrossRef](#)]
18. Kumirska, J.; Czerwicka, M.; Kaczyński, Z.; Bychowska, A.; Brzozowski, K.; Thöming, J.; Stepnowski, P. Application of Spectroscopic Methods for Structural Analysis of Chitin and Chitosan. *Mar. Drugs* **2010**, *8*, 1567–1636. [[CrossRef](#)]
19. Brugnerotto, J.; Desbrières, J.; Heux, L.; Mazeau, K.; Rinaudo, M. Overview on Structural Characterization of Chitosan Molecules in Relation with Their Behavior in Solution. *Macromol. Symp.* **2001**, *168*, 1–20. [[CrossRef](#)]
20. Rusu-Balaita, L.; Desbrières, J.; Rinaudo, M. Formation of a Biocompatible Polyelectrolyte Complex: Chitosan-Hyaluronan Complex Stability. *Polym. Bull.* **2003**, *50*, 91–98. [[CrossRef](#)]
21. Lavertu, M.; Xia, Z.; Serreqi, A.N.; Berrada, M.; Rodrigues, A.; Wang, D.; Buschmann, M.D.; Gupta, A. A Validated ¹H NMR Method for the Determination of the Degree of Deacetylation of Chitosan. *J. Pharm. Biomed. Anal.* **2003**, *32*, 1149–1158. [[CrossRef](#)]
22. Roberts, G.A.F. The Road Is Long. In Proceedings of the 8th International Conference of the European Chitin Society, Antalya, Turkey, 8–11 September 2007.
23. Basa, S.; Nampally, M.; Honorato, T.; Das, S.N.; Podile, A.R.; El Gueddari, N.E.; Moerschbacher, B.M. The Pattern of Acetylation Defines the Priming Activity of Chitosan Tetramers. *J. Am. Chem. Soc.* **2020**, *142*, 1975–1986. [[CrossRef](#)]
24. Lopez, J.M.; Sánchez, L.F.; Nakamatsu, J.; Maruenda, H. Study of the Acetylation Pattern of Chitosan by Pure Shift NMR. *Anal. Chem.* **2020**, *92*, 12250–12256. [[CrossRef](#)]
25. World Bio Mark. Insights. The Chitosan Packaging Industry Is only just Beginning. 2022. Available online: <https://worldbiomarketinsights.com/the-chitosan-packaging-industry-is-only-just-beginning/> (accessed on 22 September 2022).
26. Chitosan Market Size, Price Trends, Analysis & Forecast 2022–2027. Available online: <https://www.imarcgroup.com/chitosan-market> (accessed on 22 September 2022).
27. Pappalardo, V.; Remadi, Y.; Cipolla, L.; Scotti, N.; Ravasio, N.; Zaccheria, F. Fishery Waste Valorization: Sulfated ZrO₂ as a Heterogeneous Catalyst for Chitin and Chitosan Depolymerization. *Front. Chem.* **2022**, *10*, 1057461. [[CrossRef](#)] [[PubMed](#)]
28. Sacramento, M.M.A.; Borges, J.; Correia, F.J.S.; Calado, R.; Rodrigues, J.M.M.; Patrício, S.G.; Mano, J.F. Green Approaches for Extraction, Chemical Modification and Processing of Marine Polysaccharides for Biomedical Applications. *Front. Bioeng. Biotechnol.* **2022**, *10*, 1041102. [[CrossRef](#)] [[PubMed](#)]
29. Kou, S.G.; Peters, L.M.; Mucalo, M.R. Chitosan: A Review of Sources and Preparation Methods. *Int. J. Biol. Macromol.* **2021**, *169*, 85–94. [[CrossRef](#)] [[PubMed](#)]
30. Pellis, A.; Guebitz, G.M.; Nyanhongo, G.S. Chitosan: Sources, Processing and Modification Techniques. *Gels* **2022**, *8*, 393. [[CrossRef](#)]
31. Doan, C.T.; Tran, T.N.; Nguyen, V.B.; Vo, T.P.K.; Nguyen, A.D.; Wang, S.-L. Chitin Extraction from Shrimp Waste by Liquid Fermentation Using an Alkaline Protease-Producing Strain, *Brevibacillus Parabrevis*. *Int. J. Biol. Macromol.* **2019**, *131*, 706–715. [[CrossRef](#)] [[PubMed](#)]
32. Casadidio, C.; Peregrina, D.V.; Gigliobianco, M.R.; Deng, S.; Censi, R.; Di Martino, P. Chitin and Chitosans: Characteristics, Eco-Friendly Processes, and Applications in Cosmetic Science. *Mar. Drugs* **2019**, *17*, 369. [[CrossRef](#)] [[PubMed](#)]
33. Philibert, T.; Lee, B.H.; Fabien, N. Current Status and New Perspectives on Chitin and Chitosan as Functional Biopolymers. *Appl. Biochem. Biotechnol.* **2017**, *181*, 1314–1337. [[CrossRef](#)]
34. Ghormade, V.; Pathan, E.K.; Deshpande, M.V. Can Fungi Compete with Marine Sources for Chitosan Production? *Int. J. Biol. Macromol.* **2017**, *104*, 1415–1421. [[CrossRef](#)]
35. Kurakula, M. Prospection of Recent Chitosan Biomedical Trends: Evidence from Patent Analysis (2009–2020). *Int. J. Biol. Macromol.* **2020**, *165*, 1924–1938. [[CrossRef](#)]
36. Kurita, K. Chitin and Chitosan: Functional Biopolymers from Marine Crustaceans. *Mar. Biotechnol.* **2006**, *8*, 203–226. [[CrossRef](#)] [[PubMed](#)]
37. Brasselet, C.; Pierre, G.; Dubessay, P.; Dols-Lafargue, M.; Coulon, J.; Maupeu, J.; Vallet-Courbin, A.; de Baynast, H.; Doco, T.; Michaud, P.; et al. Modification of Chitosan for the Generation of Functional Derivatives. *Appl. Sci.* **2019**, *9*, 1321. [[CrossRef](#)]
38. Cohen, E.; Poverenov, E. Hydrophilic Chitosan Derivatives: Synthesis and Applications. *Chem. Eur. J.* **2022**, *28*, e202202156. [[CrossRef](#)] [[PubMed](#)]

39. Shariatinia, Z. Carboxymethyl Chitosan: Properties and Biomedical Applications. *Int. J. Biol. Macromol.* **2018**, *120*, 1406–1419. [[CrossRef](#)]
40. Dimassi, S.; Tabary, N.; Chai, F.; Blanchemain, N.; Martel, B. Sulfonated and Sulfated Chitosan Derivatives for Biomedical Applications: A Review. *Carbohydr. Polym.* **2018**, *202*, 382–396. [[CrossRef](#)]
41. Jayakumar, R.; Reis, R.L.; Mano, J.F. Chemistry and Applications of Phosphorylated Chitin and Chitosan. *E-Polym.* **2006**, *6*. [[CrossRef](#)]
42. Jothimani, B.; Sureshkumar, S.; Venkatachalapathy, B. Hydrophobic Structural Modification of Chitosan and Its Impact on Nanoparticle Synthesis—A Physicochemical Study. *Carbohydr. Polym.* **2017**, *173*, 714–720. [[CrossRef](#)] [[PubMed](#)]
43. Philippova, O.; Korchagina, E. Chitosan and Its Hydrophobic Derivatives: Preparation and Aggregation in Dilute Aqueous Solutions. *Polym. Sci. Ser. A* **2012**, *54*, 552–572. [[CrossRef](#)]
44. Elsabee, M.Z.; Morsi, R.E.; Al-Sabagh, A.M. Surface Active Properties of Chitosan and Its Derivatives. *Colloids Surf. B Biointerfaces* **2009**, *74*, 1–16. [[CrossRef](#)] [[PubMed](#)]
45. Desbrières, J.; Martinez, C.; Rinaudo, M. Hydrophobic Derivatives of Chitosan: Characterization and Rheological Behaviour. *Int. J. Biol. Macromol.* **1996**, *19*, 21–28. [[CrossRef](#)] [[PubMed](#)]
46. Dowling, M.B.; Smith, W.; Balogh, P.; Duggan, M.J.; MacIntire, I.C.; Harris, E.; Mesar, T.; Raghavan, S.R.; King, D.R. Hydrophobically-Modified Chitosan Foam: Description and Hemostatic Efficacy. *J. Surg. Res.* **2015**, *193*, 316–323. [[CrossRef](#)] [[PubMed](#)]
47. Alkabli, J. Progress in Preparation of Thiolated, Crosslinked, and Imino-Chitosan Derivatives Targeting Specific Applications. *Eur. Polym. J.* **2022**, *165*, 110998. [[CrossRef](#)]
48. Federer, C.; Kurpiers, M.; Bernkop-Schnürch, A. Thiolated Chitosans: A Multi-Talented Class of Polymers for Various Applications. *Biomacromolecules* **2021**, *22*, 24–56. [[CrossRef](#)] [[PubMed](#)]
49. Summonte, S.; Racaniello, G.F.; Lopodota, A.; Denora, N.; Bernkop-Schnürch, A. Thiolated Polymeric Hydrogels for Biomedical Application: Cross-Linking Mechanisms. *J. Control. Release* **2021**, *330*, 470–482. [[CrossRef](#)] [[PubMed](#)]
50. Wibel, R.; Braun, D.E.; Hämmerle, L.; Jörgensen, A.M.; Knoll, P.; Salvenmoser, W.; Steinbring, C.; Bernkop-Schnürch, A. In Vitro Investigation of Thiolated Chitosan Derivatives as Mucoadhesive Coating Materials for Solid Lipid Nanoparticles. *Biomacromolecules* **2021**, *22*, 3980–3991. [[CrossRef](#)]
51. Jin, H.; Wang, Z. Advances in Alkylated Chitosan and Its Applications for Hemostasis. *Macromol* **2022**, *2*, 346–360. [[CrossRef](#)]
52. Chapelle, C.; David, G.; Caillol, S.; Negrell, C.; Durand, G.; le Foll, M.D. Functionalization of Chitosan Oligomers: From Aliphatic Epoxide to Cardanol-Grafted Oligomers for Oil-in-Water Emulsions. *Biomacromolecules* **2021**, *22*, 846–854. [[CrossRef](#)]
53. Lu, Y.; Slomberg, D.L.; Schoenfish, M.H. Nitric Oxide-Releasing Chitosan Oligosaccharides as Antibacterial Agents. *Biomaterials* **2014**, *35*, 1716–1724. [[CrossRef](#)]
54. Hirano, S.; Ohe, Y.; Ono, H. Selective N-Acylation of Chitosan. *Carbohydr. Res.* **1976**, *47*, 315–320. [[CrossRef](#)]
55. Sashiwa, H.; Yamamori, N.; Ichinose, Y.; Sunamoto, J.; Aiba, S. Michael Reaction of Chitosan with Various Acryl Reagents in Water. *Biomacromolecules* **2003**, *4*, 1250–1254. [[CrossRef](#)]
56. Antony, R.; Arun, T.; Manickam, S.T.D. A Review on Applications of Chitosan-Based Schiff Bases. *Int. J. Biol. Macromol.* **2019**, *129*, 615–633. [[CrossRef](#)] [[PubMed](#)]
57. Fabiano, A.; Beconcini, D.; Migone, C.; Piras, A.M.; Zambito, Y. Quaternary Ammonium Chitosans: The Importance of the Positive Fixed Charge of the Drug Delivery Systems. *Int. J. Mol. Sci.* **2020**, *21*, 6617. [[CrossRef](#)] [[PubMed](#)]
58. Nagy, V.; Sahariah, P.; Hjälmarsdóttir, M.Á.; Másson, M. Chitosan-Hydroxycinnamic Acid Conjugates: Optimization of the Synthesis and Investigation of the Structure Activity Relationship. *Carbohydr. Polym.* **2022**, *277*, 118896. [[CrossRef](#)] [[PubMed](#)]
59. Guzman, J.D. Natural Cinnamic Acids, Synthetic Derivatives and Hybrids with Antimicrobial Activity. *Mol. Basel Switz.* **2014**, *19*, 19292–19349. [[CrossRef](#)]
60. Orsini, S.F.; Cipolla, L.; Petroni, S.; Dirè, S.; Ceccato, R.; Callone, E.; Bongiovanni, R.; Dalle Vacche, S.; Di Credico, B.; Mostoni, S.; et al. Synthesis and Characterization of Alkoxysilane-Bearing Photoreversible Cinnamic Side Groups: A Promising Building-Block for the Design of Multifunctional Silica Nanoparticles. *Langmuir* **2022**, *38*, 15662–15671. [[CrossRef](#)] [[PubMed](#)]
61. Kurita, K.; Ikeda, H.; Shimojoh, M.; Yang, J. N-Phthaloylated Chitosan as an Essential Precursor for Controlled Chemical Modifications of Chitosan: Synthesis and Evaluation. *Polym. J.* **2007**, *39*, 945–952. [[CrossRef](#)]
62. Kurita, K.; Ikeda, H.; Yoshida, Y.; Shimojoh, M.; Harata, M. Chemoselective Protection of the Amino Groups of Chitosan by Controlled Phthaloylation: Facile Preparation of a Precursor Useful for Chemical Modifications. *Biomacromolecules* **2002**, *3*, 1–4. [[CrossRef](#)]
63. Torii, Y.; Ikeda, H.; Shimojoh, M.; Kurita, K. Chemoselective Protection of Chitosan by Dichlorophthaloylation: Preparation of a Key Intermediate for Chemical Modifications. *Polym. Bull.* **2009**, *62*, 749–759. [[CrossRef](#)]
64. Wang, W.; Meng, Q.; Li, Q.; Liu, J.; Zhou, M.; Jin, Z.; Zhao, K. Chitosan Derivatives and Their Application in Biomedicine. *Int. J. Mol. Sci.* **2020**, *21*, 487. [[CrossRef](#)]
65. Zampano, G.; Bertoldo, M.; Ciardelli, F. Defined Chitosan-Based Networks by C-6-Azide-Alkyne “Click” Reaction. *React. Funct. Polym.* **2010**, *70*, 272–281. [[CrossRef](#)]
66. Revuelta, J.; Fraile, I.; T. Monterrey, D.; Peña, N.; Benito-Arenas, R.; Bastida, A.; Fernández-Mayoralas, A.; García-Junceda, E. Heparanized Chitosans: Towards the Third Generation of Chitinous Biomaterials. *Mater. Horiz.* **2021**, *8*, 2596–2614. [[CrossRef](#)]

67. Zhao, D.; Xu, J.; Wang, L.; Du, J.; Dong, K.; Wang, C.; Liu, X. Study of Two Chitosan Derivatives Phosphorylated at Hydroxyl or Amino Groups for Application as Flocculants. *J. Appl. Polym. Sci.* **2012**, *125*, E299–E305. [[CrossRef](#)]
68. Shokri, Z.; Seidi, F.; Saeb, M.R.; Jin, Y.; Li, C.; Xiao, H. Elucidating the Impact of Enzymatic Modifications on the Structure, Properties, and Applications of Cellulose, Chitosan, Starch and Their Derivatives: A Review. *Mater. Today Chem.* **2022**, *24*, 100780. [[CrossRef](#)]
69. Linhorst, M.; Wattjes, J.; Moerschbacher, B.M. Chitin Deacetylase as a Biocatalyst for the Selective N-Acylation of Chitosan Oligo- and Polymers. *ACS Catal.* **2021**, *11*, 14456–14466. [[CrossRef](#)]
70. Li, X.; Li, S.; Liang, X.; McClements, D.J.; Liu, X.; Liu, F. Applications of Oxidases in Modification of Food Molecules and Colloidal Systems: Laccase, Peroxidase and Tyrosinase. *Trends Food Sci. Technol.* **2020**, *103*, 78–93. [[CrossRef](#)]
71. Liu, Y.; Zhang, B.; Javvaji, V.; Kim, E.; Lee, M.E.; Raghavan, S.R.; Wang, Q.; Payne, G.F. Tyrosinase-Mediated Grafting and Crosslinking of Natural Phenols Confers Functional Properties to Chitosan. *Biochem. Eng. J.* **2014**, *89*, 21–27. [[CrossRef](#)]
72. Liu, N.; Ni, S.; Gao, H.; Chang, Y.; Fu, Y.; Liu, W.; Qin, M. Laccase-Catalyzed Grafting of Lauryl Gallate on Chitosan to Improve Its Antioxidant and Hydrophobic Properties. *Biomacromolecules* **2021**, *22*, 4501–4509. [[CrossRef](#)]
73. Xu, L.; Zhang, N.; Wang, Q.; Yuan, J.; Yu, Y.; Wang, P.; Fan, X. Eco-Friendly Grafting of Chitosan as a Biopolymer onto Wool Fabrics Using Horseradish Peroxidase. *Fibers Polym.* **2019**, *20*, 261–270. [[CrossRef](#)]
74. Aljawish, A.; Chevlot, I.; Jasniowski, J.; Scher, J.; Muniglia, L. Enzymatic Synthesis of Chitosan Derivatives and Their Potential Applications. *J. Mol. Catal. B Enzym.* **2015**, *112*, 25–39. [[CrossRef](#)]
75. Marsili, L.; Dal Bo, M.; Berti, F.; Toffoli, G. Chitosan-Based Biocompatible Copolymers for Thermoresponsive Drug Delivery Systems: On the Development of a Standardization System. *Pharmaceutics* **2021**, *13*, 1876. [[CrossRef](#)]
76. Acciaretto, F.; Vesentini, S.; Cipolla, L. Fabrication Strategies towards Hydrogels for Biomedical Application: Chemical and Mechanical Insights. *Chem. Asian J.* **2022**, *17*, e202200797. [[CrossRef](#)] [[PubMed](#)]
77. Sanchez-Salvador, J.L.; Balea, A.; Monte, M.C.; Negro, C.; Blanco, A. Chitosan Grafted/Cross-Linked with Biodegradable Polymers: A Review. *Int. J. Biol. Macromol.* **2021**, *178*, 325–343. [[CrossRef](#)] [[PubMed](#)]
78. Hasnain, M.S.; Dey, S.; Nayak, A.K. Chapter 12—Graft Copolymers of Chitosan in Drug Delivery Applications. In *Chitosan in Drug Delivery*; Hasnain, M.S., Beg, S., Nayak, A.K., Eds.; Academic Press: Cambridge, MA, USA, 2022; pp. 301–322. ISBN 978-0-12-819336-5.
79. Kumar, D.; Gihar, S.; Shrivash, M.K.; Kumar, P.; Kundu, P.P. A Review on the Synthesis of Graft Copolymers of Chitosan and Their Potential Applications. *Int. J. Biol. Macromol.* **2020**, *163*, 2097–2112. [[CrossRef](#)]
80. Bhavsar, C.; Momin, M.; Gharat, S.; Omri, A. Functionalized and Graft Copolymers of Chitosan and Its Pharmaceutical Applications. *Expert Opin. Drug Deliv.* **2017**, *14*, 1189–1204. [[CrossRef](#)] [[PubMed](#)]
81. Thakur, V.K.; Thakur, M.K. Recent Advances in Graft Copolymerization and Applications of Chitosan: A Review. *ACS Sustain. Chem. Eng.* **2014**, *2*, 2637–2652. [[CrossRef](#)]
82. Russo, L.; Battocchio, C.; Secchi, V.; Magnano, E.; Nappini, S.; Taraballi, F.; Gabrielli, L.; Comelli, F.; Papagni, A.; Costa, B.; et al. Thiol–Ene Mediated Neoglycosylation of Collagen Patches: A Preliminary Study. *Langmuir* **2014**, *30*, 1336–1342. [[CrossRef](#)]
83. Kritchenkov, A.S.; Skorik, Y.A. Click Reactions in Chitosan Chemistry. *Russ. Chem. Bull.* **2017**, *66*, 769–781. [[CrossRef](#)]
84. Bini, D.; Russo, L.; Battocchio, C.; Natalello, A.; Polzonetti, G.; Doglia, S.M.; Nicotra, F.; Cipolla, L. Dendron Synthesis and Carbohydrate Immobilization on a Biomaterial Surface by a Double-Click Reaction. *Org. Lett.* **2014**, *16*, 1298–1301. [[CrossRef](#)]
85. Negm, N.A.; Hefni, H.H.H.; Abd-Elaal, A.A.A.; Badr, E.A.; Abou Kana, M.T.H. Advancement on Modification of Chitosan Biopolymer and Its Potential Applications. *Int. J. Biol. Macromol.* **2020**, *152*, 681–702. [[CrossRef](#)]
86. Chen, Q.; Qi, Y.; Jiang, Y.; Quan, W.; Luo, H.; Wu, K.; Li, S.; Ouyang, Q. Progress in Research of Chitosan Chemical Modification Technologies and Their Applications. *Mar. Drugs* **2022**, *20*, 536. [[CrossRef](#)]
87. Bakshi, P.S.; Selvakumar, D.; Kadirvelu, K.; Kumar, N.S. Chitosan as an Environment Friendly Biomaterial—A Review on Recent Modifications and Applications. *Int. J. Biol. Macromol.* **2020**, *150*, 1072–1083. [[CrossRef](#)] [[PubMed](#)]
88. Yu, D.; Feng, J.; You, H.; Zhou, S.; Bai, Y.; He, J.; Cao, H.; Che, Q.; Guo, J.; Su, Z. The Microstructure, Antibacterial and Antitumor Activities of Chitosan Oligosaccharides and Derivatives. *Mar. Drugs* **2022**, *20*, 69. [[CrossRef](#)] [[PubMed](#)]
89. Ferreira, L.M.B.; dos Santos, A.M.; Boni, F.I.; dos Santos, K.C.; Robusti, L.M.G.; de Souza, M.P.C.; Ferreira, N.N.; Carvalho, S.G.; Cardoso, V.M.O.; Chorilli, M.; et al. Design of Chitosan-Based Particle Systems: A Review of the Physicochemical Foundations for Tailored Properties. *Carbohydr. Polym.* **2020**, *250*, 116968. [[CrossRef](#)] [[PubMed](#)]
90. Rinaudo, M. Chitin and Chitosan: Properties and Applications. *Prog. Polym. Sci.* **2006**, *31*, 603–632. [[CrossRef](#)]
91. Sogias, I.A.; Khutoryanskiy, V.V.; Williams, A.C. Exploring the Factors Affecting the Solubility of Chitosan in Water. *Macromol. Chem. Phys.* **2010**, *211*, 426–433. [[CrossRef](#)]
92. Fernando, L.D.; Dickwella Widanage, M.C.; Penfield, J.; Lipton, A.S.; Washton, N.; Latgé, J.-P.; Wang, P.; Zhang, L.; Wang, T. Structural Polymorphism of Chitin and Chitosan in Fungal Cell Walls From Solid-State NMR and Principal Component Analysis. *Front. Mol. Biosci.* **2021**, *8*, 727053. [[CrossRef](#)]
93. Faria, R.R.; Guerra, R.F.; de Sousa Neto, L.R.; Motta, L.F.; de Franca, E.F. Computational Study of Polymorphic Structures of α - and β - Chitin and Chitosan in Aqueous Solution. *J. Mol. Graph. Model.* **2016**, *63*, 78–84. [[CrossRef](#)]
94. Pillai, C.K.S.; Paul, W.; Sharma, C.P. Chitin and Chitosan Polymers: Chemistry, Solubility and Fiber Formation. *Prog. Polym. Sci.* **2009**, *34*, 641–678. [[CrossRef](#)]

95. Zargar, V.; Asghari, M.; Dashti, A. A Review on Chitin and Chitosan Polymers: Structure, Chemistry, Solubility, Derivatives, and Applications. *ChemBioEng Rev.* **2015**, *2*, 204–226. [[CrossRef](#)]
96. Li, B.; Wang, J.; Moustafa, M.E.; Yang, H. Ecofriendly Method to Dissolve Chitosan in Plain Water. *ACS Biomater. Sci. Eng.* **2019**, *5*, 6355–6360. [[CrossRef](#)]
97. Bellich, B.; D'Agostino, I.; Semeraro, S.; Gamini, A.; Cesàro, A. "The Good, the Bad and the Ugly" of Chitosans. *Mar. Drugs* **2016**, *14*, 99. [[CrossRef](#)]
98. Freitas, E.D.; Moura, C.F.; Kerwald, J.; Beppu, M.M. An Overview of Current Knowledge on the Properties, Synthesis and Applications of Quaternary Chitosan Derivatives. *Polymers* **2020**, *12*, 2878. [[CrossRef](#)]
99. Wang, Z.; Nie, J.; Qin, W.; Hu, Q.; Tang, B.Z. Gelation Process Visualized by Aggregation-Induced Emission Fluorogens. *Nat. Commun.* **2016**, *7*, 12033. [[CrossRef](#)]
100. Ru, G.; Wu, S.; Yan, X.; Liu, B.; Gong, P.; Wang, L.; Feng, J. Inverse Solubility of Chitin/Chitosan in Aqueous Alkali Solvents at Low Temperature. *Carbohydr. Polym.* **2019**, *206*, 487–492. [[CrossRef](#)] [[PubMed](#)]
101. Nishimura, S.; Kohgo, O.; Kurita, K.; Kuzuhara, H. Chemospecific Manipulations of a Rigid Polysaccharide: Syntheses of Novel Chitosan Derivatives with Excellent Solubility in Common Organic Solvents by Regioselective Chemical Modifications. *Macromolecules* **1991**, *24*, 4745–4748. [[CrossRef](#)]
102. Wang, S.; Sha, J.; Wang, W.; Qin, C.; Li, W.; Qin, C. Superhydrophobic Surfaces Generated by One-Pot Spray-Coating of Chitosan-Based Nanoparticles. *Carbohydr. Polym.* **2018**, *195*, 39–44. [[CrossRef](#)] [[PubMed](#)]
103. Tagliaro, I.; Seccia, S.; Pellegrini, B.; Bertini, S.; Antonini, C. Chitosan-Based Coatings with Tunable Transparency and Superhydrophobicity: A Solvent-Free and Fluorine-Free Approach by Stearoyl Derivatization. *Carbohydr. Polym.* **2023**, *302*, 120424. [[CrossRef](#)] [[PubMed](#)]
104. Blanco, A.; García-Abuín, A.; Gómez-Díaz, D.; Navaza, J.M. Physicochemical Characterization of Chitosan Derivatives. *CyTA J. Food* **2013**, *11*, 190–197. [[CrossRef](#)]
105. Ways, T.M.M.; Lau, W.M.; Khutoryanskiy, V.V. Chitosan and Its Derivatives for Application in Mucoadhesive Drug Delivery Systems. *Polymers* **2018**, *10*, 267. [[CrossRef](#)] [[PubMed](#)]
106. Mati-Baouche, N.; Elchinger, P.-H.; de Baynast, H.; Pierre, G.; Delattre, C.; Michaud, P. Chitosan as an Adhesive. *Eur. Polym. J.* **2014**, *60*, 198–212. [[CrossRef](#)]
107. Sharkawy, A.; Barreiro, M.F.; Rodrigues, A.E. Chitosan-Based Pickering Emulsions and Their Applications: A Review. *Carbohydr. Polym.* **2020**, *250*, 116885. [[CrossRef](#)]
108. Wang, X.-Y.; Heuzey, M.-C. Chitosan-Based Conventional and Pickering Emulsions with Long-Term Stability. *Langmuir* **2016**, *32*, 929–936. [[CrossRef](#)]
109. Yilmaz Atay, H. Antibacterial Activity of Chitosan-Based Systems. In *Functional Chitosan*; Springer: Singapore, 2020; pp. 457–489. [[CrossRef](#)]
110. Adhikari, H.S.; Yadav, P.N. Anticancer Activity of Chitosan, Chitosan Derivatives, and Their Mechanism of Action. *Int. J. Biomater.* **2018**, *2018*, 2952085. [[CrossRef](#)]
111. Dhakshinamoorthy, A.; Jacob, M.; Vignesh, N.S.; Varalakshmi, P. Pristine and Modified Chitosan as Solid Catalysts for Catalysis and Biodiesel Production: A Minireview. *Int. J. Biol. Macromol.* **2021**, *167*, 807–833. [[CrossRef](#)] [[PubMed](#)]
112. Vidal, R.R.L.; Moraes, J.S. Removal of Organic Pollutants from Wastewater Using Chitosan: A Literature Review. *Int. J. Environ. Sci. Technol.* **2019**, *16*, 1741–1754. [[CrossRef](#)]
113. Omer, A.M.; Dey, R.; Eltaweil, A.S.; Abd El-Monaem, E.M.; Ziora, Z.M. Insights into Recent Advances of Chitosan-Based Adsorbents for Sustainable Removal of Heavy Metals and Anions. *Arab. J. Chem.* **2022**, *15*, 103543. [[CrossRef](#)]
114. Annu; Raja, A.N. Recent Development in Chitosan-Based Electrochemical Sensors and Its Sensing Application. *Int. J. Biol. Macromol.* **2020**, *164*, 4231–4244. [[CrossRef](#)]
115. Jaworska, M.M.; Antos, D.; Górak, A. Review on the Application of Chitin and Chitosan in Chromatography. *React. Funct. Polym.* **2020**, *152*, 104606. [[CrossRef](#)]
116. Klinkesorn, U. The Role of Chitosan in Emulsion Formation and Stabilization. *Food Rev. Int.* **2013**, *29*, 371–393. [[CrossRef](#)]
117. Ladiè, R.; Cosentino, C.; Tagliaro, I.; Antonini, C.; Bianchini, G.; Bertini, S. Supramolecular Structuring of Hyaluronan-Lactose-Modified Chitosan Matrix: Towards High-Performance Biopolymers with Excellent Biodegradation. *Biomolecules* **2021**, *11*, 389. [[CrossRef](#)]
118. Caporale, N.; Leemans, M.; Birgersson, L.; Germain, P.-L.; Cheroni, C.; Borbély, G.; Engdahl, E.; Lindh, C.; Bressan, R.B.; Cavallo, F.; et al. From Cohorts to Molecules: Adverse Impacts of Endocrine Disrupting Mixtures. *Science* **2022**, *375*, eabe8244. [[CrossRef](#)]
119. Pavinatto, A.; de Almeida Mattos, A.V.; Malpass, A.C.G.; Okura, M.H.; Balogh, D.T.; Sanfelice, R.C. Coating with Chitosan-Based Edible Films for Mechanical/Biological Protection of Strawberries. *Int. J. Biol. Macromol.* **2020**, *151*, 1004–1011. [[CrossRef](#)] [[PubMed](#)]
120. Hoque, M.; Gupta, S.; Santhosh, R.; Syed, I.; Sarkar, P. 3—Biopolymer-Based Edible Films and Coatings for Food Applications. In *Food, Medical, and Environmental Applications of Polysaccharides*; Pal, K., Banerjee, I., Sarkar, P., Bit, A., Kim, D., Anis, A., Maji, S., Eds.; Elsevier: Amsterdam, The Netherlands, 2021; pp. 81–107. ISBN 978-0-12-819239-9.
121. Vu, K.D.; Hollingsworth, R.G.; Leroux, E.; Salmieri, S.; Lacroix, M. Development of Edible Bioactive Coating Based on Modified Chitosan for Increasing the Shelf Life of Strawberries. *Food Res. Int.* **2011**, *44*, 198–203. [[CrossRef](#)]

122. Quintana, S.E.; Llalla, O.; García-Zapateiro, L.A.; García-Risco, M.R.; Fornari, T. Preparation and Characterization of Licorice-Chitosan Coatings for Postharvest Treatment of Fresh Strawberries. *Appl. Sci.* **2020**, *10*, 8431. [[CrossRef](#)]
123. Salvati Manni, L.; Assenza, S.; Duss, M.; Vallooran, J.J.; Juranyi, F.; Jurt, S.; Zerbe, O.; Landau, E.M.; Mezzenga, R. Soft Biomimetic Nanoconfinement Promotes Amorphous Water over Ice. *Nat. Nanotechnol.* **2019**, *14*, 609–615. [[CrossRef](#)]
124. Kocherbitov, V. The Nature of Nonfreezing Water in Carbohydrate Polymers. *Carbohydr. Polym.* **2016**, *150*, 353–358. [[CrossRef](#)]
125. Harnkarnsujarit, N.; Kawai, K.; Suzuki, T. Impacts of Freezing and Molecular Size on Structure, Mechanical Properties and Recrystallization of Freeze-Thawed Polysaccharide Gels. *LWT Food Sci. Technol.* **2016**, *68*, 190–201. [[CrossRef](#)]
126. Maity, T.; Saxena, A.; Raju, P.S. Use of Hydrocolloids as Cryoprotectant for Frozen Foods. *Crit. Rev. Food Sci. Nutr.* **2018**, *58*, 420–435. [[CrossRef](#)]
127. Abdellatif, A.A.H.; Mohammed, A.M.; Saleem, I.; Alsharidah, M.; Al Rugaie, O.; Ahmed, F.; Osman, S.K. Smart Injectable Chitosan Hydrogels Loaded with 5-Fluorouracil for the Treatment of Breast Cancer. *Pharmaceutics* **2022**, *14*, 661. [[CrossRef](#)]
128. Tewari, A.K.; Upadhyay, S.C.; Kumar, M.; Pathak, K.; Kaushik, D.; Verma, R.; Bhatt, S.; Massoud, E.E.S.; Rahman, M.H.; Cavalu, S. Insights on Development Aspects of Polymeric Nanocarriers: The Translation from Bench to Clinic. *Polymers* **2022**, *14*, 3545. [[CrossRef](#)]
129. Ali, A.; Ahmed, S. A Review on Chitosan and Its Nanocomposites in Drug Delivery. *Int. J. Biol. Macromol.* **2018**, *109*, 273–286. [[CrossRef](#)] [[PubMed](#)]
130. Parhi, R. Drug Delivery Applications of Chitin and Chitosan: A Review. *Environ. Chem. Lett.* **2020**, *18*, 577–594. [[CrossRef](#)]
131. Kurakula, M.; Raghavendra Naveen, N. Electrospinning: A Facile Technology Unfolding the Chitosan Based Drug Delivery and Biomedical Applications. *Eur. Polymer J.* **2021**, *147*, 110326. [[CrossRef](#)]
132. Patel, B.; Manne, R.; Patel, D.B.; Gorityala, S.; Palaniappan, A.; Kurakula, M. Chitosan as Functional Biomaterial for Designing Delivery Systems in Cardiac Therapies. *Gels* **2021**, *7*, 253. [[CrossRef](#)] [[PubMed](#)]
133. Hu, L.; Sun, Y.; Wu, Y. Advances in Chitosan-Based Drug Delivery Vehicles. *Nanoscale* **2013**, *5*, 3103–3111. [[CrossRef](#)]
134. Kurakula, M.; Gorityala, S.; Patel, D.B.; Basim, P.; Patel, B.; Kumar Jha, S. Trends of Chitosan Based Delivery Systems in Neuroregeneration and Functional Recovery in Spinal Cord Injuries. *Polysaccharides* **2021**, *2*, 519–537. [[CrossRef](#)]
135. Naskar, S.; Kuotsu, K.; Sharma, S. Chitosan-Based Nanoparticles as Drug Delivery Systems: A Review on Two Decades of Research. *J. Drug Target.* **2019**, *27*, 379–393. [[CrossRef](#)]
136. Valachová, K.; Šoltés, L. Self-Associating Polymers Chitosan and Hyaluronan for Constructing Composite Membranes as Skin-Wound Dressings Carrying Therapeutics. *Mol. Basel Switz.* **2021**, *26*, 2535. [[CrossRef](#)]
137. Rezaei, F.S.; Sharifianjazi, F.; Esmailkhanian, A.; Salehi, E. Chitosan films and scaffolds for regenerative medicine applications: A review. *Carbohydr. Polym.* **2021**, *273*, 118631. [[CrossRef](#)]
138. Peppas, N.A.; Bures, P.; Leobandung, W.; Ichikawa, H. Hydrogels in Pharmaceutical Formulations. *Eur. J. Pharm. Biopharm.* **2000**, *50*, 27–46. [[CrossRef](#)]
139. Fu, J.; Yang, F.; Guo, Z. The Chitosan Hydrogels: From Structure to Function. *New J. Chem.* **2018**, *42*, 17162–17180. [[CrossRef](#)]
140. Sacco, P.; Furlani, F.; De Marzo, G.; Marsich, E.; Paoletti, S.; Donati, I. Concepts for Developing Physical Gels of Chitosan and of Chitosan Derivatives. *Gels Basel Switz.* **2018**, *4*, 67. [[CrossRef](#)] [[PubMed](#)]
141. Berger, J.; Reist, M.; Mayer, J.M.; Felt, O.; Gurny, R. Structure and Interactions in Chitosan Hydrogels Formed by Complexation or Aggregation for Biomedical Applications. *Eur. J. Pharm. Biopharm.* **2004**, *57*, 35–52. [[CrossRef](#)] [[PubMed](#)]
142. Berger, J.; Reist, M.; Mayer, J.M.; Felt, O.; Peppas, N.A.; Gurny, R. Structure and Interactions in Covalently and Ionically Crosslinked Chitosan Hydrogels for Biomedical Applications. *Eur. J. Pharm. Biopharm. Off. J. Arbeitsgemeinschaft Pharm. Verfahrenstechnik EV* **2004**, *57*, 19–34. [[CrossRef](#)]
143. Sheng, Y.; Cao, C.; Liang, Z.; Yin, Z.-Z.; Gao, J.; Cai, W.; Kong, Y. Construction of a Dual-Drug Delivery System Based on Oxidized Alginate and Carboxymethyl Chitosan for Chemo-Photothermal Synergistic Therapy of Osteosarcoma. *Eur. Polym. J.* **2022**, *174*, 111331. [[CrossRef](#)]
144. García-Couce, J.; Tomás, M.; Fuentes, G.; Que, I.; Almirall, A.; Cruz, L.J. Chitosan/Pluronic F127 Thermosensitive Hydrogel as an Injectable Dexamethasone Delivery Carrier. *Gels* **2022**, *8*, 44. [[CrossRef](#)] [[PubMed](#)]
145. Hendi, A.; Hassan, M.U.; Elsherif, M.; Alqattan, B.; Park, S.; Yetisen, A.K.; Butt, H. Healthcare Applications of PH-Sensitive Hydrogel-Based Devices: A Review. *Int. J. Nanomed.* **2020**, *15*, 3887–3901. [[CrossRef](#)]
146. Qu, J.; Zhao, X.; Ma, P.X.; Guo, B. Injectable Antibacterial Conductive Hydrogels with Dual Response to an Electric Field and PH for Localized “Smart” Drug Release. *Acta Biomater.* **2018**, *72*, 55–69. [[CrossRef](#)]
147. Sgambato, A.; Cipolla, L.; Russo, L. Bioresponsive Hydrogels: Chemical Strategies and Perspectives in Tissue Engineering. *Gels* **2016**, *2*, 28. [[CrossRef](#)]
148. Sgambato, A.; Pastori, V.; Russo, L.; Vesentini, S.; Lecchi, M.; Cipolla, L. Neoglycosylated Collagen: Effect on Neuroblastoma F-11 Cell Lines. *Molecules* **2020**, *25*, 4361. [[CrossRef](#)]
149. Russo, L.; Cipolla, L. Glycomics: New Challenges and Opportunities in Regenerative Medicine. *Chem. Eur. J.* **2016**, *22*, 13380–13388. [[CrossRef](#)] [[PubMed](#)]
150. Russo, L.; Sgambato, A.; Lecchi, M.; Pastori, V.; Raspanti, M.; Natalello, A.; Doglia, S.M.; Nicotra, F.; Cipolla, L. Neoglycosylated Collagen Matrices Drive Neuronal Cells to Differentiate. *ACS Chem. Neurosci.* **2014**, *5*, 261–265. [[CrossRef](#)] [[PubMed](#)]
151. Liang, Y.; He, J.; Guo, B. Functional Hydrogels as Wound Dressing to Enhance Wound Healing. *ACS Nano* **2021**, *15*, 12687–12722. [[CrossRef](#)]

152. Morrish, C.; Whitehead, F.; Istivan, T.; Kasapis, S. The Effect of Trisodium Phosphate Crosslinking on the Diffusion Kinetics of Caffeine from Chitosan Networks. *Food Chem.* **2022**, *381*, 132272. [[CrossRef](#)] [[PubMed](#)]
153. Sacco, P.; Brun, F.; Donati, I.; Porrelli, D.; Paoletti, S.; Turco, G. On the Correlation between the Microscopic Structure and Properties of Phosphate-Cross-Linked Chitosan Gels. *ACS Appl. Mater. Interfaces* **2018**, *10*, 10761–10770. [[CrossRef](#)] [[PubMed](#)]
154. Martínez-Martínez, M.; Rodríguez-Berna, G.; Gonzalez-Alvarez, I.; Hernández, M.J.; Corma, A.; Bermejo, M.; Merino, V.; Gonzalez-Alvarez, M. Ionic Hydrogel Based on Chitosan Cross-Linked with 6-Phosphogluconic Trisodium Salt as a Drug Delivery System. *Biomacromolecules* **2018**, *19*, 1294–1304. [[CrossRef](#)]
155. Sacco, P.; Borgogna, M.; Travan, A.; Marsich, E.; Paoletti, S.; Asaro, F.; Grassi, M.; Donati, I. Polysaccharide-Based Networks from Homogeneous Chitosan-Tripolyphosphate Hydrogels: Synthesis and Characterization. *Biomacromolecules* **2014**, *15*, 3396–3405. [[CrossRef](#)]
156. Sacco, P.; Paoletti, S.; Cok, M.; Asaro, F.; Abrami, M.; Grassi, M.; Donati, I. Insight into the Ionotropic Gelation of Chitosan Using Tripolyphosphate and Pyrophosphate as Cross-Linkers. *Int. J. Biol. Macromol.* **2016**, *92*, 476–483. [[CrossRef](#)]
157. Supper, S.; Anton, N.; Seidel, N.; Riemenschnitter, M.; Schoch, C.; Vandamme, T. Rheological Study of Chitosan/Polyol-Phosphate Systems: Influence of the Polyol Part on the Thermo-Induced Gelation Mechanism. *Langmuir ACS J. Surf. Colloids* **2013**, *29*, 10229–10237. [[CrossRef](#)]
158. Supper, S.; Anton, N.; Seidel, N.; Riemenschnitter, M.; Curdy, C.; Vandamme, T. Thermosensitive Chitosan/Glycerophosphate-Based Hydrogel and Its Derivatives in Pharmaceutical and Biomedical Applications. *Expert Opin. Drug Deliv.* **2014**, *11*, 249–267. [[CrossRef](#)]
159. Saravanan, S.; Vimalraj, S.; Thanikaivelan, P.; Banudevi, S.; Manivasagam, G. A Review on Injectable Chitosan/Beta Glycerophosphate Hydrogels for Bone Tissue Regeneration. *Int. J. Biol. Macromol.* **2019**, *121*, 38–54. [[CrossRef](#)] [[PubMed](#)]
160. Supper, S.; Anton, N.; Boisclair, J.; Seidel, N.; Riemenschnitter, M.; Curdy, C.; Vandamme, T. Chitosan/Glucose 1-Phosphate as New Stable in Situ Forming Depot System for Controlled Drug Delivery. *Eur. J. Pharm. Biopharm. Off. J. Arbeitsgemeinschaft Pharm. Verfahrenstechnik EV* **2014**, *88*, 361–373. [[CrossRef](#)] [[PubMed](#)]
161. He, Y.; Guo, S.; Chang, R.; Zhang, D.; Ren, Y.; Guan, F.; Yao, M. Facile Preparation of Antibacterial Hydrogel with Multi-Functions Based on Carboxymethyl Chitosan and Oligomeric Procyanidin. *RSC Adv.* **2022**, *12*, 20897–20905. [[CrossRef](#)] [[PubMed](#)]
162. Wu, T.; Huang, J.; Jiang, Y.; Hu, Y.; Ye, X.; Liu, D.; Chen, J. Formation of Hydrogels Based on Chitosan/Alginate for the Delivery of Lysozyme and Their Antibacterial Activity. *Food Chem.* **2018**, *240*, 361–369. [[CrossRef](#)] [[PubMed](#)]
163. Neufeld, L.; Bianco-Peled, H. Pectin-Chitosan Physical Hydrogels as Potential Drug Delivery Vehicles. *Int. J. Biol. Macromol.* **2017**, *101*, 852–861. [[CrossRef](#)]
164. Zuliani, C.C.; Damas, I.I.; Andrade, K.C.; Westin, C.B.; Moraes, Â.M.; Coimbra, I.B. Chondrogenesis of Human Amniotic Fluid Stem Cells in Chitosan-Xanthan Scaffold for Cartilage Tissue Engineering. *Sci. Rep.* **2021**, *11*, 3063. [[CrossRef](#)]
165. Vieira de Souza, T.; Malmonge, S.M.; Santos, A.R. Development of a Chitosan and Hyaluronic Acid Hydrogel with Potential for Bioprinting Utilization: A Preliminary Study. *J. Biomater. Appl.* **2021**, *36*, 358–371. [[CrossRef](#)]
166. Quadrado, R.F.N.; Fajardo, A.R. Vapor-Induced Polyelectrolyte Complexation of Chitosan/Pectin: A Promising Strategy for the Preparation of Hydrogels for Controlled Drug Delivery. *J. Mol. Liq.* **2022**, *361*, 119604. [[CrossRef](#)]
167. Zarandona, I.; Bengoechea, C.; Álvarez-Castillo, E.; de la Caba, K.; Guerrero, A.; Guerrero, P. 3D Printed Chitosan-Pectin Hydrogels: From Rheological Characterization to Scaffold Development and Assessment. *Gels* **2021**, *7*, 175. [[CrossRef](#)]
168. Mousavi, S.; Khoshfetrat, A.B.; Khatami, N.; Ahmadian, M.; Rahbarghazi, R. Comparative Study of Collagen and Gelatin in Chitosan-Based Hydrogels for Effective Wound Dressing: Physical Properties and Fibroblastic Cell Behavior. *Biochem. Biophys. Res. Commun.* **2019**, *518*, 625–631. [[CrossRef](#)]
169. Li, Y.; Rodrigues, J.; Tomás, H. Injectable and Biodegradable Hydrogels: Gelation, Biodegradation and Biomedical Applications. *Chem. Soc. Rev.* **2012**, *41*, 2193–2221. [[CrossRef](#)] [[PubMed](#)]
170. Sánchez-Cid, P.; Jiménez-Rosado, M.; Rubio-Valle, J.F.; Romero, A.; Ostos, F.J.; Rafii-El-Idrissi Benhnia, M.; Perez-Puyana, V. Biocompatible and Thermoresistant Hydrogels Based on Collagen and Chitosan. *Polymers* **2022**, *14*, 272. [[CrossRef](#)] [[PubMed](#)]
171. Sergeeva, Y.N.; Huang, T.; Felix, O.; Jung, L.; Tropel, P.; Viville, S.; Decher, G. What Is Really Driving Cell-Surface Interactions? Layer-by-Layer Assembled Films May Help to Answer Questions Concerning Cell Attachment and Response to Biomaterials. *Biointerphases* **2016**, *11*, 019009. [[CrossRef](#)] [[PubMed](#)]
172. Chen, L.; Yan, C.; Zheng, Z. Functional Polymer Surfaces for Controlling Cell Behaviors. *Mater. Today* **2018**, *21*, 38–59. [[CrossRef](#)]
173. IUPAC. *Compendium of Chemical Terminology*, 2nd ed.; Blackwell Scientific Publications: Oxford, UK, 1997; ISBN 0-9678550-9-8.
174. Cui, L.; Jia, J.; Guo, Y.; Liu, Y.; Zhu, P. Preparation and Characterization of IPN Hydrogels Composed of Chitosan and Gelatin Cross-Linked by Genipin. *Carbohydr. Polym.* **2014**, *99*, 31–38. [[CrossRef](#)]
175. Wahid, F.; Hu, X.-H.; Chu, L.-Q.; Jia, S.-R.; Xie, Y.-Y.; Zhong, C. Development of Bacterial Cellulose/Chitosan Based Semi-Interpenetrating Hydrogels with Improved Mechanical and Antibacterial Properties. *Int. J. Biol. Macromol.* **2019**, *122*, 380–387. [[CrossRef](#)]
176. Dash, M.; Ferri, M.; Chiellini, F. Synthesis and Characterization of Semi-Interpenetrating Polymer Network Hydrogel Based on Chitosan and Poly(Methacryloylglycylglycine). *Mater. Chem. Phys.* **2012**, *135*, 1070–1076. [[CrossRef](#)]
177. Catoira, M.C.; González-Payo, J.; Fusaro, L.; Ramella, M.; Boccafoschi, F. Natural Hydrogels R&D Process: Technical and Regulatory Aspects for Industrial Implementation. *J. Mater. Sci. Mater. Med.* **2020**, *31*, 64. [[CrossRef](#)]

178. Song, J.; Zhang, C.; Kong, S.; Liu, F.; Hu, W.; Su, F.; Li, S. Novel Chitosan Based Metal-Organic Polyhedrons/Enzyme Hybrid Hydrogel with Antibacterial Activity to Promote Wound Healing. *Carbohydr. Polym.* **2022**, *291*, 119522. [[CrossRef](#)]
179. Mio, L.; Sacco, P.; Donati, I. Influence of Temperature and Polymer Concentration on the Nonlinear Response of Highly Acetylated Chitosan–Genipin Hydrogels. *Gels* **2022**, *8*, 194. [[CrossRef](#)]
180. Andrade del Olmo, J.; Alonso, J.M.; Sáez-Martínez, V.; Benito-Cid, S.; Moreno-Benítez, I.; Bengoa-Larrauri, M.; Pérez-González, R.; Vilas-Vilela, J.L.; Pérez-Álvarez, L. Self-Healing, Antibacterial and Anti-Inflammatory Chitosan-PEG Hydrogels for Ulcerated Skin Wound Healing and Drug Delivery. *Biomater. Adv.* **2022**, *139*, 212992. [[CrossRef](#)] [[PubMed](#)]
181. Moreira Teixeira, L.S.; Feijen, J.; van Blitterswijk, C.A.; Dijkstra, P.J.; Karperien, M. Enzyme-Catalyzed Crosslinkable Hydrogels: Emerging Strategies for Tissue Engineering. *Biomaterials* **2012**, *33*, 1281–1290. [[CrossRef](#)] [[PubMed](#)]
182. Zhou, S.; Bei, Z.; Wei, J.; Yan, X.; Wen, H.; Cao, Y.; Li, H. Mussel-Inspired Injectable Chitosan Hydrogel Modified with Catechol for Cell Adhesion and Cartilage Defect Repair. *J. Mater. Chem. B* **2022**, *10*, 1019–1030. [[CrossRef](#)] [[PubMed](#)]
183. Francis Suh, J.-K.; Matthew, H.W.T. Application of Chitosan-Based Polysaccharide Biomaterials in Cartilage Tissue Engineering: A Review. *Biomaterials* **2000**, *21*, 2589–2598. [[CrossRef](#)]
184. Liang, Y.; Zhao, X.; Ma, P.X.; Guo, B.; Du, Y.; Han, X. PH-Responsive Injectable Hydrogels with Mucosal Adhesiveness Based on Chitosan-Grafted-Dihydrocaffeic Acid and Oxidized Pullulan for Localized Drug Delivery. *J. Colloid Interface Sci.* **2019**, *536*, 224–234. [[CrossRef](#)]
185. Ryu, J.H.; Hong, S.; Lee, H. Bio-Inspired Adhesive Catechol-Conjugated Chitosan for Biomedical Applications: A Mini Review. *Acta Biomater.* **2015**, *27*, 101–115. [[CrossRef](#)]
186. Donati, I.; Stredanska, S.; Silvestrini, G.; Vetere, A.; Marcon, P.; Marsich, E.; Mozetic, P.; Gamini, A.; Paoletti, S.; Vittur, F. The Aggregation of Pig Articular Chondrocyte and Synthesis of Extracellular Matrix by a Lactose-Modified Chitosan. *Biomaterials* **2005**, *26*, 987–998. [[CrossRef](#)]
187. Furlani, F.; Sacco, P.; Scognamiglio, F.; Asaro, F.; Travan, A.; Borgogna, M.; Marsich, E.; Cok, M.; Paoletti, S.; Donati, I. Nucleation, Reorganization and Disassembly of an Active Network from Lactose-Modified Chitosan Mimicking Biological Matrices. *Carbohydr. Polym.* **2019**, *208*, 451–456. [[CrossRef](#)]
188. Scognamiglio, F.; Travan, A.; Donati, I.; Borgogna, M.; Marsich, E. A Hydrogel System Based on a Lactose-Modified Chitosan for Viscosupplementation in Osteoarthritis. *Carbohydr. Polym.* **2020**, *248*, 116787. [[CrossRef](#)]
189. Yeh, Y.Y.; Tsai, Y.T.; Wu, C.Y.; Tu, L.H.; Bai, M.Y.; Yeh, Y.C. The Role of Aldehyde-Functionalized Crosslinkers on the Property of Chitosan Hydrogels. *Macromol. Biosci.* **2022**, *22*, 2100477, Erratum in: *Macromol. Biosci.* **2022**, *22*, e2200366. [[CrossRef](#)]
190. Iftime, M.-M.; Morariu, S.; Marin, L. Salicyl-Imine-Chitosan Hydrogels: Supramolecular Architecturing as a Crosslinking Method toward Multifunctional Hydrogels. *Carbohydr. Polym.* **2017**, *165*, 39–50. [[CrossRef](#)] [[PubMed](#)]
191. Iftime, M.-M.; Mititelu Tartau, L.; Marin, L. New Formulations Based on Salicyl-Imine-Chitosan Hydrogels for Prolonged Drug Release. *Int. J. Biol. Macromol.* **2020**, *160*, 398–408. [[CrossRef](#)] [[PubMed](#)]
192. Marin, L.; Moraru, S.; Popescu, M.-C.; Nicolescu, A.; Zgardan, C.; Simionescu, B.C.; Barboiu, M. Out-of-Water Constitutional Self-Organization of Chitosan-Cinnamaldehyde Dynagels. *Chem. Weinh. Bergstr. Ger.* **2014**, *20*, 4814–4821. [[CrossRef](#)] [[PubMed](#)]
193. Iftime, M.-M.; Rosca, I.; Sandu, A.-I.; Marin, L. Chitosan Crosslinking with a Vanillin Isomer toward Self-Healing Hydrogels with Antifungal Activity. *Int. J. Biol. Macromol.* **2022**, *205*, 574–586. [[CrossRef](#)]
194. Faustini, M.; Nicole, L.; Ruiz-Hitzky, E.; Sanchez, C. History of Organic–Inorganic Hybrid Materials: Prehistory, Art, Science, and Advanced Applications. *Adv. Funct. Mater.* **2018**, *28*, 1704158. [[CrossRef](#)]
195. Jones, J.R. Review of Bioactive Glass: From Hench to Hybrids. *Acta Biomater.* **2013**, *9*, 4457–4486. [[CrossRef](#)]
196. Tallia, F.; Russo, L.; Li, S.; Orrin, A.L.H.; Shi, X.; Chen, S.; Steele, J.A.M.; Meille, S.; Chevalier, J.; Lee, P.D.; et al. Bouncing and 3D Printable Hybrids with Self-Healing Properties. *Mater. Horiz.* **2018**, *5*, 849–860. [[CrossRef](#)]
197. Connell, L.S.; Gabrielli, L.; Mahony, O.; Russo, L.; Cipolla, L.; Jones, J.R. Functionalizing Natural Polymers with Alkoxysilane Coupling Agents: Reacting 3-Glycidoxypropyl Trimethoxysilane with Poly(γ -Glutamic Acid) and Gelatin. *Polym. Chem.* **2017**, *8*, 1095–1103. [[CrossRef](#)]
198. Russo, L.; Landi, E.; Tampieri, A.; Natalello, A.; Doglia, S.M.; Gabrielli, L.; Cipolla, L.; Nicotra, F. Sugar-Decorated Hydroxyapatite: An Inorganic Material Bioactivated with Carbohydrates. *Carbohydr. Res.* **2011**, *346*, 1564–1568. [[CrossRef](#)]
199. Sandri, M.; Natalello, A.; Bini, D.; Gabrielli, L.; Cipolla, L.; Nicotra, F. Sweet and Salted: Sugars Meet Hydroxyapatite. *Synlett* **2011**, *2011*, 1845–1848. [[CrossRef](#)]
200. Russo, L.; Gabrielli, L.; Valliant, E.M.; Nicotra, F.; Jiménez-Barbero, J.; Cipolla, L.; Jones, J.R. Novel Silica/Bis(3-Aminopropyl) Polyethylene Glycol Inorganic/Organic Hybrids by Sol–Gel Chemistry. *Mater. Chem. Phys.* **2013**, *140*, 168–175. [[CrossRef](#)]
201. El Kadib, A.; Bousmina, M. Chitosan Bio-Based Organic–Inorganic Hybrid Aerogel Microspheres. *Chem. Eur. J.* **2012**, *18*, 8264–8277. [[CrossRef](#)] [[PubMed](#)]
202. Liang, J.-N.; Yan, L.-P.; Dong, Y.-F.; Liu, X.; Wu, G.; Zhao, N.-R. Robust and Nanostructured Chitosan–Silica Hybrids for Bone Repair Application. *J. Mater. Chem. B* **2020**, *8*, 5042–5051. [[CrossRef](#)]
203. Zhu, L.; Liu, Y.; Wang, A.; Zhu, Z.; Li, Y.; Zhu, C.; Che, Z.; Liu, T.; Liu, H.; Huang, L. Application of BMP in Bone Tissue Engineering. *Front. Bioeng. Biotechnol.* **2022**, *10*, 810880. [[CrossRef](#)]
204. Bessa, P.C.; Casal, M.; Reis, R.L. Bone Morphogenetic Proteins in Tissue Engineering: The Road from Laboratory to Clinic, Part II (BMP Delivery). *J. Tissue Eng. Regen. Med.* **2008**, *2*, 81–96. [[CrossRef](#)] [[PubMed](#)]

205. Gritsch, L.; Maqbool, M.; Mouriño, V.; Ciraldo, F.E.; Cresswell, M.; Jackson, P.R.; Lovell, C.; Boccaccini, A.R. Chitosan/Hydroxyapatite Composite Bone Tissue Engineering Scaffolds with Dual and Decoupled Therapeutic Ion Delivery: Copper and Strontium. *J. Mater. Chem. B* **2019**, *7*, 6109–6124. [[CrossRef](#)]
206. Mouriño, V.; Cattalini, J.P.; Boccaccini, A.R. Metallic Ions as Therapeutic Agents in Tissue Engineering Scaffolds: An Overview of Their Biological Applications and Strategies for New Developments. *J. R. Soc. Interface* **2012**, *9*, 401–419. [[CrossRef](#)]
207. Russo, L.; Taraballi, F.; Lupo, C.; Poveda, A.; Jiménez-Barbero, J.; Sandri, M.; Tampieri, A.; Nicotra, F.; Cipolla, L. Carbonate Hydroxyapatite Functionalization: A Comparative Study towards (Bio)Molecules Fixation. *Interface Focus* **2014**, *4*, 20130040. [[CrossRef](#)]
208. Gabrielli, L.; Connell, L.; Russo, L.; Jiménez-Barbero, J.; Nicotra, F.; Cipolla, L.; Jones, J.R. Exploring GPTMS Reactivity against Simple Nucleophiles: Chemistry beyond Hybrid Materials Fabrication. *RSC Adv.* **2013**, *4*, 1841–1848. [[CrossRef](#)]
209. Gabrielli, L.; Russo, L.; Poveda, A.; Jones, J.R.; Nicotra, F.; Jiménez-Barbero, J.; Cipolla, L. Epoxide Opening versus Silica Condensation during Sol–Gel Hybrid Biomaterial Synthesis. *Chem. Eur. J.* **2013**, *19*, 7856–7864. [[CrossRef](#)]
210. Wang, D.; Romer, F.; Connell, L.; Walter, C.; Saiz, E.; Yue, S.; Lee, P.D.; McPhail, D.S.; Hanna, J.V.; Jones, J.R. Highly Flexible Silica/Chitosan Hybrid Scaffolds with Oriented Pores for Tissue Regeneration. *J. Mater. Chem. B* **2015**, *3*, 7560–7576. [[CrossRef](#)] [[PubMed](#)]
211. Jayash, S.N.; Cooper, P.R.; Shelton, R.M.; Kuehne, S.A.; Poologasundarampillai, G. Novel Chitosan-Silica Hybrid Hydrogels for Cell Encapsulation and Drug Delivery. *Int. J. Mol. Sci.* **2021**, *22*, 12267. [[CrossRef](#)]
212. Borges, J.; Mano, J.F. Molecular Interactions Driving the Layer-by-Layer Assembly of Multilayers. *Chem. Rev.* **2014**, *114*, 8883–8942. [[CrossRef](#)]
213. Iler, R.K. Multilayers of Colloidal Particles. *J. Colloid Interface Sci.* **1966**, *21*, 569–594. [[CrossRef](#)]
214. Decher, G.; Hong, J.-D. Buildup of Ultrathin Multilayer Films by a Self-Assembly Process, I Consecutive Adsorption of Anionic and Cationic Bipolar Amphiphiles on Charged Surfaces. *Makromol. Chem. Macromol. Symp.* **1991**, *46*, 321–327. [[CrossRef](#)]
215. Decher, G. Fuzzy Nanoassemblies: Toward Layered Polymeric Multicomposites. *Science* **1997**, *277*, 1232–1237. [[CrossRef](#)]
216. Decher, G.; Hong, J.D. Buildup of Ultrathin Multilayer Films by a Self-Assembly Process: II. Consecutive Adsorption of Anionic and Cationic Bipolar Amphiphiles and Polyelectrolytes on Charged Surfaces. *Berichte Bunsenges. Für Phys. Chem.* **1991**, *95*, 1430–1434. [[CrossRef](#)]
217. Li, Y.; Wang, X.; Sun, J. Layer-by-Layer Assembly for Rapid Fabrication of Thick Polymeric Films. *Chem. Soc. Rev.* **2012**, *41*, 5998–6009. [[CrossRef](#)]
218. Richardson, J.J.; Cui, J.; Björnmalm, M.; Braunger, J.A.; Ejima, H.; Caruso, F. Innovation in Layer-by-Layer Assembly. *Chem. Rev.* **2016**, *116*, 14828–14867. [[CrossRef](#)]
219. Richardson, J.J.; Björnmalm, M.; Caruso, F. Technology-Driven Layer-by-Layer Assembly of Nanofilms. *Science* **2015**, *348*, aaa2491. [[CrossRef](#)]
220. Andres, C.M.; Kotov, N.A. Inkjet Deposition of Layer-by-Layer Assembled Films. *J. Am. Chem. Soc.* **2010**, *132*, 14496–14502. [[CrossRef](#)] [[PubMed](#)]
221. Liu, X.; Luo, C.; Jiang, C.; Shao, L.; Zhang, Y.; Shi, F. Rapid Multilayer Construction on a Non-Planar Substrate by Layer-by-Layer Self-Assembly under High Gravity. *RSC Adv.* **2014**, *4*, 59528–59534. [[CrossRef](#)]
222. Ma, L.; Cheng, M.; Jia, G.; Wang, Y.; An, Q.; Zeng, X.; Shen, Z.; Zhang, Y.; Shi, F. Layer-by-Layer Self-Assembly under High Gravity Field. *Langmuir* **2012**, *28*, 9849–9856. [[CrossRef](#)] [[PubMed](#)]
223. Akagi, T.; Fujiwara, T.; Akashi, M. Inkjet Printing of Layer-by-Layer Assembled Poly(Lactide) Stereocomplex with Encapsulated Proteins. *Langmuir* **2014**, *30*, 1669–1676. [[CrossRef](#)] [[PubMed](#)]
224. Suntivich, R.; Shchepelina, O.; Choi, I.; Tsukruk, V.V. Inkjet-Assisted Layer-by-Layer Printing of Encapsulated Arrays. *ACS Appl. Mater. Interfaces* **2012**, *4*, 3102–3110. [[CrossRef](#)] [[PubMed](#)]
225. Correia, C.R.; Reis, R.L.; Mano, J.F. Multilayered Hierarchical Capsules Providing Cell Adhesion Sites. *Biomacromolecules* **2013**, *14*, 743–751. [[CrossRef](#)]
226. Correia, C.R.; Sher, P.; Reis, R.L.; Mano, J.F. Liquified Chitosan–Alginate Multilayer Capsules Incorporating Poly(L-Lactic Acid) Microparticles as Cell Carriers. *Soft Matter* **2013**, *9*, 2125–2130. [[CrossRef](#)]
227. Tang, Z.; Wang, Y.; Podsiadlo, P.; Kotov, N.A. Biomedical Applications of Layer-by-Layer Assembly: From Biomimetics to Tissue Engineering. *Adv. Mater.* **2006**, *18*, 3203–3224. [[CrossRef](#)]
228. Zhang, Z.; Zeng, J.; Groll, J.; Matsusaki, M. Layer-by-Layer Assembly Methods and Their Biomedical Applications. *Biomater. Sci.* **2022**, *10*, 4077–4094. [[CrossRef](#)]
229. Criado-Gonzalez, M.; Mijangos, C.; Hernández, R. Polyelectrolyte Multilayer Films Based on Natural Polymers: From Fundamentals to Bio-Applications. *Polymers* **2021**, *13*, 2254. [[CrossRef](#)]
230. Alkekha, D.; Hammond, P.T.; Shukla, A. Layer-by-Layer Biomaterials for Drug Delivery. *Annu. Rev. Biomed. Eng.* **2020**, *22*, 1–24. [[CrossRef](#)] [[PubMed](#)]
231. Ren, K.; Hu, M.; Zhang, H.; Li, B.; Lei, W.; Chen, J.; Chang, H.; Wang, L.; Ji, J. Layer-by-Layer Assembly as a Robust Method to Construct Extracellular Matrix Mimic Surfaces to Modulate Cell Behavior. *Prog. Polym. Sci.* **2019**, *92*, 1–34. [[CrossRef](#)]
232. Silva, J.M.; Reis, R.L.; Mano, J.F. Biomimetic Extracellular Environment Based on Natural Origin Polyelectrolyte Multilayers. *Small* **2016**, *12*, 4308–4342. [[CrossRef](#)] [[PubMed](#)]

233. Monge, C.; Almodóvar, J.; Boudou, T.; Picart, C. Spatio-Temporal Control of LbL Films for Biomedical Applications: From 2D to 3D. *Adv. Healthc. Mater.* **2015**, *4*, 811–830. [[CrossRef](#)] [[PubMed](#)]
234. Costa, R.R.; Mano, J.F. Polyelectrolyte Multilayered Assemblies in Biomedical Technologies. *Chem. Soc. Rev.* **2014**, *43*, 3453–3479. [[CrossRef](#)] [[PubMed](#)]
235. Hammond, P.T. Building Biomedical Materials Layer-by-Layer. *Mater. Today* **2012**, *15*, 196–206. [[CrossRef](#)]
236. Sousa, M.P.; Arab-Tehrany, E.; Cleymand, F.; Mano, J.F. Surface Micro- and Nanoengineering: Applications of Layer-by-Layer Technology as a Versatile Tool to Control Cellular Behavior. *Small* **2019**, *15*, 1901228. [[CrossRef](#)]
237. Criado-Gonzalez, M.; Fernandez-Gutierrez, M.; San Roman, J.; Mijangos, C.; Hernández, R. Local and Controlled Release of Tamoxifen from Multi (Layer-by-Layer) Alginate/Chitosan Complex Systems. *Carbohydr. Polym.* **2019**, *206*, 428–434. [[CrossRef](#)]
238. Silva, J.M.; García, J.R.; Reis, R.L.; García, A.J.; Mano, J.F. Tuning Cell Adhesive Properties via Layer-by-Layer Assembly of Chitosan and Alginate. *Acta Biomater.* **2017**, *51*, 279–293. [[CrossRef](#)]
239. Wu, L.; Wu, C.; Liu, G.; Liao, N.; Zhao, F.; Yang, X.; Qu, H.; Peng, B.; Chen, L.; Yang, G. A Surface-Mediated SiRNA Delivery System Developed with Chitosan/Hyaluronic Acid-SiRNA Multilayer Films through Layer-by-Layer Self-Assembly. *Appl. Surf. Sci.* **2016**, *389*, 395–403. [[CrossRef](#)]
240. Couto, D.S.; Alves, N.M.; Mano, J.F. Nanostructured Multilayer Coatings Combining Chitosan with Bioactive Glass Nanoparticles. *J. Nanosci. Nanotechnol.* **2009**, *9*, 1741–1748. [[CrossRef](#)] [[PubMed](#)]
241. Park, S.; Choi, D.; Jeong, H.; Heo, J.; Hong, J. Drug Loading and Release Behavior Depending on the Induced Porosity of Chitosan/Cellulose Multilayer Nanofilms. *Mol. Pharm.* **2017**, *14*, 3322–3330. [[CrossRef](#)] [[PubMed](#)]
242. Cai, K.; Rechtenbach, A.; Hao, J.; Bossert, J.; Jandt, K.D. Polysaccharide-Protein Surface Modification of Titanium via a Layer-by-Layer Technique: Characterization and Cell Behaviour Aspects. *Biomaterials* **2005**, *26*, 5960–5971. [[CrossRef](#)] [[PubMed](#)]
243. Huang, J.; Moghaddam, S.Z.; Thormann, E. Chitosan/Alginate Dialdehyde Multilayer Films with Modulated PH-Responsiveness and Swelling. *Macromol. Chem. Phys.* **2020**, *221*, 1900499. [[CrossRef](#)]
244. Silva, J.M.; Caridade, S.G.; Costa, R.R.; Alves, N.M.; Groth, T.; Picart, C.; Reis, R.L.; Mano, J.F. PH Responsiveness of Multilayered Films and Membranes Made of Polysaccharides. *Langmuir* **2015**, *31*, 11318–11328. [[CrossRef](#)]
245. Neto, A.I.; Cibrão, A.C.; Correia, C.R.; Carvalho, R.R.; Luz, G.M.; Ferrer, G.G.; Botelho, G.; Picart, C.; Alves, N.M.; Mano, J.F. Nanostructured Polymeric Coatings Based on Chitosan and Dopamine-Modified Hyaluronic Acid for Biomedical Applications. *Small* **2014**, *10*, 2459–2469. [[CrossRef](#)]
246. Costa, R.R.; Neto, A.I.; Calgeris, I.; Correia, C.R.; Pinho, A.C.M.; Fonseca, J.; Öner, E.T.; Mano, J.F. Adhesive Nanostructured Multilayer Films Using a Bacterial Exopolysaccharide for Biomedical Applications. *J. Mater. Chem. B* **2013**, *1*, 2367–2374. [[CrossRef](#)]
247. Boddohi, S.; Almodóvar, J.; Zhang, H.; Johnson, P.A.; Kipper, M.J. Layer-by-Layer Assembly of Polysaccharide-Based Nanostructured Surfaces Containing Polyelectrolyte Complex Nanoparticles. *Colloids Surf. B Biointerfaces* **2010**, *77*, 60–68. [[CrossRef](#)]
248. Alves, N.M.; Picart, C.; Mano, J.F. Self Assembling and Crosslinking of Polyelectrolyte Multilayer Films of Chitosan and Alginate Studied by QCM and IR Spectroscopy. *Macromol. Biosci.* **2009**, *9*, 776–785. [[CrossRef](#)]
249. Urbaniak, T.; García-Briones, G.S.; Zhigunov, A.; Hladys, S.; Adrian, E.; Lobaz, V.; Krunclová, T.; Janoušková, O.; Pop-Georgievski, O.; Kubies, D. Quaternized Chitosan/Heparin Polyelectrolyte Multilayer Films for Protein Delivery. *Biomacromolecules* **2022**, *23*, 4734–4748. [[CrossRef](#)]
250. Neto, A.I.; Vasconcelos, N.L.; Oliveira, S.M.; Ruiz-Molina, D.; Mano, J.F. High-Throughput Topographic, Mechanical, and Biological Screening of Multilayer Films Containing Mussel-Inspired Biopolymers. *Adv. Funct. Mater.* **2016**, *26*, 2745–2755. [[CrossRef](#)]
251. Sousa, M.P.; Cleymand, F.; Mano, J.F. Elastic Chitosan/Chondroitin Sulfate Multilayer Membranes. *Biomed. Mater.* **2016**, *11*, 035008. [[CrossRef](#)] [[PubMed](#)]
252. Caridade, S.G.; Monge, C.; Gilde, F.; Boudou, T.; Mano, J.F.; Picart, C. Free-Standing Polyelectrolyte Membranes Made of Chitosan and Alginate. *Biomacromolecules* **2013**, *14*, 1653–1660. [[CrossRef](#)]
253. Silva, J.M.; Duarte, A.R.C.; Caridade, S.G.; Picart, C.; Reis, R.L.; Mano, J.F. Tailored Freestanding Multilayered Membranes Based on Chitosan and Alginate. *Biomacromolecules* **2014**, *15*, 3817–3826. [[CrossRef](#)]
254. Silva, J.M.; Caridade, S.G.; Oliveira, N.M.; Reis, R.L.; Mano, J.F. Chitosan–Alginate Multilayered Films with Gradients of Physicochemical Cues. *J. Mater. Chem. B* **2015**, *3*, 4555–4568. [[CrossRef](#)] [[PubMed](#)]
255. Hautmann, A.; Kedilaya, D.; Stojanović, S.; Radenković, M.; Marx, C.K.; Najman, S.; Pietzsch, M.; Mano, J.F.; Groth, T. Free-Standing Multilayer Films as Growth Factor Reservoirs for Future Wound Dressing Applications. *Biomater. Adv.* **2022**, *142*, 213166. [[CrossRef](#)] [[PubMed](#)]
256. Silva, J.M.; Caridade, S.G.; Reis, R.L.; Mano, J.F. Polysaccharide-Based Freestanding Multilayered Membranes Exhibiting Reversible Switchable Properties. *Soft Matter* **2016**, *12*, 1200–1209. [[CrossRef](#)]
257. Borges, J.; Caridade, S.G.; Silva, J.M.; Mano, J.F. Unraveling the Effect of the Hydration Level on the Molecular Mobility of Nanolayered Polymeric Systems. *Macromol. Rapid Commun.* **2015**, *36*, 405–412. [[CrossRef](#)]
258. Gil, S.; Silva, J.M.; Mano, J.F. Magnetically Multilayer Polysaccharide Membranes for Biomedical Applications. *ACS Biomater. Sci. Eng.* **2015**, *1*, 1016–1025. [[CrossRef](#)]
259. Sousa, M.P.; Mano, J.F. Cell-Adhesive Bioinspired and Catechol-Based Multilayer Freestanding Membranes for Bone Tissue Engineering. *Biomimetics* **2017**, *2*, 19. [[CrossRef](#)]
260. Sousa, M.P.; Neto, A.I.; Correia, T.R.; Miguel, S.P.; Matsusaki, M.; Correia, I.J.; Mano, J.F. Bioinspired Multilayer Membranes as Potential Adhesive Patches for Skin Wound Healing. *Biomater. Sci.* **2018**, *6*, 1962–1975. [[CrossRef](#)] [[PubMed](#)]

261. Rodrigues, J.R.; Alves, N.M.; Mano, J.F. Biomimetic Polysaccharide/Bioactive Glass Nanoparticles Multilayer Membranes for Guided Tissue Regeneration. *RSC Adv.* **2016**, *6*, 75988–75999. [[CrossRef](#)]
262. Sousa, M.P.; Caridade, S.G.; Mano, J.F. Control of Cell Alignment and Morphology by Redesigning ECM-Mimetic Nanotopography on Multilayer Membranes. *Adv. Healthc. Mater.* **2017**, *6*, 1601462. [[CrossRef](#)] [[PubMed](#)]
263. Martins, N.I.; Sousa, M.P.; Custódio, C.A.; Pinto, V.C.; Sousa, P.J.; Minas, G.; Cleymand, F.; Mano, J.F. Multilayered Membranes with Tuned Well Arrays to Be Used as Regenerative Patches. *Acta Biomater.* **2017**, *57*, 313–323. [[CrossRef](#)]
264. Ribeiro, C.; Borges, J.; Costa, A.M.S.; Gaspar, V.M.; Bermudez, V.D.Z.; Mano, J.F. Preparation of Well-Dispersed Chitosan/Alginate Hollow Multilayered Microcapsules for Enhanced Cellular Internalization. *Molecules* **2018**, *23*, 625. [[CrossRef](#)]
265. Costa, R.R.; Girotti, A.; Santos, M.; Arias, F.J.; Mano, J.F.; Rodríguez-Cabello, J.C. Cellular Uptake of Multilayered Capsules Produced with Natural and Genetically Engineered Biomimetic Macromolecules. *Acta Biomater.* **2014**, *10*, 2653–2662. [[CrossRef](#)]
266. Costa, R.R.; Custódio, C.A.; Arias, F.J.; Rodríguez-Cabello, J.C.; Mano, J.F. Nanostructured and Thermoresponsive Recombinant Biopolymer-Based Microcapsules for the Delivery of Active Molecules. *Nanomed. Nanotechnol. Biol. Med.* **2013**, *9*, 895–902. [[CrossRef](#)]
267. Correia, C.R.; Nadine, S.; Mano, J.F. Cell Encapsulation Systems Toward Modular Tissue Regeneration: From Immunoisolation to Multifunctional Devices. *Adv. Funct. Mater.* **2020**, *30*, 1908061. [[CrossRef](#)]
268. Correia, C.R.; Pirraco, R.P.; Cerqueira, M.T.; Marques, A.P.; Reis, R.L.; Mano, J.F. Semipermeable Capsules Wrapping a Multifunctional and Self-Regulated Co-Culture Microenvironment for Osteogenic Differentiation. *Sci. Rep.* **2016**, *6*, 21883. [[CrossRef](#)]
269. Correia, C.R.; Gil, S.; Reis, R.L.; Mano, J.F. A Closed Chondromimetic Environment within Magnetic-Responsive Liquefied Capsules Encapsulating Stem Cells and Collagen II/TGF- β 3 Microparticles. *Adv. Healthc. Mater.* **2016**, *5*, 1346–1355. [[CrossRef](#)]
270. Correia, C.R.; Santos, T.C.; Pirraco, R.P.; Cerqueira, M.T.; Marques, A.P.; Reis, R.L.; Mano, J.F. In Vivo Osteogenic Differentiation of Stem Cells inside Compartmentalized Capsules Loaded with Co-Cultured Endothelial Cells. *Acta Biomater.* **2017**, *53*, 483–494. [[CrossRef](#)] [[PubMed](#)]
271. Correia, C.R.; Bjørge, I.M.; Zeng, J.; Matsusaki, M.; Mano, J.F. Liquefied Microcapsules as Dual-Microcarriers for 3D+3D Bottom-Up Tissue Engineering. *Adv. Healthc. Mater.* **2019**, *8*, 1901221. [[CrossRef](#)] [[PubMed](#)]
272. Costa, R.R.; Castro, E.; Arias, F.J.; Rodríguez-Cabello, J.C.; Mano, J.F. Multifunctional Compartmentalized Capsules with a Hierarchical Organization from the Nano to the Macro Scales. *Biomacromolecules* **2013**, *14*, 2403–2410. [[CrossRef](#)]
273. Silva, J.M.; Duarte, A.R.C.; Custódio, C.A.; Sher, P.; Neto, A.I.; Pinho, A.C.M.; Fonseca, J.; Reis, R.L.; Mano, J.F. Nanostructured Hollow Tubes Based on Chitosan and Alginate Multilayers. *Adv. Healthc. Mater.* **2014**, *3*, 433–440. [[CrossRef](#)]
274. Silva, J.M.; Custódio, C.A.; Reis, R.L.; Mano, J.F. Multilayered Hollow Tubes as Blood Vessel Substitutes. *ACS Biomater. Sci. Eng.* **2016**, *2*, 2304–2314. [[CrossRef](#)] [[PubMed](#)]
275. Yang, Y.; He, Q.; Duan, L.; Cui, Y.; Li, J. Assembled Alginate/Chitosan Nanotubes for Biological Application. *Biomaterials* **2007**, *28*, 3083–3090. [[CrossRef](#)]
276. Sher, P.; Custódio, C.A.; Mano, J.F. Layer-By-Layer Technique for Producing Porous Nanostructured 3D Constructs Using Moldable Freeform Assembly of Spherical Templates. *Small* **2010**, *6*, 2644–2648. [[CrossRef](#)]
277. Silva, J.M.; Georgi, N.; Costa, R.; Sher, P.; Reis, R.L.; Blitterswijk, C.A.V.; Karperien, M.; Mano, J.F. Nanostructured 3D Constructs Based on Chitosan and Chondroitin Sulphate Multilayers for Cartilage Tissue Engineering. *PLoS ONE* **2013**, *8*, e5451. [[CrossRef](#)]
278. Sher, P.; Oliveira, S.M.; Borges, J.; Mano, J.F. Assembly of Cell-Laden Hydrogel Fiber into Non-Liquefied and Liquefied 3D Spiral Constructs by Perfusion-Based Layer-by-Layer Technique. *Biofabrication* **2015**, *7*, 011001. [[CrossRef](#)]
279. Sher, P.; Correia, C.R.; Costa, R.R.; Mano, J.F. Compartmentalized Bioencapsulated Liquefied 3D Macro-Construct by Perfusion-Based Layer-by-Layer Technique. *RSC Adv.* **2014**, *5*, 2511–2516. [[CrossRef](#)]
280. Oliveira, S.M.; Reis, R.L.; Mano, J.F. Assembling Human Platelet Lysate into Multiscale 3D Scaffolds for Bone Tissue Engineering. *ACS Biomater. Sci. Eng.* **2015**, *1*, 2–6. [[CrossRef](#)] [[PubMed](#)]
281. Guo, Z.; Jiang, N.; Moore, J.; McCoy, C.P.; Ziminska, M.; Rafferty, C.; Sarri, G.; Hamilton, A.R.; Li, Y.; Zhang, L.; et al. Nanoscale Hybrid Coating Enables Multifunctional Tissue Scaffold for Potential Multimodal Therapeutic Applications. *ACS Appl. Mater. Interfaces* **2019**, *11*, 27269–27278. [[CrossRef](#)] [[PubMed](#)]
282. Yan, Y.; Chen, H.; Zhang, H.; Guo, C.; Yang, K.; Chen, K.; Cheng, R.; Qian, N.; Sandler, N.; Zhang, Y.S.; et al. Vascularized 3D Printed Scaffolds for Promoting Bone Regeneration. *Biomaterials* **2019**, *190–191*, 97–110. [[CrossRef](#)] [[PubMed](#)]
283. Sousa, C.F.V.; Saraiva, C.A.; Correia, T.R.; Pesqueira, T.; Patrício, S.G.; Rial-Hermida, M.I.; Borges, J.; Mano, J.F. Bioinstructive Layer-by-Layer-Coated Customizable 3D Printed Perfusible Microchannels Embedded in Photocrosslinkable Hydrogels for Vascular Tissue Engineering. *Biomolecules* **2021**, *11*, 863. [[CrossRef](#)] [[PubMed](#)]
284. Oliveira, M.B.; Hatami, J.; Mano, J.F. Coating Strategies Using Layer-by-Layer Deposition for Cell Encapsulation. *Chem. Asian J.* **2016**, *11*, 1753–1764. [[CrossRef](#)] [[PubMed](#)]
285. Li, W.; Lei, X.; Feng, H.; Li, B.; Kong, J.; Xing, M. Layer-by-Layer Cell Encapsulation for Drug Delivery: The History, Technique Basis, and Applications. *Pharmaceutics* **2022**, *14*, 297. [[CrossRef](#)]
286. Liu, T.; Wang, Y.; Zhong, W.; Li, B.; Mequanint, K.; Luo, G.; Xing, M. Biomedical Applications of Layer-by-Layer Self-Assembly for Cell Encapsulation: Current Status and Future Perspectives. *Adv. Healthc. Mater.* **2019**, *8*, 1800939. [[CrossRef](#)]
287. Geng, W.; Wang, L.; Jiang, N.; Cao, J.; Xiao, Y.-X.; Wei, H.; Yetisen, A.K.; Yang, X.-Y.; Su, B.-L. Single Cells in Nanoshells for the Functionalization of Living Cells. *Nanoscale* **2018**, *10*, 3112–3129. [[CrossRef](#)]
288. Hong, D.; Yang, S.H. Cationic Polymers for Coating Living Cells. *Macromol. Res.* **2018**, *26*, 1185–1192. [[CrossRef](#)]

289. Anselmo, A.C.; McHugh, K.J.; Webster, J.; Langer, R.; Jaklenec, A. Layer-by-Layer Encapsulation of Probiotics for Delivery to the Microbiome. *Adv. Mater.* **2016**, *28*, 9486–9490. [[CrossRef](#)]
290. Jonas, A.M.; Glinel, K.; Behrens, A.; Anselmo, A.C.; Langer, R.S.; Jaklenec, A. Controlling the Growth of *Staphylococcus Epidermidis* by Layer-By-Layer Encapsulation. *ACS Appl. Mater. Interfaces* **2018**, *10*, 16250–16259. [[CrossRef](#)] [[PubMed](#)]
291. Pawlak, A.; Belbekhouche, S. Controlling the Growth of *Escherichia Coli* by Layer-by-Layer Encapsulation. *Colloids Surf. B Biointerfaces* **2021**, *206*, 111950. [[CrossRef](#)]
292. Speth, M.T.; Repnik, U.; Griffiths, G. Layer-by-Layer Nanocoating of Live Bacille-Calmette-Guérin Mycobacteria with Poly(I:C) and Chitosan Enhances pro-Inflammatory Activation and Bactericidal Capacity in Murine Macrophages. *Biomaterials* **2016**, *111*, 1–12. [[CrossRef](#)]
293. Groll, J.; Boland, T.; Blunk, T.; Burdick, J.A.; Cho, D.-W.; Dalton, P.D.; Derby, B.; Forgacs, G.; Li, Q.; Mironov, V.A.; et al. Biofabrication: Reappraising the Definition of an Evolving Field. *Biofabrication* **2016**, *8*, 013001. [[CrossRef](#)]
294. Maia, J.R.; Sobreiro-Almeida, R.; Cleymand, F.; Mano, J. Biomaterials of Human Source for 3D Printing Strategies. *J. Phys. Mater.* **2023**, *6*, 012002. [[CrossRef](#)]
295. Lobo, D.A.; Ginestra, P.; Ceretti, E.; Miquel, T.P.; Ciurana, J. Cancer Cell Direct Bioprinting: A Focused Review. *Micromachines* **2021**, *12*, 764. [[CrossRef](#)]
296. Groll, J.; Burdick, J.A.; Cho, D.-W.; Derby, B.; Gelinsky, M.; Heilshorn, S.C.; Jüngst, T.; Malda, J.; Mironov, V.A.; Nakayama, K.; et al. A Definition of Bioinks and Their Distinction from Biomaterial Inks. *Biofabrication* **2018**, *11*, 013001. [[CrossRef](#)]
297. Lazaridou, M.; Bikiaris, D.N.; Lamprou, D.A. 3D Bioprinted Chitosan-Based Hydrogel Scaffolds in Tissue Engineering and Localised Drug Delivery. *Pharmaceutics* **2022**, *14*, 1978. [[CrossRef](#)]
298. Parhi, R. A Review of Three-Dimensional Printing for Pharmaceutical Applications: Quality Control, Risk Assessment and Future Perspectives. *J. Drug Deliv. Sci. Technol.* **2021**, *64*, 102571. [[CrossRef](#)]
299. Di Luca, M.; Hoskins, C.; Corduas, F.; Onchuru, R.; Oluwasanmi, A.; Mariotti, D.; Conti, B.; Lamprou, D.A. 3D Printed Biodegradable Multifunctional Implants for Effective Breast Cancer Treatment. *Int. J. Pharm.* **2022**, *629*, 122363. [[CrossRef](#)] [[PubMed](#)]
300. Xu, J.; Fang, H.; Su, Y.; Kang, Y.; Xu, D.; Cheng, Y.Y.; Nie, Y.; Wang, H.; Liu, T.; Song, K. A 3D Bioprinted Decellularized Extracellular Matrix/Gelatin/Quaternized Chitosan Scaffold Assembling with Poly(Ionic Liquid)s for Skin Tissue Engineering. *Int. J. Biol. Macromol.* **2022**, *220*, 1253–1266. [[CrossRef](#)] [[PubMed](#)]
301. Maturavongsadit, P.; Narayanan, L.K.; Chansoria, P.; Shirwaiker, R.; Benhabbour, S.R. Cell-Laden Nanocellulose/Chitosan-Based Bioinks for 3D Bioprinting and Enhanced Osteogenic Cell Differentiation. *ACS Appl. Bio Mater.* **2021**, *4*, 2342–2353. [[CrossRef](#)]
302. Yu, K.-F.; Lu, T.-Y.; Li, Y.-C.E.; Teng, K.-C.; Chen, Y.-C.; Wei, Y.; Lin, T.-E.; Cheng, N.-C.; Yu, J. Design and Synthesis of Stem Cell-Laden Keratin/Glycol Chitosan Methacrylate Bioinks for 3D Bioprinting. *Biomacromolecules* **2022**, *23*, 2814–2826. [[CrossRef](#)] [[PubMed](#)]
303. Coşkun, S.; Akbulut, S.O.; Sarıkaya, B.; Çakmak, S.; Gümüşderelioğlu, M. Formulation of Chitosan and Chitosan-NanoHAp Bioinks and Investigation of Printability with Optimized Bioprinting Parameters. *Int. J. Biol. Macromol.* **2022**, *222*, 1453–1464. [[CrossRef](#)] [[PubMed](#)]
304. Gwak, M.A.; Lee, S.J.; Lee, D.; Park, S.A.; Park, W.H. Highly Gallol-Substituted, Rapidly Self-Crosslinkable, and Robust Chitosan Hydrogel for 3D Bioprinting. *Int. J. Biol. Macromol.* **2022**, *227*, 493–504. [[CrossRef](#)]
305. Condi Mainardi, J.; Rezwan, K.; Maas, M. Genipin-Crosslinked Chitosan/Alginate/Alumina Nanocomposite Gels for 3D Bioprinting. *Bioprocess Biosyst. Eng.* **2022**, *45*, 171–185. [[CrossRef](#)]
306. Riofrio, A.; Alcivar, T.; Baykara, H. Environmental and Economic Viability of Chitosan Production in Guayas-Ecuador: A Robust Investment and Life Cycle Analysis. *ACS Omega* **2021**, *6*, 23038–23051. [[CrossRef](#)]

Disclaimer/Publisher’s Note: The statements, opinions and data contained in all publications are solely those of the individual author(s) and contributor(s) and not of MDPI and/or the editor(s). MDPI and/or the editor(s) disclaim responsibility for any injury to people or property resulting from any ideas, methods, instructions or products referred to in the content.